8-2007

Functional Genomics of the Angiotensin II Type 2 Receptor in the Developing Brain

Traci Pawlowski
Clemson University, tpawlow@clemson.edu

Follow this and additional works at: https://tigerprints.clemson.edu/all_dissertations

Part of the Genetics Commons

FUNCTIONAL GENOMICS OF THE ANGIOTENSIN II TYPE TWO
RECEPTOR IN THE DEVELOPING BRAIN

A Dissertation
Presented to
the Graduate School of
Clemson University

In Partial Fulfillment
of the Requirements for the Degree
Doctor of Philosophy
Genetics

by
Traci Bryant-Pawlowski
August 2007

Accepted by:
Anand K. Srivastava PhD, Committee Chair
Albert Abbott PhD
Chin-Fu Chen PhD
Barbara Dupont PhD
James Morris PhD

ABSTRACT

The mammalian brain expresses two angiotensin II specific receptors, the angiotensin II type 1 (AGTR1) and type 2 (AGTR2). Studies in humans and mice indicate a possible role for AGTR2 in learning, memory and behavior. However, *AGTR2* gene function in the brain, and the molecular mechanisms by which AGTR2 exerts its physiological action, remains elusive. This study examines the possible role of AGTR2 in the developing brain and in brain function by employing three different approaches.

To identify genes in the developing brain that depend on AGTR2 function, a microarray analysis was conducted that compared the gene expression of $Agtr2^{-/y}$ mouse brains to normal controls at embryonic day 15 and postnatal day 1. Genes involved in microtubule regulation, cell adhesion and glutamate metabolism were found to be up-regulated in $Agtr2^{-/y}$ mouse brains. These results suggest that AGTR2 may contribute to the developing brain by influencing cell morphology and synaptic connectivity.

Using a yeast two-hybrid system, the amino-terminal extracellular domain and carboxy-terminal intracellular domain of AGTR2 were screened against a human fetal brain cDNA library to identify AGTR2 interacting proteins. Three novel AGTR2 interacting proteins, ASMTL, GNB2L1 and NGLY1 were identified.

Lastly, a brain-specific isoform of a previously identified AGTR2 interacting protein, ATIP, was explored as a potential candidate gene for mental retardation.

Limited screening of the *ATIP* gene in 80 patients with mental retardation identified two non-pathogenic sequence variants but no disease causing mutations.

In summary, this study unveils several functional classes of genes as potential downstream targets of AGTR2 and identifies three new AGTR2 interacting proteins in the developing brain. Further functional studies of the newly identified AGTR2 interacting proteins and some of the genes influenced by AGTR2 may provide clues to AGTR2-mediated signaling in the developing brain and in brain function.

DEDICATION

I dedicate this dissertation to my husband Joseph Pawlowski, whose love, support, patience and unwavering confidence in my abilities made graduate school possible. Also, to my son Christopher Pawlowski, whose love, idealism, curiosity and joie de vivre are a constant inspiration.

ACKNOWLEDGEMENTS

TABLE OF CONTENTS

TABLE OF CONTENTS (continued)

LIST OF TABLES

LIST OF TABLES (continued)

LIST OF FIGURES

LIST OF FIGURES (continued)

LIST OF FIGURES (continued)

Figure   Page

PREFACE

Mental retardation (MR), defined by an IQ score less than 70, affects approximately 1-3% of the human population (Chelly and Mandel 2001). The causes of MR are many, and in up to 40% of cases the cause is unknown (Chelly and Mandel 2001). When the cause is known, mental retardation can result from prenatal insults, environmental factors, injuries and genetic causes. The genetic component of MR likely includes mutations in a large number of genes distributed throughout the genome. X-linked mental retardation is the most common cause of MR in males (Stevenson 2005).

The role of angiotensin II (Ang II) in the renin-angiotensin system (RAS) has been well characterized as an enzyme-neuropeptide system in the brain, as well as for its role in blood pressure control and fluid homeostasis. The action of the Ang II peptide is primarily mediated by its two receptors, Angiotensin II type 1 receptor (AGTR1) and Angiotensin II type 2 receptor (AGTR2). The RAS has been shown to regulate sensory information, learning and emotional response (von Bohlen und Halbach and Albrecht 2006). Several components of the RAS have been implicated as having roles in brain development and function. Mutations in the *AGTR2* gene have been found in individuals with MR (Vervoort et al. 2002; Ylisaukko-ojo et al. 2004), and a family with X-linked MR and epilepsy has been found to have a mutation in the renin receptor (Ramser et al. 2005).

All components of the RAS are present in several areas of the body including the kidney, blood vessel walls, heart and brain (Lavoie and Sigmund 2003). In the classic RAS, angiotensinogen is converted to angiotensin I by renin. Angiotensin I is cleaved by angiotensin converting enzyme (ACE) to make angiotensin II (Figure P.1). Angiotensinogen can also be cleaved by cathespin D or tonin to make angiotensin II. Cathespin G, chymostatin-sensitive angiotensin II generating enzyme (CAGE), and chymase can also cleave angiotensin I to make angiotensin II (Lavoie and Sigmund 2003; von Bohlen und Halbach and Albrecht 2006). Ang II is likely the first neuroactive form of the angiotensins. Other neuroactive angiotensins include angiotensin IV and angiotensin (1-7) and are produced by the actions of other enzymes (von Bohlen und Halbach and Albrecht 2006).

Physiologically AGTR2 has been shown to balance the actions of AGTR1 (Hein et al. 1995; Ichiki et al. 1995; AbdAlla et al. 2001). AGTR2 has been shown to inhibit AGTR1 actions by directly binding to AGTR1 (AbdAlla et al. 2001). The role of AGTR1 is very well characterized, but the functions of AGTR2 remain elusive. The purpose of this study is to elucidate the physiological function of AGTR2 in the developing brain.

The RAS mediates the expression of AGTR1 and AGTR2 by the level of angiotensin II produced, and thus the signaling cascades controlled by each respective receptor. Stimulation of AGTR1 raises blood pressure, increases cellular Ca^{2+}, depolarizes sodium channels and contributes to cell proliferation (Allen et al.

1998; Berry et al. 2001). Conversely, activation of AGTR2 lowers blood pressure, hyper-polarizes sodium channels and induces apoptosis (Berry et al. 2001). Different signaling cascades are mediated by angiotensin II depending on whether it is bound by AGTR2 or AGTR1. Binding of angiotensin II to AGTR1 causes endocytosis of AGTR1 but not AGTR2 (Hein et al. 1997).   AGTR1 induces phosphorylation by tyrosine kinase and up-regulates Map kinases (MAPK), which up-regulates transcription of various genes affecting cell proliferation (Berry et al. 2001). AGTR1 also induces vasoconstriction via the phosphatidyl inositol pathway (Berry et al. 2001). Conversely, AGTR2 through the activation of protein phosphatase 2A (PP2A), inhibits MAPK expression.   Through stimulating ERK phosphatase, AGTR2 also promotes apoptosis as well as vasodilation through nitrous oxide synthetase and phospholipase A2 (Berry et al. 2001). AGTR2 has also been shown to regulate cell growth (Goto et al. 1997). These functions are summarized in Figure P.1.

Functional studies of AGTR2 in neuronal cells suggest it has a role in apoptosis and cell differentiation. AGTR2 has been found to mediate apoptosis in PC12W and R3T3 cells (Yamada et al. 1996) AGTR2 has been localized to neurons but not glial cells and has been shown to influence morphology of several cell types including NG-108-15, PC12W and rat neuronal cell lines (Gendron et al. 2003). Its effects on neuronal growth and differentiation are complex.   In PC12W cells, AGTR2 was found to up-regulate MAP2, polymerize beta-tubulin levels and down-

regulate MAP1B protein levels. MAP2 has been associated with elongation of axons

(Shea and Flanagan 2001).   Thus a possible role for AGTR2 in nerve regeneration

and cell differentiation was suggested (Stroth et al. 1998).
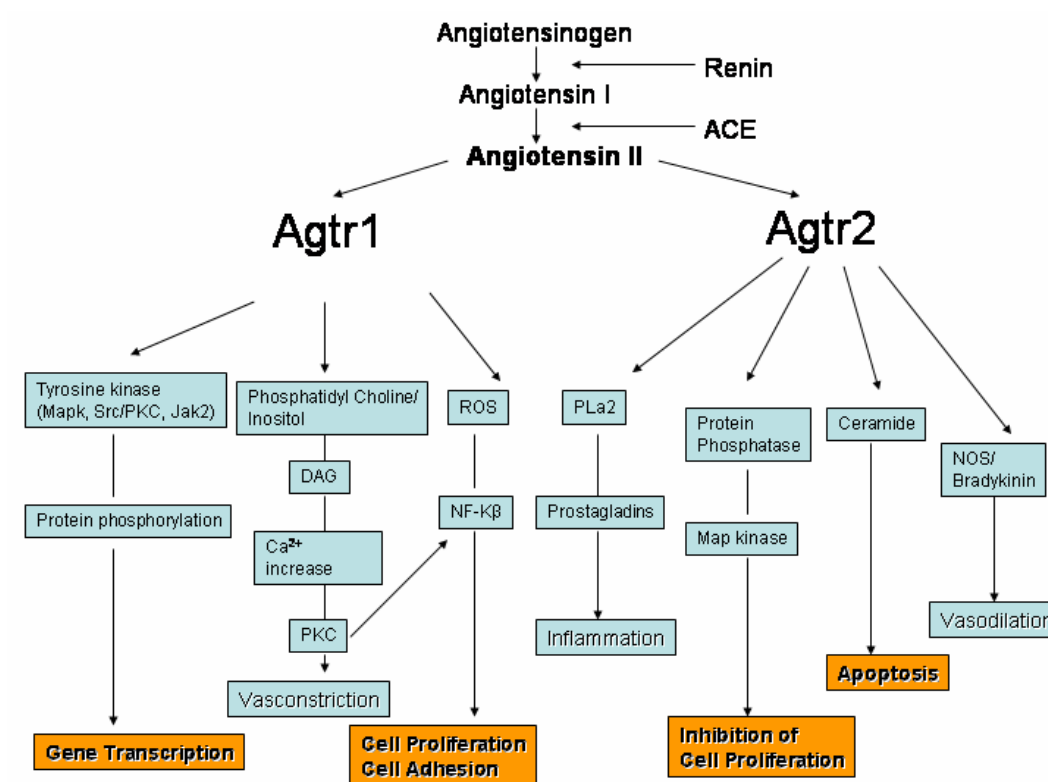
<u>Figure P.1</u> The angiotensin II receptors signaling cascade. The physiological
functions affecting the developing brain are highlighted in orange.

Using NG-108-15 cells, Gendron and associates (1999) found that AGTR2

stimulates neurite outgrowth via an increase in MAPK activity and a decrease in

$p21^{ras}$ activity in a time dependent manner. The inhibition of protein kinase C

(PKC) by AGTR2 has also been shown to inhibit cell proliferation by PKC

inhibiting $p21^{ras}$ and then up-regulating Rap1 and the $p42/p44^{mapk}$ pathway to allow

neurite elongation (Beaudry et al. 2006). AGTR2 has also been shown to stimulate neuronal differentiation by its association with MMS2 and a complex of ATIP and SHP-1 in rat neuronal cells (Li et al. 2007).

Both receptors are expressed in the hippocampus, the cingulate cortex, parts of the amygdala, the anterior thalamus, the paraventricular nucleus, the supraoptic nucleus, the superior and inferior colliculi, the locus coeruleus, the inferior olive and the vagal nucleus (reviewed in von Bohlen und Halbach and Albrecht 2006). AGTR2 is uniquely expressed in the lateral septal area, habenula, centromedial thalamus, medial geniculate nucleus, reticular nucleus, ventral segmental area, hypoglossal nucleus, motor trigeminal nucleus and the cerebellum (von Bohlen und Halbach and Albrecht 2006).

In the mouse fetus, expression of AGTR2 has been shown to be relatively higher and more diverse in the developing brain than in adulthood (Johren and Saavedra 1996; Nuyt et al. 1999; Saavedra 2005). Using a cRNA probe, Nuyt and co-workers (1999) found AGTR2 in the developing rat brain beginning at E11 in the lateral hypothalamic area and then increasing in expression and location throughout gestation and 28 days postnatally.

A female patient with mental retardation and absence *AGTR2* gene expression was described previously (Vervoort et al. 2002). A subsequent screening of 590 unrelated patients with MR revealed one frame shift and three missense mutations in eight patients (Vervoort et al. 2002). In a separate screening of 360 unrelated males

with non-syndromic X-linked mental retardation, one patient was found to have a p.C117F change in the N-terminal domain of AGTR2 which was determined to be a rare polymorphic variant (Bienvenu et al. 2003). A study of 57 similarly affected Finnish male patients found one patient with the G21V mutation and one with an I53F in the transmembrane domain (Ylisaukko-ojo et al. 2004). However, Erdman and co-workers (2004) found in a screening of 631 males and 277 females, that 1 male with dilated cardiomyopathy and another male with hypertrophic cardiomyopathy had the G21V mutation as well as 2 normal controls. None of these patients had reported mental deficits. Several proteins (Erb3, PLZF, ATIP, NHE6) have been found to interact with AGTR2 through in-vivo and in-vitro studies (Knowle et al. 2000; Senbonmatsu et al. 2003; Nouet et al. 2004; Pulakat et al. 2005). The sequence changes detected in patients with MR and the location known AGTR2 interacting proteins are indicated in Figure P.2.
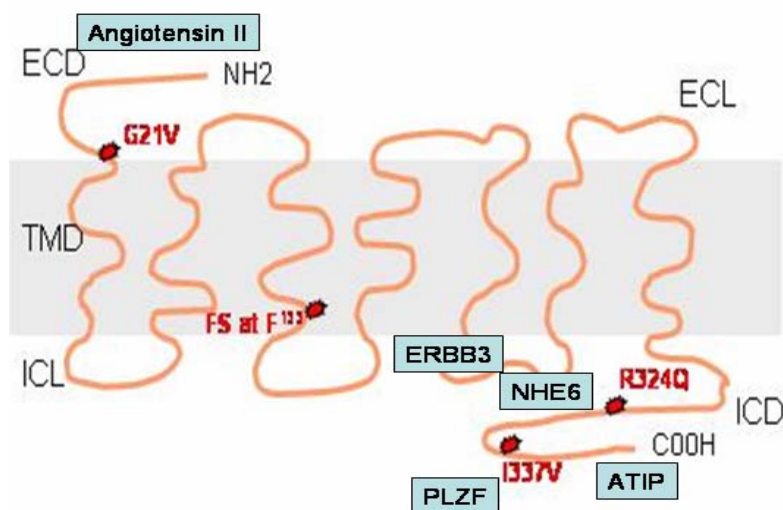
Figure P.2 Summary of mutations and interactions of AGTR2. Mutations are in red, blue boxes are interacting proteins. ECD=extra-cellular domain, ECL = Extra-cellular loop, TMD = transmembrane domain, ICL = intracellular loop, ICD = intracellular domain.

The *AGTR2* gene is located at chromosome Xq23 in humans. The gene is 4250 bp long, consisting of 3 exons. The entire open reading frame is contained in exon 3 and transcribes a 2882 bp transcript. The AGTR2 protein is a seven transmembrane receptor consisting of 363 amino acids of 41.2 kDa (Koike et al. 1994). AGTR2 is highly expressed in fetal tissues with expression reducing rapidly after birth and then predominately only being expressed in the cerebellum, kidney, heart, adrenals, vasculature and pancreas (Berry et al. 2001).

In the mouse, the *Agtr2* gene is located on XA1.3. The gene is 4539 bp long, consisting of 4 exons making a 3204 bp transcript. The coding region has been

found in exons 3 and 4, and encodes a 363 amino acid protein with a 95% homology

to the human receptor (Eppig and Bult 2005).

The first AGTR2 knock-out mouse models were described in 1995 (Hein et

al. 1995; Ichiki et al. 1995). These mice were viable and fertile. The mutant males

showed increased fear and a reduction in exploratory behavior and decreased body

temperature, sensitivity to pain, startle response and drinking response. Cell number

in the brains of the *Agtr2$^{-/y}$* mice was increased, but cell size was not affected (von

Bohlen und Halbach et al. 2001) Sakagawa and collaborators (2000) found that

AGTR2 knockout mice had an increased sensitivity to pain and lower levels of brain

β-endorphin.

Microarrays are used in Chapter 1 to elucidate the differences in gene

expression in the brains of *Agtr2$^{-/y}$* versus normal embryonic day 15 (E15) and

postnatal day one (P1) mice. Our findings point to predicted and novel pathways for

AGTR2 in brain development, as well as differences in its function at different

points in development.

In Chapter 2, the screening of a human fetal brain library with the N-terminal

and C-terminal domains of AGTR2 utilizing a yeast two-hybrid system is discussed.

The screening with the N-terminal domain found three novel interacting proteins:

GNB2L1, (also known as RACK-1), NGLY1 and ASTML.

In Chapter 3, angiotensin II interacting protein (ATIP) is partially

characterized. ATIP has previously been shown to interact with the C-terminal

intracellular domain of AGTR2 (Nouet et al. 2004; Wruck et al. 2005). One isoform of the ATIP gene is characterized in the central nervous system. A mutation screen of ATIP in patients with MR was undertaken, but no disease causing mutations were identified.

A female patient with an X;7 translocation and an absence of *AGTR2* gene expression (Vervoort et al. 2002), is discussed in the appendix. This patient did not have a disrupted *AGTR2* gene, so several molecular methods were employed to attempt to find a regulatory region for *AGTR2*. A deletion in the patient's Xq22 chromosome region was found. This region contained a pseudogene for SUMO2 was found, which may contribute to the absent expression of *AGTR2*. Though the patient's *CUTL1* gene was disrupted on chromosome 7, the patient demonstrated expression of this gene.

In summary, work in this dissertation includes identification of genes whose functions are likely influenced by AGTR2 in the developing brain. Three proteins that interact with AGTR2 were identified and partially characterized in patients with AGTR2 defects. A previously identified AGTR2 interacting protein, ATIP, was characterized and tested as a candidate gene for mental retardation. Altogether, the results support a likely role of AGTR2 mediated signaling in brain development and function.

.

MICROARRAY ANALYSIS REVEALS GENES CONTRIBUTING TO ABNORMAL DENDRITIC SPINES IN $AGTR2^{-/Y}$ MOUSE

Mental retardation (MR) is the most common developmental disability, affecting cognitive function in about 1-3% of the human population. Studies in humans and mice indicated a possible role for the angiotensin II type 2 receptor (AGTR2) in learning, memory and behavior. However, AGTR2 gene function in the brain and the molecular mechanism by which AGTR2 exerts is physiological action remains elusive.

The role of the renin-angiotensin system in blood pressure control and fluid homeostasis is well established. Angiotensin II binds to angiotensin II type one receptor (AGTR1) and type 2 receptor (AGTR2) receptor. Both receptors have been shown to have opposing physiological effects (Berry et al. 2001). AGTR1 affects vasoconstriction, cell proliferation, cell hypertrophy, superoxide production, endothelin release, lipid peroxidation, adhesion molecule expression and vascular matrix expression primarily through phospholipases C, D and A2 (Berry et al., 2001; (Csikos et al. 1998). The AGTR2 receptor has been shown to have a balancing effect to AGTR1 in regard to blood pressure and natriuresis (Berry et al. 2001). It has also been shown to inhibit growth and induce apoptosis (Yamada et al. 1996). It also decreases cyclic guanosine monophosphate levels (GMP) and increases the production of arachidonic acid (Nahmias and Strosberg 1995). AGTR2 activates serine/threonine protein phosphatase two A (PP2A), the nitric oxide pathway as

well as phospholipase A2 which contribute to vasodilation through the upregulation of prostaglandins, bradykinin and nitric oxide (Berry et al. 2001). The synthesis of ceramide also has been associated with stimulation of AGTR2 which in turn induces apoptosis (Lehtonen et al. 1999; Berry et al. 2001).

AGTR2 has also been shown to up-regulate the microtubule proteins polymerized β-tubulin and MAP2 in PC12W cells (Stroth et al. 1998). It has also been demonstrated that stimulation of AGTR2 inhibits cell proliferation and induces neurite outgrowth (Meffert et al. 1996). AGTR2 knockout mice showed an increase in cell number in the brain, especially in the ventral thalamic nuclei and medial nucleus of the amygdala that persists into adulthood (von Bohlen und Halbach et al. 2001).

Previous findings have shown that AGTR2 knockout mice were viable and fertile (Hein et al. 1995; Ichiki et al. 1995). However, the behavior and learning abilities of AGTR2 knockout mice differ from normal mice. AGTR2 knockout mice demonstrate a lowered pain threshold than normal mice (Sakagawa et al. 2000). These mice also show more anxiety type behaviors (Okuyama et al. 1999). Mutant mice lacking the Agtr2 gene (*Agtr2$^{-/y}$*) were found to be significantly impaired in their learning performance and exhibited abnormal dendritic spine morphology (C. Maul, unpublished data), a feature consistently found to be associated with MR. In a test of spatial memory, six month old AGTR2 knockout mice exhibited impaired performance in a maze and also demonstrated impaired learning in a one-way active

avoidance task (Maul unpublished data). These mice also have a decrease in spontaneous movement (Hein et al. 1995) and exploratory behavior (Ichiki et al. 1995).

Expression of AGTR2 has been shown to be ubiquitous in the fetus and then declines rapidly after birth (Grady et al. 1991). Expression in the rat brain is detectable at embryonic day 13 (E13) and its expression changes in both intensity and locality in the brain throughout prenatal development and postnatally (Nuyt et al. 1999).

In order to identify transcripts in the developing brain that depend on AGTR2 function, we analyzed RNA isolated from brains of $Agtr2^{-/y}$ and control mice at developmental stage E15 and at birth using Agilent Whole Mouse Genome 44K arrays. Gene expression profiles of the $Agtr2^{-/y}$ brain samples were compared to profiles of the control brains. Furthermore, the expression profiling data generated in this study point to a role for AGTR2 that is likely independent of the renin-angiotensin system.

<div align="center">Methods</div>

Animals

Pre-dissected organs from animals were provided from $Agtr2^{-/y}$ breeding stocks by Dr. T. Walther at the Charité, Campus Benjamin Franklin, Berlin, Germany. These mice are from the 129/sv strain on a C57BL/6 x 129 mixed genetic background with a disrupted $Agtr2$ gene.

Genotyping of animals was performed after isolating DNA from liver. PCR was performed with the following primer sets: knockout- NeoPvu-F – 5' GGCAGCGCGGCTATCGTGG 3' and control – AT25 (F) 5' CCACCAGCAGA-AACATTACC 3' and the same reverse primer was used for both: AT23 (R) 5' GAA-CTACATAAGATGCTTGCCAGG 3'. (Primer sequences provided by T. Walther) The following conditions were used for amplification: 95ºC for 5 min., 95ºC for 30 sec., 60ºC for 30 sec., 72ºC for 45 sec. for 30 cycles followed by 72ºC for 7 min. Sex was determined by genotyping with an X-linked gene *Jarid1 C*, using the following primers: Forward 5' CTGAAGCTTTTGGCTTTGAG 3' and reverse – 5' CCACTGCC-AAATTCTTTGG 3' with the following conditions: 95ºC for 5 min., 95ºC for 20 sec., 56ºC for 30 sec., 72ºC for 40 sec. for 30 cycles followed by 72ºC for 7 min. (Clapcote and Roder 2005) *Jarid1 C* primers will produce a 331 bp and 302 bp band in males and a single 331 bp band in females, as there is a homologue to *Jarid1 C* on the Y chromosome (Figure 1.1).
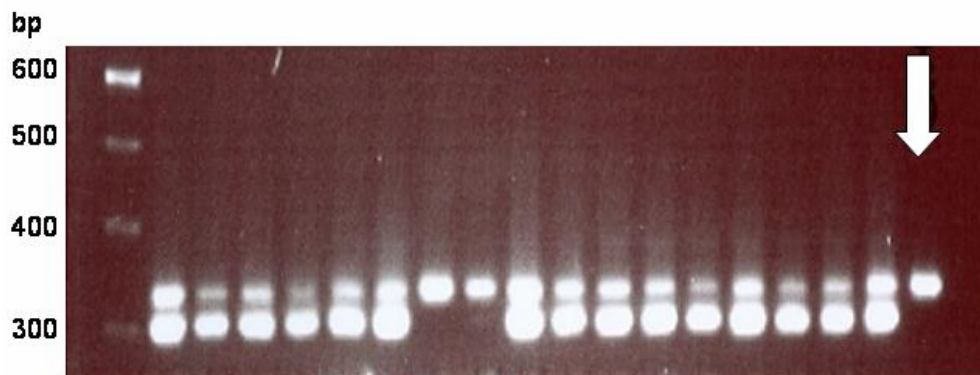
Figure 1.1 Agarose gel of *Jarid1C* PCR of E15 *Agtr2$^{-/y}$* mouse DNA. Males have a 331 bp and 302 bp band and females have a 331bp band. Control female is indicated by the arrow.

RNA extraction

Total RNA was extracted from frozen slices of whole brain weighing less than 30µg using the Qiagen RNeasy kit (Qiagen) according to manufacturer instructions. Samples were cleaned with DNase using the Ambion Turbo DNase-free kit (Ambion Inc.). RNA samples were analyzed on the Agilent 2100 expert bioanalyzer (Agilent) for purity and concentration. Two microliters of purified RNA were loaded on a RNA 6000 Nano LabChip (Agilent) along with 2 µl of RNA ladder (Ambion) and fluorescent marker from the Nano LabChip kit. The chip was read by the Agilent 2100 Bioanalyzer. The bioanalyzer software computed sample concentration, ratio of 18S to 28S ribosomal RNA and produced a gel image and electropherogram.

Microarray hybridization

RNA from 6 male controls and 8 male knockouts at stage E15 was amplified individually and labeled with the Agilent low RNA Input Linear Amplification Kit (Agilent) according to manufacturer instructions. In brief, cDNA was synthesized using a T7 primer and was then labeled with Cy3- or Cy5-CTP. Samples were purified with Qiagen RNasey mini spin columns (Qiagen).   Equal amounts of control sample and *Agtr2$^{-/y}$* sample were labeled with Cy3 or Cy5 respectively and were hybridized to the first set of 8 Agilent Whole Mouse Genome Oligo 44K Microarrays slides (Agilent) according to the Agilent protocol. On the second set of microarray slides, the control samples were paired with a different knockout sample. The experimental strategy is outlined in figure 1.2. Arrays were hybridized for 17 hours at 65°C and then washed with 6X SSC, 0.005% Triton X-102 for one minute and then with 0.1X SSC, 0.005% Triton X-102 for one minute and then for 30 seconds in ozone scavenging solution (Agilent #5185-5979) . The microarray slides were scanned on an Agilent microarray scanner and data was normalized and extracted with Feature Extraction 8.0 software (Agilent). RNA from 4 male control and 4 P1 *Agtr2 $^{-/y}$* brains was handled in the same fashion, with all controls being dye-swapped with a different knockout in each dye selection (Figure 1.2).
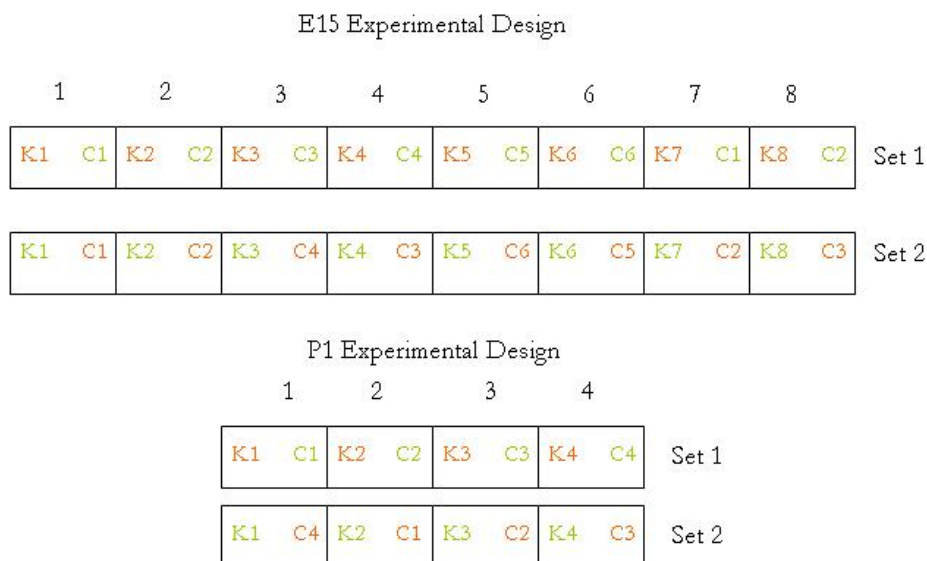
Figure 1.2 Experimental design for E15 and P1 mouse brains on Agilent Whole
Mouse Genome 44K expression arrays demonstrating dye-swap strategy. K =
Agtr2$^{-/y}$ samples, C = control samples.

Data analysis

Normalized data from each array were reviewed to determine hybridization

efficiency. Two arrays were not included due to poor hybridization. A list of over

and under expressed genes for each developmental stage was generated using a

Student's t-test with a Benjamini and Hochberg false discovery rate (Benjamini 2000)

statistic using both GeneSpring GX (Agilent) and Bioconductor marray and limma

software (Smyth 2005; Team 2005; Yee 2005). A list was produced using

GeneSpring GX© using a p≤ 0.001 and a FDR ≤ 0.3 for stage E15 of 88 up-

regulated and 45 down-regulated genes. Ninety-five genes had on-chip replicates and 5,996 genes had insufficient data for a comparison. Also using GeneSpring GX with a p ≤ .005 and a FDR ≤ .3, for the newborn stage, a list of 270 up-regulated and 127 down-regulated genes was produced. There were 2971 genes that had insufficient data for comparison. Using the R statistical language (Team 2005) Bioconductor with the marray (Yee 2005) and limma (Smyth 2005) packages were implemented to provide a second analysis. The p-values with a Benjamini and Hochberg false discovery rate and the fold change using a log2 transformation of all genes on all arrays were calculated using limma. A summary of the creation of the final lists is seen in Figures 1.3a and 1.3b. Annotation of genes in the list were enhanced buy using the DAVID Gene Id Conversion Tool (Dennis et al. 2003).

Hierarchical clustering (condition tree) of the embryo arrays was performed by GeneSpring GX using a Pearson correlation with a clustering algorithm = average linkage, with a separation ratio of 1 and a minimum distance of 0.001 using the E15 final list. Clustering of the P1 arrays (gene tree) was performed in the same way using a Pearson correlation with a clustering algorithm = average linkage, discarding genes with no data in half the starting conditions and bootstrapping 100 sets. Gene tree clustering on the entire embryo set was not possible due to computing limitations.

E15 Data, **14 Arrays**

Data Normalized Log2 -5996 genes

Data Normalized Log2

GeneSpring GX T-test p≤.001

GeneSpring GX T-test FDR≤0.3

Bioconductor Limma Compute FDR and Fold Change

GeneSpring GX List 133 genes

List of all genes by Fold change

Final List p≤.001 FDR≤0.3 FC>1.3 62 genes
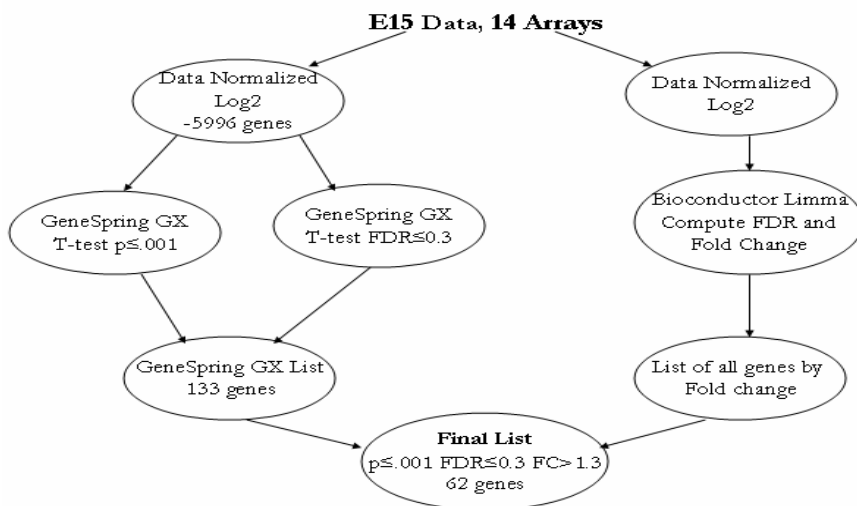
Figure 1.3a Flow chart of creation of E15 final list. Normalized data was analyzed with GeneSpring GX and Bioconductor Limma to add strength to the results.

P1 Data, 8 Arrays

Data Normalized Log2 -2971

Data Normalized Log2

GeneSpring GX T-test p≤.005

GeneSpring GX T-test FDR≤0.3

Bioconductor Limma Compute FDR and Fold Change

GeneSpring GX List 377 genes

List of all genes by Fold change

Final List p≤.005 FDR≤0.3 FC>1.4 62 genes
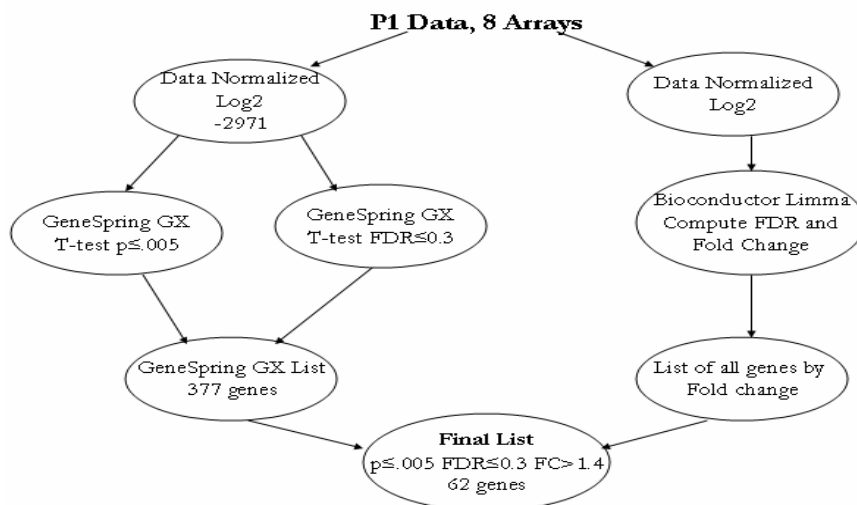
Figure 1.3b Flow chart of creation of P1 final list. Normalized data was analyzed with GeneSpring GX and Bioconductor Limma to add strength to the results.

Quantitative PCR

RNA was isolated as previously described on 4 controls and 4 knockouts from each developmental stage, and from mice other than ones used in the microarray experiment previously. Primers were designed using the Primer3 program (http://frodo.wi.mit.edu/cgi-bin/primer3/primer3_www.cgi) (Rozen and Skaletsky 2000). Biorad I-Script 1 step RT-PCR with SYBR green (Biorad) was used according to manufacturer instructions with 5 ng of RNA per sample used. Samples were run in triplicate on a Biorad i-cycler and analyzed using a standard curve method (Larionov et al. 2005)A control gene, AK029535 (Riken cDNA493050c13) was selected from a list of genes showing the least difference in expression generated by limma using the model 1a algorithm as described by Szabo et. al (Szabo et al. 2004).   The list of primers used is in Table1.1.

Table 1.1
Primers for Quantitative RT-PCR of E15 and P1 Mouse Brains

Primer Name	Genebank Accession	Annealing Temperature ºC	Sequence 5' – 3'	Product Size (bp)
AK029535	AK029535	55	F-GACAGTGGAGGGGAGAATGA R -ACCGAGTTCTGGGTGTTGAC	240
Prdm16	NM_027504	63	F-AGGGCAAGAACCATTACACG R-AGAGGTGGTCGTGGGTACAG	247
Bmp2kb	NM_080708	60	F-CATTTCCGATTCCAAGGAGA R-GGAAGGACCCGTGTACTGAA	224
Pisd	AK005333	61	F-GGAGCAGTGACCACACTGAA R-ACATCTTGCGTAGGCACAGG	150
013803	AK013803	53	F-TGGCTCTCTTCCTGATTGGT R-CCAAACAAGGGTCTTCCAAA	190

Table 1.1 (continued)

Prosc	BC047992	64	F-AGGGTGTGGTGAGGATTCTG R-GACGAGAACTGTGCACCTGA	209
C77370	XM_205178	57	F-GCAGGACTTGCTTAGGTTGC R-TTGACTTATGCAGGGGGAAG	210
050558	AK050558	64	F-TCTTTCCCGAGTTCTGCTGT R-GGGAACAACCAGGCTCATAA	225
Syn2	NM_013681	57	F-ATGGCAAAGATGGCAAAGAC R-CCGGTTCCTTAAGTGTTCCA	204
Mtap2	AK086484	55	F-CTGGACATCAGCCTCACTCA R-AATAGGTGCCCTGTGACCTG	164
Casc4	NM_177054	55	F-GAAGCAGATCGACCAGAAGG R-TTCTAGCCGCTTGACAAGGT	163
Prie4	AK009137	56	F-TGTAACTGGGCTCCTTGCTT R-TTGCAAAGACCTCTCCTGGT	195
Ube2m	NM_145578	61	F-CGACCTCCTCAACTTCAAGC R-CTGGCTTCCAGTCCTCTCTG	200
Gnb2l1	NM_008143	55	F-GCAAGTACACGGTCCAGGAT R-GGGATCCATCTGGAGAGACA	204
Achy	L32836	50	F-CGTGATGAGCAACTCCTTCA R-TGGTCAGCTTCACATTCAGC	155
Gls	AK047664	65	F-TCAGTGCCCTTAATTGCTGA R-CTTGCATAGGTCACGGGTTT	249
Rbm26	NM_134077	55	F-CTCCACTTCCTCCTTTGCAG R-CTTGGGGCTTCAGGATTGTA	187
Add1	AK031960	62	F-TCCTTCCCTTTTGGCTTTTT R-ACCCTCTTCCCGAGTAAGGA	192
S3fb	AK017529	62	F-TCCGTTTGTTTTGGTGTTGA R-TACAAGGCTGTCACGGATGA	236
Chuk	NM_007700	61	F-TGGAGCCTACGAAGCTGTTT R-CCCTCATTAGTTGCGGTGTT	234
Gpi	AK051363	56	F-ATGAACAGGCCTTCAGCATT R-AAAGCCTTGCTCCCTACACA	215
Atp6	AF093677	55	F-CCTTCCACAAGGAACTCCAA R-GGTAGCTGTTGGTGGGCTAA	187
Pp2cb	NM_017374	53	F-CTATCCAGAGCGCATCACAA R-TCCAGGGCTCTTATGTGGTC	234
Frg1	NM_013522	60	F-GGGAGCTCCACACAGAGAAG R-GCCATCTTCCCATCTTGAAA	204
Nasp	NM_016777	60	F-TGGCTGTACTCCATGAGCAG R-TCATGGATACTGAGGCACCA	228
At2b	NM_007429	55	F-AGCAGCCGTCCTTTTGATAA R-TGCTGGACACCTTTTTAGGG	196
Ace	NM_207624	61	F-CAGTGTCTACCCCCAAGCAT R-TTCCATCAAAGACCCTCCAG	165
Agtr1a	NM_177322	57	F-GGAAACAGCTTGGTGGTGAT R-TGAGACACGTGAGCAGGAAC	235

Table 1.1 (continued)

Agt	NM_007428	57	F-CACCCCTGCTACAGTCCATT R-GTCTGTACTGACCCCCTCCA	221

Results

Gene expression profiles of the *Agtr2*[-/y] brain samples were compared to

profiles of the control brains for two developmental stages, E15 and at birth (P1).

The graphed log ratios by dye swap are presented in Figures 1.4 and 1.5.

Hierarchical clustering of each developmental set demonstrated that the *Agtr2*[-/y]

mouse brains had an overall different expression pattern than did those of controls,

as controls and *Agtr2*[-/y] samples clustered separately and are shown in Figure 1.6.
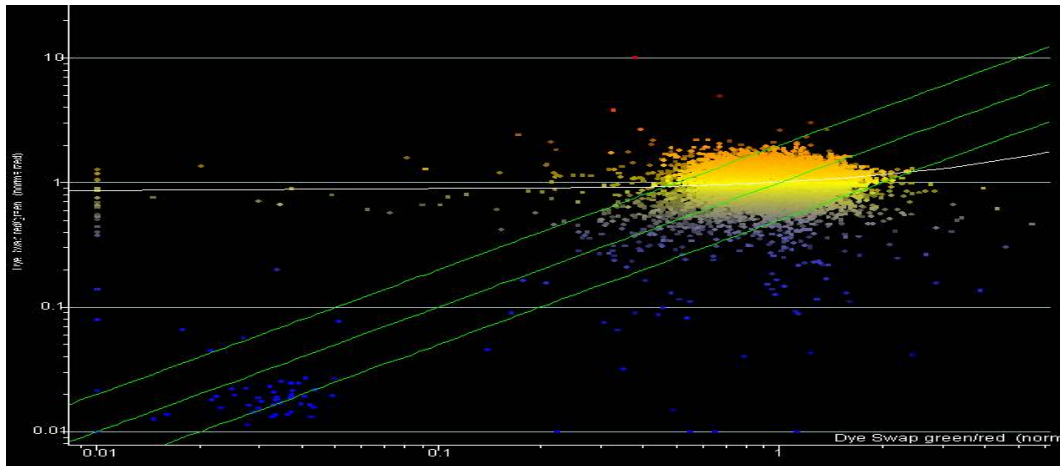
Figure 1.4 Log ratios of all embryo (E15) arrays by dye-swap. X axis = knockouts labeled blue, controls red; Y axis = knockouts labeled red, controls blue.
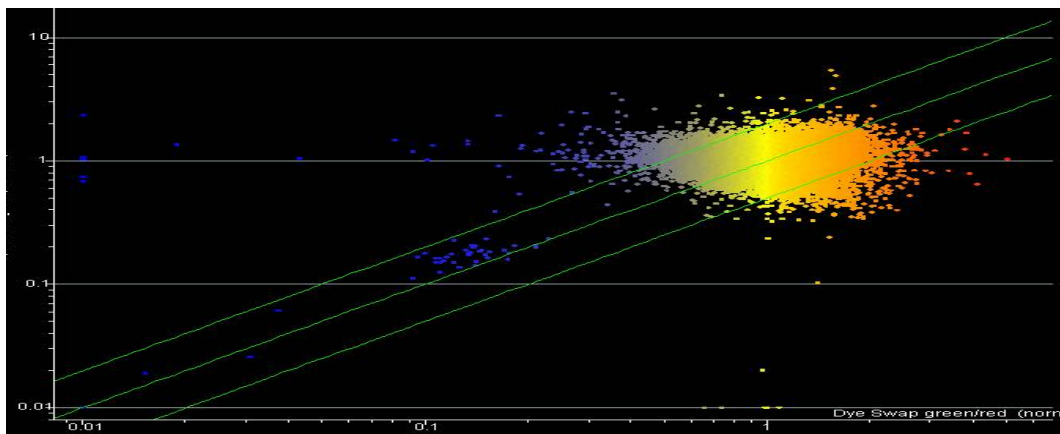
 Figure 1.5 Log ratios of all postnatal day one (P1) by dye-swap. X axis = knockouts labeled blue, controls labeled red; Y ax is = knockouts labeled red, controls blue.
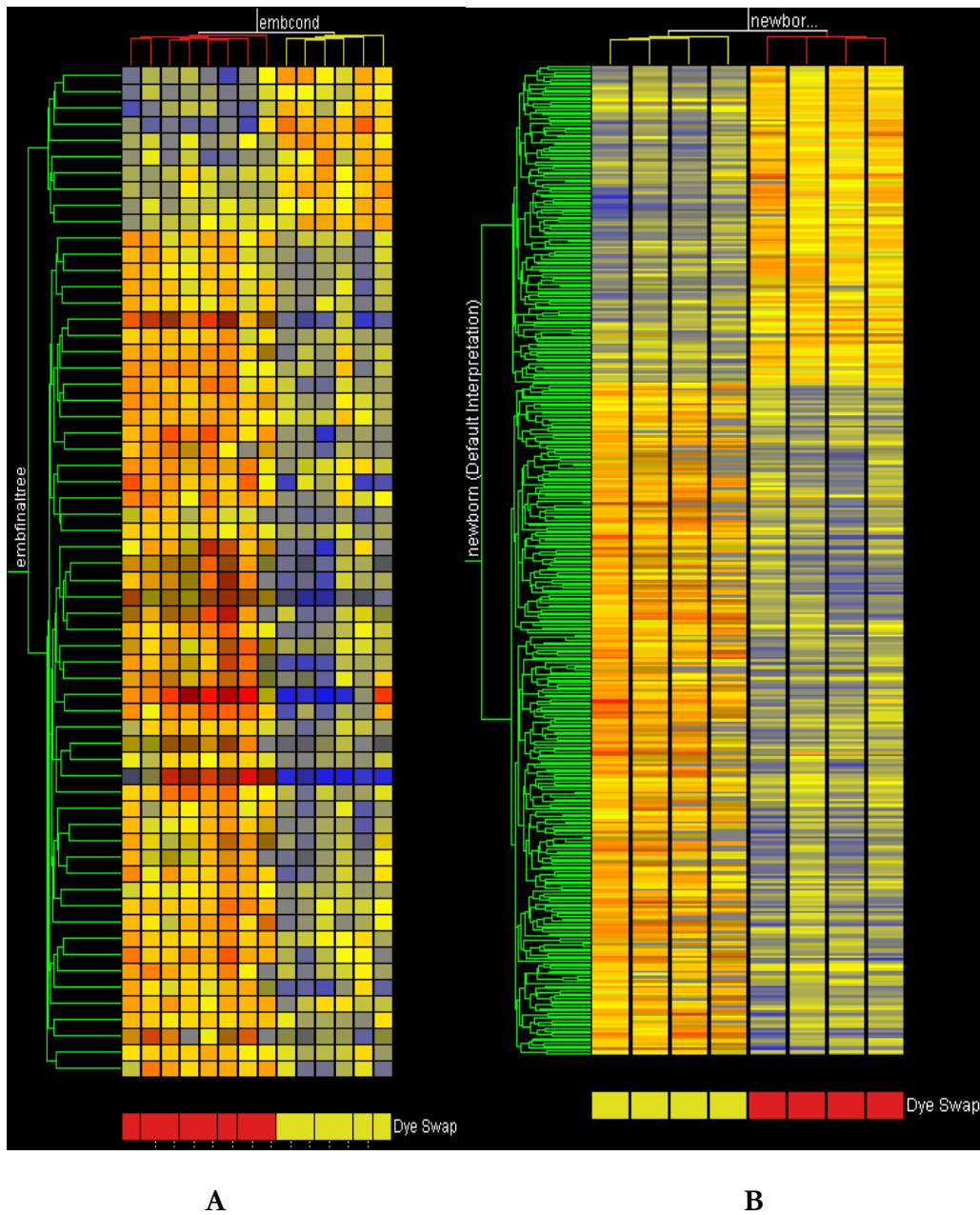
Figure 1.6 Hierarchal clustering showing knockout animals have different expression profiles as represented by the dye swap color coding below the tree. A) embryo (E15) arrays B) postnatal day one (P1) arrays.

Data analysis using GeneSpring GX© (FDR ≤ 0.3 and p ≤ 0.001) produced a

list of 133 genes (88 up-regulated, 45 down-regulated) differentially expressed at E15.

A similar analysis (FDR ≤ 0.3 and p≤ 0.005) in newborn brains identified a list of

397 differentially expressed genes (270 up-regulated, 127 down-regulated) in *Agtr2*^{-/y}

mouse brains. To further narrow the gene lists, genes that had a fold change greater

than or equal to 1.3 and a p-value less than 0.001 in the E15 were selected (Figure

1.3a). This resulted in a list of 62 genes (52 up-regulated and 10 down-regulated) for

the E15 brains (Table 1 .2 and Figure 1.7 and 1.8). In the P1 samples, a fold change

greater than or equal to 1.4 and p-value less than 0.005 was selected for a final list

(Figure 1.3b). This resulted in a list of 62 genes (50 up-regulated and 12 down-

regulated) in the neonates (Table 1.3 and Figure 1.9 and 1.10). Fold change was

computed with Bioconductor software with a log2 transformation. The final E15

and P1 lists had AK005333 (phosphatidyl decarboxylase) and AK084084 (Rab30) in

common. AK005003 was up-regulated 1.6 fold (p = 1.08E-04) in the E15 and 1.9

fold (p = 3.39E-04) in the P1, while AK084084 was up-regulated 1.5 fold (p =

6.86E-04) in the E15 brains and 1.7 (p = 1.22E-04) in the P1. The E15 list had two

genes listed twice with two separate probes: NM_177054 (Casc4) and NM_033563

(Klf7).
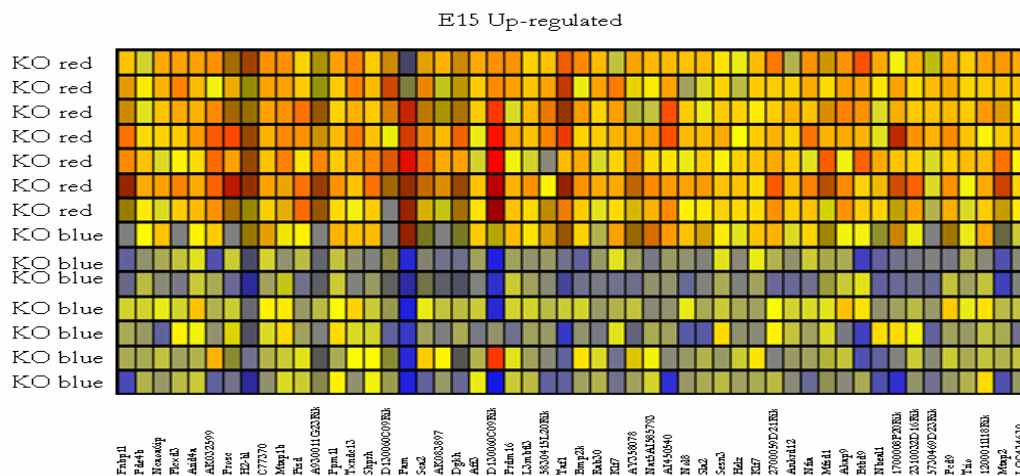
Figure 1.7 Tile view of final list of up-regulated genes in *Agtr2^{-/y}* E15 brains. Each row is an individual array KO red = arrays with *Agtr2^{-/y}* samples labeled red, KO blue = arrays with *Agtr2^{-/y}* samples labeled blue. Expression is represented as a gradient from red to blue, red being the highest expression and blue being the lowest. Each column represents an individual gene spot. Gene names are listed below each column.
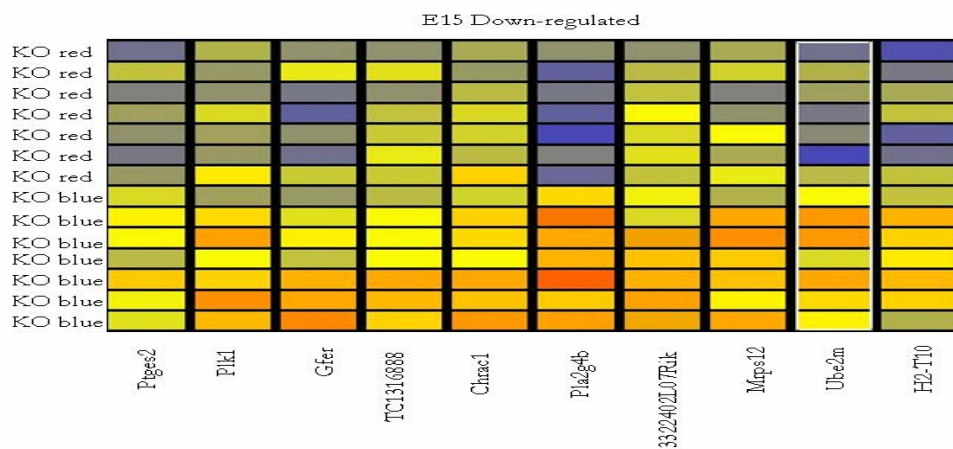
Figure 1.8 Tile view of final list of down-regulated genes in *Agtr2^{-/y}* E15 brains. Each row is an individual array KO red = arrays with *Agtr2^{-/y}* samples labeled red, KO blue = arrays with *Agtr2^{-/y}* samples labeled blue. Expression is represented as a gradient from red to blue, red being the highest expression and blue being the lowest. Each column represents an individual gene spot. Gene names are listed below each column.

Table 1.2
Genes at Day E15 Showing Fold Change ≥ 1.3 and p < .001 in *Agtr2*[-/y] Brains

Probe set	Genebank	Gene Symbol	Gene Name	P value	Fold Change
A_51_P514139	NM_027504	Prdm16	PR domain containing 16	1.97E-04	+3.1
A_52_P546610	NM_013626	Pam	peptidylglycine alpha-amidating monooxygenase	6.72E-05	+2.1
A_51_P337944	NM_080708	Bmp2k	BMP2 inducible kinase	7.96E-07	+1.9
A_52_P561377	NM_145505	AI450540	expressed sequence AI450540	1.88E-05	+1.9
A_52_P542860	NM_172618	Btbd9	BTB (POZ) domain containing 9	1.61E-03	+1.8
A_52_P135424	AK032599			1.45E-03	+1.6
A_52_P654624	AK005333;	Pisd	phosphatidyl decarboxlyase	1.08E-04	+1.6
A_52_P342836	BC055351	AY358078		2.83E-03	+1.6
A_52_P150396	AK013803;	male hippocampus	RIKEN cDNA 2700059D21 gene	9.00E-05	+1.6
A_52_P54666	AK086484;	Mtap2	microtubule associated protein2	4.68E-04	+1.6
A_52_P188425	BC047992;	Prosc	proline synthetase co-transcribed	5.66E-04	+1.5
A_51_P247114	NM_008199	H2-BL	histocompatibility 2, blastocyst	8.23E-06	+1.5
A_52_P617386	AK084084	Rab 30		6.86E-04	+1.5
A_51_P393161	AK049497	Zfp291		1.33E-04	+1.5
A_51_P496779	NM_194462	Akap9	A kinase (PRKA) anchor protein (yotiao) 9	1.40E-04	+1.5
A_51_P446575	AK044903;	Fnbp1l	Formin binding protein 1-like	2.56E-04	+1.4
A_52_P207132	AK044972;	Plcxd3	phosphatidylinositol-specific phospholipase C, X domain containing 3	5.10E-04	+1.4
A_52_P462472	XM_205178	C77370	expressed sequence C77370	9.91E-05	+1.4
A_52_P110581	AK050558;	pancreas islet cells cDNA	RIKEN cDNA A930011G23 gene	1.13E-04	+1.4
A_51_P212515	NM_178726	Ppm1l	protein phosphatase 1 (formerly 2C)-like	1.55E-03	+1.4
A_51_P227866	AK030696	Txndc13	Thioredoxin domain containing 13	2.31E-04	+1.4
A_52_P503135	NM_177054	Casc4	RIKEN cDNA D130060C09 gene	1.47E-03	+1.4

Table 1.2 (continued)

A_52_P90101	AK036209;	Atxn2	spinocerebellar ataxia 2 homolog (human)	1.85E-03	+1.4
A_51_P172241	TC1312974			4.07E-05	+1.4
A_52_P660753	XM_194622	Taf1	TAF1 RNA poly II TATA box binding protein	8.54E-04	+1.4
A_52_P239424	AK086122	Klf7	Kruppel-like factor 7 (ubiquitous)	8.96E-04	+1.4
A_52_P424197	AK029131	AI585793		4.43E-04	+1.4
A_51_P366277	BC049166	Nol8		1.14E-03	+1.4
A_52_P16346	AK012005;	Sla2	SRC like adaptor 2	1.93E-04	+1.4
A_52_P268720	BC021818	Helz		2.30E-04	+1.4
A_51_P134801	XM_619483	Ankrd12	Ankyrin repeat domain 12	2.95E-04	+1.4
A_51_P308628	XM_619630	Nbeal	Neurobeachin like 1	1.07E-03	+1.4
A_51_P128075	NM_027028	Ca binding riken gene	RIKEN cDNA 1700008P20 gene	1.16E-03	+1.4
A_52_P407755	AK009137;	Prei4	Preimplantation protein 4	1.14E-03	+1.4
A_51_P512340	NM_019840	Pde4b	phosphodiesterase 4B, cAMP specific	1.35E-04	+1.3
A_51_P364894	NM_054089	Ncoa6ip	nuclear receptor coactivator 6 interacting protein	2.90E-03	+1.3
A_52_P462171	XM_354675	Arid4a	AT rich interactive domain 4A (Rbp1 like)	6.96E-04	+1.3
A_51_P217878	AK043468;	Mtap1b	microtubule associated protein 1B	3.78E-04	+1.3
A_52_P167166	AK047842;	Shprh		4.26E-04	+1.3
A_52_P540045	AK083897;	Dgkh	Diacylglycerol kinase, ETA	1.39E-03	+1.3
A_52_P289071	NM_177054	Casc4	cancer susceptibility candidate 4	5.10E-04	+1.3
A_51_P115940	NM_172787	L3mbtl3	l(3)mbt-like 3 (Drosophila)	3.44E-04	+1.3
A_52_P5549	NM_026583	discontinued record	RIKEN cDNA 5830415L20 gene	1.11E-04	+1.3
A_52_P38317	AK046153;	Nat5	N-acetyltransferase 5 (ARD1 homolog, S. cerevisiae)	1.36E-03	+1.3
A_51_P127215	BC003348;	Sesn3	sestrin 3	3.77E-03	+1.3
A_51_P405280	NM_033563	Klf7	Kruppel-like factor 7 (ubiquitous)	5.19E-04	+1.3
A_52_P190807	AK032690			9.75E-04	+1.3

<u>Table 1.2</u> (continued)

A_52_P519538	NM_172712	Ube1l2	RIKEN cDNA 5730469D23 gene	1.11E-04	+1.3
A_52_P197199	XM_139187	Pcdh9	protocadherin 9	2.01E-04	+1.3
A_52_P521507	BC051169	Trio	Trio	5.54E-04	+1.3
A_52_P621817	AK173240	Zfp46		2.49E-04	+1.3
A_52_P651784	XM_486486	discontinued record	similar to S-adenosylmethionine decarboxylase	1.15E-04	+1.3
A_51_P349008	NM_133783	Ptges2	prostaglandin E synthase 2	3.86E-04	-1.3
A_51_P218805	NM_212443	Gfer	growth factor, erv1 (S. cerevisiae)-like (augmenter of liver regeneration)	9.44E-04	-1.3
A_52_P108808	TC1316888	TC1316888		5.85E-04	-1.3
A_52_P20639	NM_023727	hypoth. Protein	RIKEN cDNA 3322402L07 gene	2.41E-04	-1.3
A_51_P506937	NM_011885	Mrps12	mitochondrial ribosomal protein S12	5.48E-04	-1.3
A_51_P432538	NM_010395	H2-t10	histocompatibility 2, T region locus 10	5.17E-04	-1.3
A_51_P344566	NM_011121	Plk1	polo-like kinase 1 (Drosophila)	2.81E-05	-1.4
A_51_P272172	NM_053068	Chrac1	chromatin accessibility complex 1	3.74E-04	-1.4
A_51_P100246	NM_145578	Ube2m	ubiquitin-conjugating enzyme E2M	1.00E-03	-1.4
A_51_P288549	BC016255	Pla2g4b	phospholipase A2, group IVB (cytosolic)	1.54E-05	-1.7
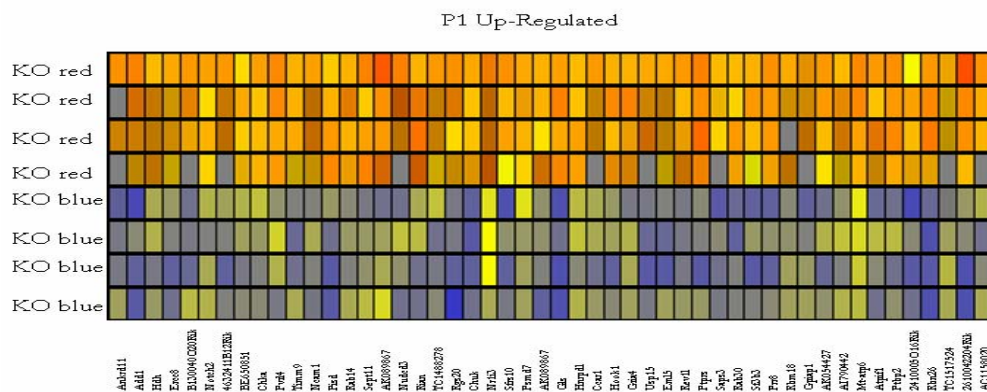
Figure 1.9 Tile view of final list of up-regulated genes in *Agtr2*^{-/y} P1 brains. Each row is an individual array KO red = arrays with *Agtr2*^{-/y} samples labeled red, KO blue = arrays with *Agtr2*^{-/y} samples labeled blue. Expression is represented as a gradient from red to blue, red being the highest expression and blue being the lowest. Each column represents an individual gene spot. Gene names are listed below each column.
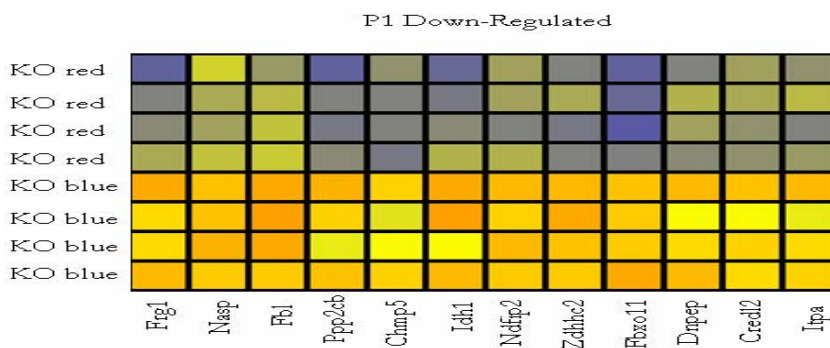
Figure 1.10   Tile view of final list of down-regulated genes in *Agtr2*^{-/y} P1 brains. Each row is an individual array KO red = arrays with *Agtr2*^{-/y} samples labeled red, KO blue = arrays with *Agtr2*^{-/y} samples labeled blue. Expression is represented as a gradient from red to blue, red being the highest expression and blue being the lowest. Each column represents an individual gene spot. Gene names are listed below each column.

Table 1.3
Genes at P1 Showing Fold Change ≥ 1.4 and p < .005 in *Agtr2^(-/y)* Brains

Probe Set	Genebank	Gene Symbol	Gene Name	P Value	Fold Change
A_51_P222953	AK047664	Gls		8.890E-06	+2.2
A_52_P329105	NM_134077	1700009P03Rik	RIKEN cDNA 1700009P03 gene	4.510E-03	+2.1
A_52_P386075	XM_622182			1.040E-03	+2.1
A_51_P304449	AK031960	Add1		1.270E-04	+2.0
A_51_P390755	AK035845	Ptprs	RIKEN cDNA 9630010G10 gene	1.380E-04	+2.0
A_52_P654624	AK005333	Pisd	RIKEN cDNA 4933439C20 gene	3.390E-04	+1.9
A_52_P657817	AK030767	Mapk8	mitogen activated protein kinase 8	5.090E-04	+1.9
A_52_P368881	TC1323355			3.770E-04	+1.9
A_52_P102630	AB063319	Rian		4.280E-04	+1.8
A_52_P320822	NM_177199	Sfrs10	RIKEN cDNA 5730405G21 gene	7.950E-04	+1.8
A_52_P236097	AK017529	Sf3b3	splicing factor 3b, subunit 3	7.340E-04	+1.8
A_52_P92213	AK089867			8.570E-04	+1.7
A_52_P386468	NM_007700	Chuk	conserved helix-loop-helix ubiquitous kinase	2.200E-06	+1.7
A_52_P475033	AK088515			9.930E-04	+1.7
A_52_P617386	AK084084	Rab 30		1.220E-04	+1.7
A_52_P422088	AK084846	Ptbp2	PTBP2	5.190E-04	+1.7
A_52_P440027	AK014565	4632411B12Rik	RIKEN cDNA 4632411B12 gene	9.200E-04	+1.6
A_52_P24835	NM_027893	Pvrl4	poliovirus receptor-related 4	5.330E-04	+1.6
A_52_P484519	AK171368	Sept 11		8.820E-04	+1.6
A_52_P319752	AK046219	Nudcd3	NudC domain containing 3	4.860E-04	+1.6
A_52_P527329	AK089867			8.570E-04	+1.6
A_51_P183154	AK049897	Hook1		6.280E-04	+1.6
A_52_P955951	AK048907	Gria4		2.170E-04	+1.6
A_52_P340618	BC030361	Eml5	echinoderm microtubule associated protein like 5	7.360E-04	+1.6
A_52_P323215	NM_019570	Rev1l	REV1-like (S. cerevisiae)	3.080E-05	+1.6

Table 1.3 (continued)

A_52_P433	AK129392			5.040E-04	+1.6
A_52_P671465	AK051363	Gpiap1		2.720E-04	+1.6
A_51_P458230	AK054427			8.970E-04	+1.6
A_52_P276412	AK011886	Atpif1		6.450E-04	+1.6
A_52_P620432	AK019968	2410005O16Rik	RIKEN cDNA 2410005O16 gene	6.000E-04	+1.6
A_52_P398494	XM_902635	Ankrd11		7.040E-04	+1.5
A_52_P113585	AK084575	Hdh	HDH	1.000E-04	+1.5
A_52_P411015	NM_177300	B130040O20Rik	RIKEN cDNA B130040O20 gene	6.150E-04	+1.5
A_52_P61903	AK014174	Chka	choline kinase alpha	4.240E-04	+1.5
A_52_P182520	BC028435	Timm9		3.110E-04	+1.5
A_52_P668157	AK011905	Ncam1		8.800E-05	+1.5
A_52_P124105	AK083451	Rab14	RAB14, member RAS oncogene family	1.110E-04	+1.5
A_52_P98160	TC268598			5.940E-04	+1.5
A_52_P188026	BC051052	Ccar1	CCAR	3.710E-04	+1.5
A_52_P59544	AK036220	Rbm18		3.110E-04	+1.5
A_52_P72938	AK039096	AI790442	expressed sequence AI790442	8.760E-04	+1.5
A_52_P321318	AF093677	mt-Atp6	ATP synthase 6, mitochondrial	3.140E-04	+1.5
A_52_P236607	BC066170	Ercc8	excision repaiross-complementing rodent repair deficiency, complementation group 8	3.100E-04	+1.4
A_52_P289213	BC059256	Notch2	Notch2	8.250E-04	+1.4
A_52_P454703	BE650851			3.580E-04	+1.4
A_51_P358256	NM_009803	Nr1i3	nuclear receptor subfamily 1, group I, member 3	6.810E-04	+1.4
A_52_P171993	AK012463	Psmd7	proteasome (prosome, macropain) 26S subunit, non-ATPase, 7	7.320E-04	+1.4
A_52_P146848	NM_016690	Hnrpdl	heterogeneous nuclear ribonucleoprotein D-like	2.740E-04	+1.4

Table 1.3 (continued)

A_52_P237755	TC1517524			8.580E-04	+1.4
A_52_P860487	ac1158020			6.740E-04	+1.4
A_51_P122246	NM_029720	Creld2	RIKEN cDNA 5730592L21 gene	3.360E-04	-1.4
A_51_P281255	NM_016777	Nasp	nuclear autoantigenic sperm protein (histone-binding)	1.840E-04	-1.4
A_52_P576863	NM_025922	Itpa	inosine triphosphatase (nucleoside triphosphate pyrophosphatase)	8.830E-04	-1.4
A_51_P259001	NM_029814	Chmp5	RIKEN cDNA 2210412K09 gene	3.150E-04	-1.4
A_52_P476357	NM_016878	Dnpep	aspartyl aminopeptidase	8.290E-04	-1.4
A_52_P141786	NM_029561	Ndfip2	Nedd4 family interacting protein 2	3.940E-04	-1.4
A_51_P349142	NM_007991	Fbl	fibrillarin	1.640E-04	-1.4
A_51_P479802	XM_110248	Fbxo11	F-box protein 11	2.630E-05	-1.4
A_51_P125535	NM_017374	Ppp2cb	protein phosphatase 2a, catalytic subunit, beta isoform	5.120E-04	-1.6
A_51_P132978	NM_010497	Idh1	isocitrate dehydrogenase 1 (NADP+), soluble	7.520E-04	-1.6
A_51_P117226	AK046533			1.020E-04	-1.6
A_51_P267544	NM_013522	Frg1	FSHD region gene 1	6.180E-04	-1.6

Randomly selected genes from each list (Table 1.1) were validated by

quantitative RT-PCR. In the majority of cases the fold change levels found by RT-

PCR correlated well with the expression profile array data (Tables 1.4 and 1.5).

Table 1.4
RT-PCR Results of Selected Genes at E15

Probe ID	Primary Accession	Gene Name	FC	RT-PCR FC
a_51_P514139	NM_027504	Prdm16	3.1	1.3
a_51_P337944	NM_080708	Bmp2 inducible kinase	1.9	1.4
a_52_P654624	AK005333	Pisd	1.6	2.3
a_52_P150396	AK013803	RIKEN CDNA 2700059D21 GENE	1.6	no change
a_52_P188425	BC047992	proline synthestase	1.5	1.1
a_52_P462472	XM_205178	expressed seq. C77370	1.4	no change
a_52_P110581	AK050558	RIKEN CDNA A930011G23 GENE	1.4	no change
a_51_P396325	NM_013681	synapsin 2	1.3	1.3
A_52_P54666	AK086484	Mtap2	1.6	1.3
a_52_P503135 a_52_P289071	NM_177054	Casc4	1.4	1.2
a_52_P407755	AK009137	Prei4	1.4	1.7
a_51_P100246	NM_145578	Ube2m	-1.4	-1.2
a_51_P488673 a_52_P404108	NM_008143	Gnb2L1	-1.3 -1.2	-1.5
a_51_P473533	L32836	Ahcy	-1.2	-1.7

Table 1.5
RT-PCR Results of Selected Genes at Postnatal Day 1

Primary Accession	Gene Name	Probe ID	FC	RT-PCR FC
AK047664	Glutaminase	a_51_P222953	2.2	1.4
NM_134077	Rbm26	a_52_P329105	2.1	1.3
AK031960	Adducin 1 (alpha)	a_51_P304449	2	1.7
AK005333	Pisd	a_52_P654624	1.9	1.7
AK017529	splicing factor 3b	a_52_P236097	1.8	1.4
NM_007700	Conserved helix loop helix	a_52_P386468	1.7	1.4
AK051363	Gpi-anchored membrane protein 1	a_52_P671465	1.6	1.7
AF093677	ATP synthase 6	a_52_P321317	1.5	no change

Table 1.5 (continued)

NM_008143	Gnb2L1	a_51_P488673 a_52_P404108	1.0 -1.0	No change
NM_017374	Protein phosphastase2cb	a_51_P125535	-1.6	-1.4
NM_013522	Frg1	a_51_P267544	-1.6	-1.7
NM_016777	Nasp	a_51_P281255	-1.4	-1.3

The expression of genes involved in the renin-angiotensin pathway was also
examined by RT-PCR and microarray values. No significant differences were found
for these genes at either time point on the arrays (Table 1.6).

Table 1.6
Comparison of E15 and P1 Values of Renin-Angiotensin System Genes

Gene	spotnumber	E15 RT-p-value	E15 Array pvalue	E15 Array fold chg	P1 RT P-value	P1 array pvalue	P1 Array foldchange
Agtr2	A51P437978	.1	0.92	0.9	.04	0.741	1.23
Agtr1	A51P236439	.84	0.92	0.97	.32	0.85	0.94
	A52P645862		0.79	1.08		0.99	0.98
Agtr1b	A52P53617		0.86	1.03		0.98	0.98
Ace	A52P72297	.65	0.88	1.03	.16	0.91	0.95
	A51P310523		0.93	1.06		0.95	1.07
	A52P68028		0.84	0.95		0.94	0.94
Agtrl1	A52P97572		0.71	0.89	.32	0.99	1.01
	A51P299055		0.98	1		0.92	1.04
Agtrap	A52P330667		0.73	0.94		0.96	1.03
	A51P271208		0.76	1.06		0.81	1.08
	A52P552550		0.95	0.98		0.92	0.97
	A52P480709		0.98	1.01		0.81	1.11
Ace2	A51P257496		0.93	1.02		0.936	0.97
Ren1	A52P652885		0.84	1.04		0.96	0.96

(continued)

	A52P544060		0.86	0.96		0.95	0.96
	A51P316661		0.57	1.2		0.98	1.02
Renbp	A51P123765		0.44	0.88		0.99994	1
Agt	A51P323712	.37	0.92	1.02	.51	0.988	1.06
	A51P436690		0.94	0.98		0.96	0.96

A list of 388 genes was also produced that were found NOT to be expressed at either time point (data not shown). Data analysis also revealed that there were 694 genes with no expression in the embryos and 862 genes not expressed in the P1 (data not shown). These genes were involved in a variety of physiological processes and/or cDNAs from adult tissues.

To create a list of genes that were significantly differentially expressed at both developmental stages and to investigate which genes expression was affected by developmental stage, a two way ANOVA analysis was performed. This analysis used developmental age and absence of Agtr2 as parameters and a Benjamini and Hochberg false discovery rate of 0.05. This created a list of 118 (87 up and 31 down) differentially regulated genes in all knockouts and 3 (2 up and 1 down in neonates) differentially regulated genes for developmental stage (table 1.8). The list of differentially regulated genes in all *Agtr2$^{-/y}$* mouse brains was compressed to 82 genes, by eliminating genes with less than a 1.3 fold change (Table 1.7). This list had 15 genes in common with the E15 t-test list and 16 genes in common with the P1 t-test list.

Table 1.7
Significantly differentially regulated genes in *Agtr2⁻/ʸ* ANOVA FDR=.05,
fold change ≥ 1.3

Probe	Genebank	Gene symbol	Common Name	FC
A_52_P386075	AK004071			+1.9
A_52_P654624	AK005333;	4933439C20 Rik	RIKEN cDNA 4933439C20 gene	+1.7
A_52_P561377	NM_145505	AI450540	expressed sequence AI450540	+1.7
A_52_P381009	AK009502;	Tia1	cytotoxic granule-associated RNA binding protein 1	+1.7
A_52_P82704	AK122557	Bcl11a	Mus musculus mRNA for mKIAA1809 protein	+1.7
A_52_P617386	AK084084	Rab 30		+1.6
A_52_P368881	TC1323355			+1.6
A_51_P222953	AK047664;			+1.6
A_52_P54666	AK086484;			+1.6
A_51_P337944	NM_080708	Bmp2k	BMP2 inducible kinase	+1.6
A_52_P564625	TC1362404			+1.6
A_52_P135424	AK032599			+1.6
A_51_P247114	NM_008199	H2-Bl	histocompatibility 2, blastocyst	+1.6
A_52_P150396	AK013803;	2700059D21 Rik	RIKEN cDNA 2700059D21 gene	+1.5
A_52_P236097	AK017529;	Sf3b3	splicing factor 3b, subunit 3	+1.5
A_51_P136820	NM_011179	Psap	Prosaposin	+1.5
A_52_P504460	AK013634;	Ccnt2	cyclin T2	+1.5
A_51_P154668	NM_001004146	MGC65558	similar to phosphatidylserine decarboxylase	+1.5
A_52_P372843	AK005295;			+1.5
A_52_P320822	NM_177199	5730405G21 Rik	RIKEN cDNA 5730405G21 gene	+1.5
A_52_P280448	TC1254974			+1.5
A_52_P342836	BC055351	AY358078		+1.5
A_51_P183154	AK049897	Hook1		+1.5
A_52_P422088	AK084846;	Ptbp2		+1.4
A_52_P4148	BC056964			+1.4
A_52_P167166	AK047842;			+1.4
A_52_P623457	NM_178922	Hic2	hypermethylated in cancer 2	+1.4
A_51_P172241	TC1312974			+1.4
A_52_P90101	AK036209;	Sca2	spinocerebellar ataxia 2 homolog (human)	+1.4
A_52_P360453	AK084271;	3110052M02 Rik	RIKEN cDNA 3110052M02 gene	+1.4

Table 1.7 (continued)

A_52_P102022	AK017641;	5730446C15 Rik	RIKEN cDNA 5730446C15 gene	+1.4
A_52_P369946	CB850089			+1.4
A_51_P461947	NM_177298	9030221M09 Rik	RIKEN cDNA 9030221M09 gene	+1.4
A_52_P407755	AK009137;	2310032D16 Rik	RIKEN cDNA 2310032D16 gene	+1.4
A_52_P499917	AK051838;	D930046L20 Rik	RIKEN cDNA D930046L20 gene	+1.4
A_52_P386468	NM_007700	Chuk	conserved helix-loop-helix ubiquitous kinase	+1.4
A_52_P481097	AK086528;	Lztfl1		+1.4
A_51_P458230	AK054427;			+1.4
A_52_P676492	AK032320	Brd8		+1.4
A_52_P432464	AK053863;	Luc7l2	LUC7-like 2 (S. cerevisiae)	+1.4
A_52_P1100217	AK051484;			+1.4
A_52_P337948	AK088459	Tnik		+1.3
A_52_P323215	NM_019570	Rev1l	REV1-like (S. cerevisiae)	+1.3
A_52_P6451	AK090341			+1.3
A_52_P374669	XM_359326	Jarid1a		+1.3
A_52_P190807	AK032690			+1.3
A_52_P276412	AK011886;	Atipif11		+1.3
A_52_P456702	AK045162;	B930046C15 Rik	RIKEN cDNA B930046C15 gene	+1.3
A_52_P376103	AK042630;			+1.3
A_52_P273674	BC019581;XM_619603	4930413O22 Rik	RIKEN cDNA 4930413O22 gene	+1.3
A_52_P5549	NM_026583	5830415L20 Rik	RIKEN cDNA 5830415L20 gene	+1.3
A_52_P61273	BC066768	Leng8		+1.3
A_52_P527329	AK089867;	9030025P20 RIK		+1.3
A_52_P577116	AK029399;	Pik3ca	phosphatidylinositol 3-kinase, catalytic, alpha polypeptide	+1.3
A_51_P476660	XM_139743	Mllt4	myeloid/lymphoid or mixed lineage-leukemia translocation to 4 homolog (Drosophila)	+1.3
A_52_P268720	AK122645	Helz		+1.3
A_52_P107681	AK028731;	Ylpm1	YLP motif containing 1	+1.3
A_51_P221008	AK028276;	3222401L13 Rik	RIKEN cDNA 3222401L13 gene	+1.3
A_51_P133037	NM_008889	Ppp1r14b	protein phosphatase 1, regulatory (inhibitor) subunit 14B	+1.3

Table 1.7 (continued)

A_52_P668157	AK011905;	NCAM1	Neural cell adhesion molecule1	+1.3
A_52_P342202	NM_027696	4933425I22R ik	RIKEN cDNA 4933425I22 gene	+1.3
A_52_P283055	TC1248463			+1.3
A_51_P261107	NM_139144	Ogt	O-linked N-acetylglucosamine (GlcNAc) transferase (UDP-N-acetylglucosamine:polypeptide-N-acetylglucosaminyl transferase)	+1.3
A_52_P620432	AK019968;	2410005O16 Rik	RIKEN cDNA 2410005O16 gene	+1.3
A_51_P192089	NM_028228	Pinx1	PIN2/TRF1-interacting protein	+1.3
A_52_P507277	NM_025789	Rshl2	radial spokehead-like 2	-1.3
A_51_P486479	NM_024456	Rab5c	RAB5C, member RAS oncogene family	-1.3
A_51_P267544	NM_013522	Frg1	FSHD region gene 1	-1.3
A_51_P110576	NM_011175	Lgmn	legumain	-1.3
A_51_P261689	AK003078;	UBE2S		-1.3
A_52_P476357	NM_016878	Dnpep	aspartyl aminopeptidase	-1.3
A_51_P439824	NM_018771	Rgs19ip1	regulator of G-protein signaling 19 interacting protein 1	-1.3
A_52_P461292	NM_008753	Oaz1	ornithine decarboxylase antizyme	-1.3
A_51_P261351	NM_026246	Mrpl49	mitochondrial ribosomal protein L49	-1.3
A_52_P614336	NM_011116	Pld3	phospholipase D3	-1.3
A_51_P140141	AK013263;	1500019G21 Rik	RIKEN cDNA 1500019G21 gene	-1.3
A_51_P375227	NM_009954	Bcar1	breast cancer anti-estrogen resistance 1	-1.3
A_52_P362128	BC025640;X M_130932	Pygo2	pygopus 2	-1.3
A_52_P187787	NM_023231	Stoml2	stomatin (Epb7.2)-like 2	-1.3
A_51_P435333	NM_027151	Dctn2	dynactin 2	-1.4
A_52_P585104	NM_010219	Fkbp4	FK506 binding protein 4	-1.4

Table 1.8

Significantly differentially expressed genes by developmental stage ANOVA FDR .05

Probe Set	P Value	Gene Name	Gene Symbol	Genebank	Expression with age
A_51_P431397	0.0199	Nucleoporin 214	Nup214	AK040284	Down
A_52_P98630	0.0195	interleukin 3	Il3	NM_010556	Up
A_51_P314161	0.0195	queuine tRNA-ribosyltransferase 1	Qtrt1	NM_021888	Up

Discussion

Angiotensin II binds to two receptors, AGTR1 and AGTR2. In the absence of AGRT2, it would be expected that all angiotensin II would be bound to AGTR1. Without the regulating effect of AGTR2, the AGTR1 signaling cascades should be unchecked. The absence of AGTR2 did not cause a detectable increased expression of AGTR1 in the brains of E15 or P1 *Agtr2$^{-/y}$* mice. There was also no difference in expression of genes in the RAS between knockouts and controls. Our results show that genes downstream of AGTR1 are up-regulated in the absence of AGTR2.

Our results also suggest that AGTR2 may have different effects on the developing brain at different developmental stages as only two genes, Pisd and Rab 30 were found to be in common between the two developmental stages in the final lists of significantly differentially expressed genes.

The largest gene categories represented as over-expressed in E15 Agtr2$^{-/y}$ brains are transcription factors and genes in the AGTR1 pathway (Table 1.9). Other categories of genes are transferases, kinases, genes involved in microtubule and actin processing, cell adhesion, protein transport and/or binding, nucleic acid binding,

immunity, cell cycle arrest, ubiquitin/proteasome function and a protein

phosphatase. Two genes, Akap9 and Mtap2 are involved in the up-regulation of

NMDA receptors (Lin et al. 1998).

In the E15 *Agtr2$^{-/y}$* brains, genes predominantly involved in apoptosis were

found to be down-regulated. This is consistent with previous findings that AGTR2

is a mediator of apoptosis (Yamada et al. 1996). A summary of functions for

dysregulated genes in the E15 knockouts is presented in Table 1.9 and Table 1.10.

Table 1.9
Up-regulated Gene Categories of E15 *Agtr2$^{-/y}$* Brains

Agtr1-related Functions	Transferases	Transcription Factors	
Pisd	Ncoa6Ip	Prdm16	L3mbtl3
Pde4B	Dgkh	Zfp291	Zfp46
Plcxd3	Nat5	C77370	
Prei4	Trio	Aff3	
Dgkh		Taf1	
Sla2		Klf7	
Ca^{2+} binding Riken		Arid4a	
Kinases	**Microtubules/Actin**	**Protein Transport/Binding**	
Bmp2k	Mtap2 Fnbpi1	Pam	Nbeal1
Akap9	Mtap1B	Rab30	Ncoa6Ip
	Akap9	Atxn2	Shprh
Cell Adhesion	**Nucleic Acid Binding**	**Immunity**	
Btbd9	Nol8	H2-Bl	
Pcdh9	Helz	Sla2	
Sla2	Trio		
Cell Cycle Arrest	**Ubiquitin/Proteasome**	**Protein Phosphatase**	
Sesn3	Ube1l2	Ppm1l	

Table 1.10
Down-regulated Gene Categories of E15 *Agtr2$^{-/y}$* Brain**s**

Agtr2-related Functions	Cell Cycle Arrest	Transferase
Ptges2	Plk1	Plk1
Pla2g4b		Chrac1
Ube2m		
Cell Proliferation	**Translation**	**Immunity**
Gfer	Mrps12	H2-t10

Up-regulated genes in the P1 *Agtr2$^{-/y}$* brains were over-represented by genes involved in protein binding and transport (Ercc8, Notch2, Hdh, Timm9, Rev1l, Rab14, Rab30, Sept11 and Hook1). Also up- regulated were genes involved in RNA processing, (Rbm26, Rbm18, Sfrs10, Rian, Sf3b3, Hnrpd1), DNA binding, (Ankrd 11, Rab14, Ccar1), transcription (Prr8, Ercc8, Nr1i3) and glutamate metabolism (Gls and Gria4). Several genes involved in cell adhesion (Ptprs, Pvr14, Ncam1 and Nrli3) as well as cytoskeleton and microtubule expression (Add1, Hook1 and Eml5) were also represented. A complete summary of the categories is found in Table 1.11.

Examination of the P1 results show that some of the genes involved histone modification (Nasp and Ppp2cb), nucleotide metabolism (Itpa), NADP+ activity (Idh1), protein ubiquination (Fbox11 and Ndfip2) rRNA processing (Frg1), chromatin remodeling (CHMP5) and calcium ion binding (Creld1). The list is summarized in Table 1.12.

Table 1.11
Functions of Up-regulated Genes of P1 *Agtr2^{-/y}* Brains

Agtr1 Pathway	Protein Binding/Transport		RNA Processing
Mapk8	Ercc8	Rab30	Rbm26
Pisd	Notch2	Rab14	Rbm18
Chka	Hdh	Sept11	Sfrs10
	Timm9	Hook1	Rian
	Rev1L		Sf3b3
			Hnrpdl
Cell Adhesion	**Cytoskeleton/Microtubules**		**DNA Binding**
Ptprs	Add1		Ankrd 11
Pvr14	Hook1		Rab14
Ncam1	Eml5		Ccar1
Nrli3			
Transcription	**Cell Cycle Control**		**Kinases**
Prr8	Nudcd3	Atpif1	Mapk8
Ercc8	Gpiap1		Chuk
Nr1i3	Ccar1		
Anti-apoptosis	**Perception of Sound**		**Ubiquitin/Proteasome**
Hdh	Timm9		Usp15
Notch2	Ercc8		Psmd7
Glutamate Metabolism	**Protein Phosphatase**		
Gls	Ptprs		
Gria4			

Table 1.12
Functions of Down-regulated Genes of *Agtr2^{-/y}* P1 Brains

Chromatin Remodeling	Histone Binding	Nucleotide Metabolism
Chmp5	Nasp	Itpa
	Ppp2cb	
Lysosome Organization	**Proteolysis**	**Protein Ubiquination**
Chmp5	Dnpep	Fbxo11
		Ndfip2
Protein Modification	**rRNA Processing**	**Ca²⁺ Binding**
Zdhhc2	Fbl	Creld2
NADP+ Activity		
Idh1		

Pathway Studio (Ariadne, Rockville, MD USA) was used to visualize common functions for the genes down-regulated in the E15 *Agtr2*^{-/y} brains. Three genes down-regulated in E15 *Agtr2*^{-/y} brains Ptges2, H2-T10 (HLA-F) and Ube2m, are all involved in inducing apoptosis (Figure 1.11), consistent with previous findings that AGTR2 induces apoptosis. Plk1 has been shown to cause cell proliferation and inhibit apoptosis (Reagan-Shaw and Ahmad 2005; Jang et al. 2006). Pla2g4b is a phospholipase and phospholipases are in the AGTR2 signaling pathway.
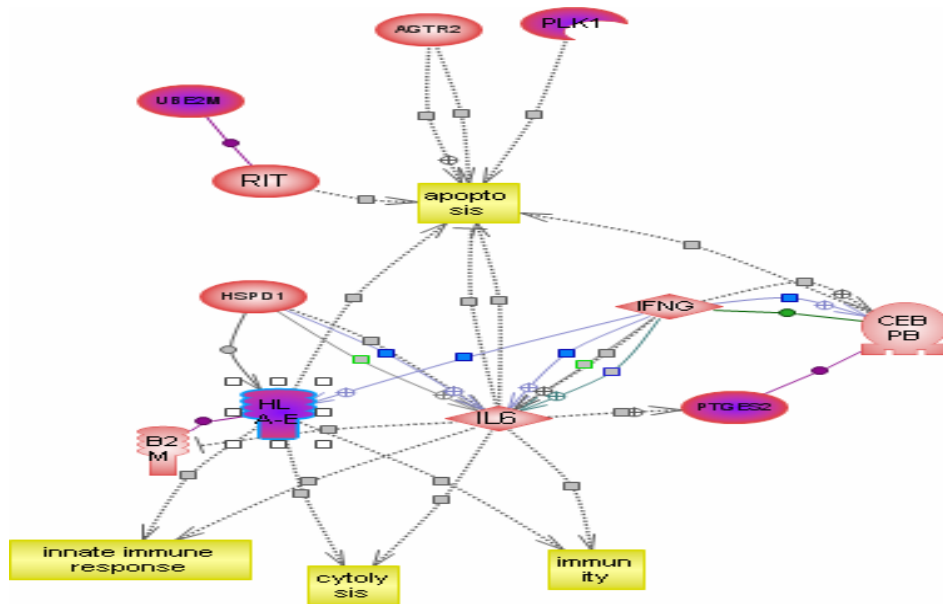
Figure 1.11 E15 down-regulated genes involved in apoptosis. Yellow squares = cell functions, pink shapes = proteins, purple gradient = E15 list.

Examining the genes up-regulated in the *Agtr2*^{-/y} E15 brains with 1.5 fold or greater expression reveals a complex picture. AGTR2 has previously been shown to

down-regulate MAP1B but up-regulate MAP2 in PC12W cells (Stroth et al. 1998). In

this study Mtap2 and Mtap1b are both up-regulated in the E15 *Agtr2⁻/ʸ* brains.

MAP2 (Mtap2) has previously been shown to be phosphorylated by JNK and

subsequently defines dendritic shape in the brain (Bjorkblom et al. 2005) Map2 is

found in the dendrites and is crucial for microtubule stability (Stroth et al. 1998).

Map1b is found in growth cones and is needed for neurite outgrowth (Stroth et al.

1998).   It remains to be seen if these two genes (Mtap2 and Map1b) play a role in

the defective dendritic spine morphology noted in *Agtr2⁻/ʸ* mice (Maul, unpublished

data).   These genes also regulate actin along with two genes C1orf39 (also known as

Fnbp1l) (Ho et al. 2004) and Sla2 (Sun et al. 2005) which are also up-regulated in

E15 *Agtr2⁻/ʸ* brain. Several other up-regulated genes, Akap9, Fnbp1l, as well as

Mtap2 and Map 1B are associated with microtubule function (Figure 1.12).
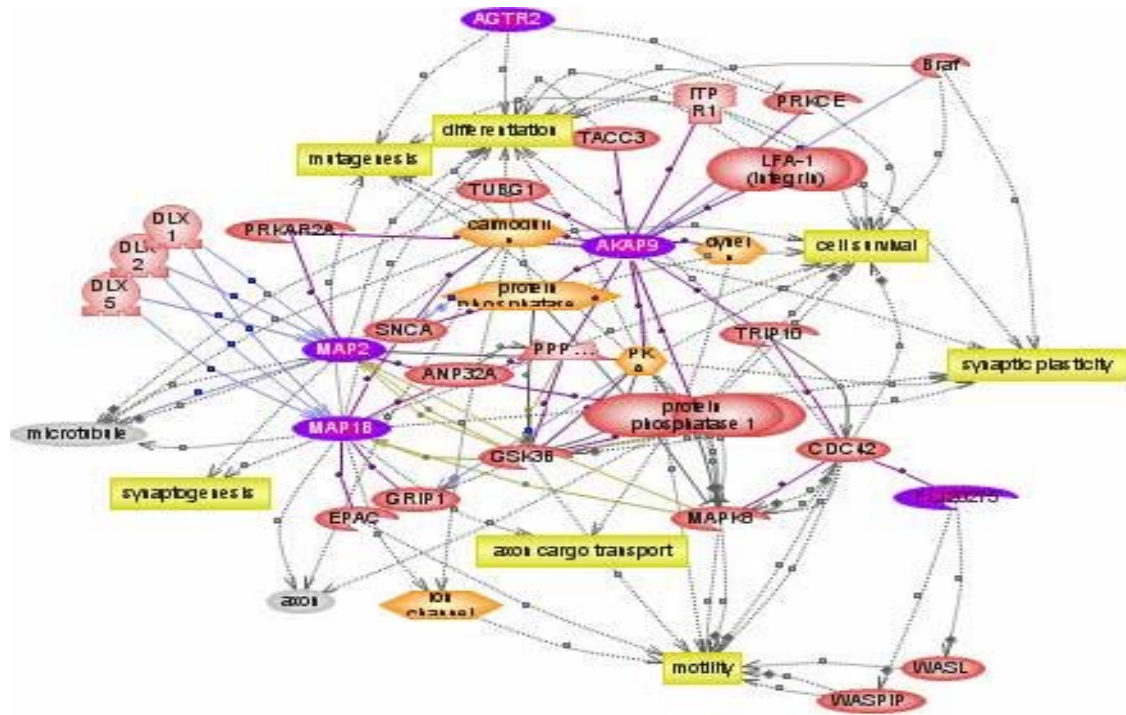
Figure 1.12 Genes up-regulated in *Agtr2*^{-/y} brains affecting microtubule expression as well as other cell functions vital to brain development and function. Genes highlighted in purple are from the E15 list. (FLJ20274 = Fbl)   Yellow squares = cell function, orange hexagons = functional class, pink ovals = proteins, gray ovals = cell part

Peptidylglycine alpha-amidating monooxygenase (Pam), was found to be more than two-fold up-regulated in the E15 knockouts (Table 1.2). This gene contains two catalytic domains that work sequentially to catalyze neuroendocrine peptides and is needed for signal transduction and receptor recognition (Driscoll et al. 2006).

Prdm16, PR domain containing 16, (also known as Mel 1) shared the highest level of expression in the E15 knockouts. This gene codes for a transcription factor containing several zinc finger domains and is associated with myelodysplastic syndrome and acute myloid leukemia(Nishikata et al. 2003; Xinh et al. 2003). Several zinc fingers and helicases are up-regulated in the E15 knockouts: Zfp291, Zfp46, Helz and Shprh.

Genes involved in regulation of microtubules are also well represented in the over-expressed genes of the P1 knockouts. Add1, Eml5, Hdh, Hook1, Nudcd3 and Sept11 all affect microtubules.

Notch2 and Hdh are up-regulated in P1 knockouts and both have anti-apoptotic effects (Rigamonti et al. 2000; Duechler et al. 2005; Leavitt et al. 2006). Hdh up-regulates brain derived neurotrophic factor (BDNF) (Zuccato et al. 2003) and associates with the EGF pathway potentially causing overgrowth of neuronal cells. Notch2 is also negatively associated with glial differentiation (Tanaka et al. 1999).

In the P1 knockouts several overexpressed genes, Hdh, Gria4, and Gls, were found to be involved in glutamate metabolism. Glutamate metabolism is integral to NMDA receptors which are essential in neuronal development and synaptic plasticity.

Down-regulated in the P1 brains are Fbox11 and Ndfip2, which are involved in the ubiquitin-proteasome system which contributes to cellular differentiation (Li et

al. 2007). Also down-regulated in the P1s are Nasp and Snf7 which are involved in histone modification. Cells preparing to undergo apoptosis often have histone modification (Janigro 2006). Several other genes involved in Agtr2 functions, such as two phosphataseses, Itpa and Pp2cb are also down-regulated in the P1 brains. Idh1 and Ndfip2 are genes involved in the NF-Kappa pathway in apoptosis. Fbl and Frg1 are involved in RNA processing, and are also nucleolar proteins.

Mapk8, map kinase 8, (also known as JNK1) is part of the AGTR1 signaling cascade and is one of the most significantly up-regulated genes in the P1 knockout brains. It has been shown to be a regulator of morphogenesis in early nervous system development (Tararuk et al. 2006). JNK1 (Mapk8) phosphorylates the microtubule depolymerizing factor SCG10 which determines microtubule stability and axodendritic length (Tararuk et al. 2006).

The up-regulation of Chuk (also known as IKK1) is significant in that it is also influenced by angiotensin II (Wu et al. 2006), and activates the NF-kappa-B complex, which in turn causes cell proliferation and anti-apoptotic effects (Luo et al. 2005). (Figure 1.13).
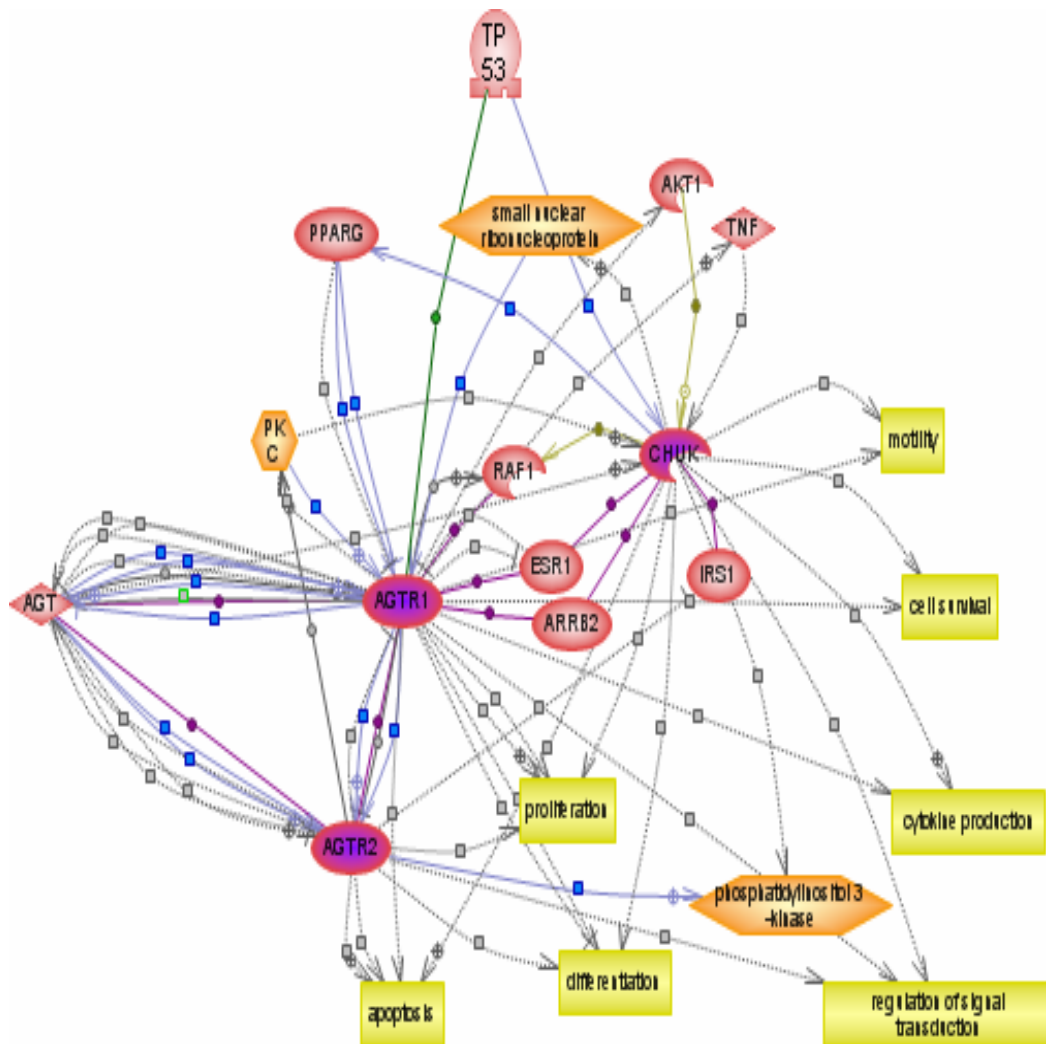
Figure 1.13   Interaction and common targets of Chuk, Agtr1 and Agtr2.   Note that Chuk, Agtr2 and Agtr1 up-regulate cell proliferation, but also are involved in apoptosis. Purple shapes = genes from P1 list, pink shapes = proteins, orange hexagons = functional classes, yellow squares = cellular functions.

Other important up-regulated genes in the P1 list are cell adhesion genes. Ncam1, neural cell adhesion molecule 1, has been associated with NMDA receptors (Sytnyk et al. 2006) and the inhibition of cell death (Bussolati et al. 2006). Pvrl4 is also a cell to cell adhesion gene (Reymond et al. 2001). Ncam1, Gria4, Nr1i3 and Mapk8 all share several important neurological functions (Figure 1.14).
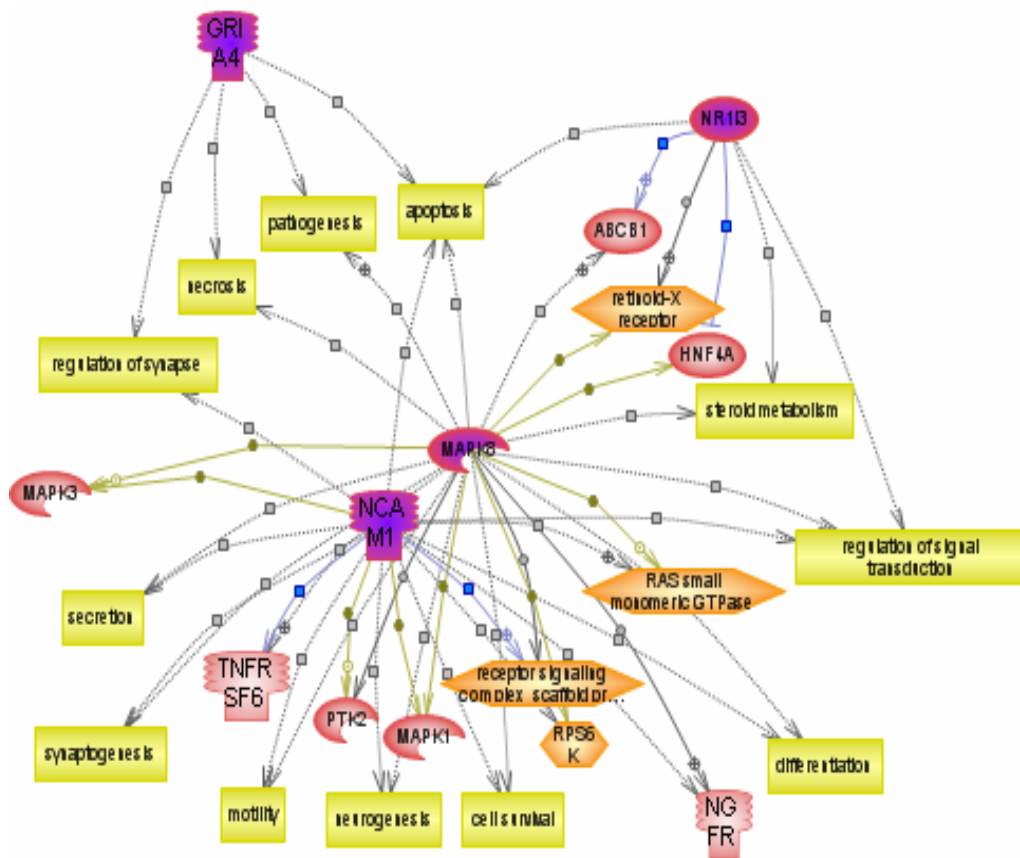
Figure 1.14 Genes with common neurological functions that are up-regulated in P1 knockouts. Purple shapes = genes from P1 list, pink shapes = proteins, orange hexagons = functional classes, yellow squares = cellular functions

It is important to note that this study used total RNA isolated from whole brain for gene expression profiling. Previous in-situ hybridization work (Nuyt et al. 1999) has shown that *Agtr2* gene expression is varied in both expression level and location dependent upon developmental stage. In-situ hybridization of the dysregulated genes may further elucidate potential roles of these genes in the developing brain.

Our study shows that the absence of *Agtr2* gene expression in the developing brain causes an up-regulation in AGTR1 activities such as cell proliferation. A more novel finding for both developmental stages E15 and P1 is genes connecting with NMDA receptor function are increased in the *Agtr2^{-/y}* brain, and may possibly contribute to abnormal brain development. The up-regulation of genes involved in cell adhesion point to a contribution to abnormal synaptic connectivity. Our results support other studies that have shown abnormal dendritic spines in *Agtr2^{-/y}* mice might be caused by abnormal microtubule activity. We found genes that affect micro-tubules are up-regulated at both developmental stages in the *Agtr2^{-/y}* mouse brains. This study further adds to the hypothesis that AGTR2 contributes to the developing brain by influencing cell morphology and synaptic connectivity. Further analysis might reveal if some of the genes influenced by AGTR2 may also contribute to the pathophysiology of mental retardation.

IDENTIFICATION OF AGTR2 INTERACTING PROTEINS
IN FETAL BRAIN

Many genes can have different expression patterns and functions depending on the developmental state of the organism. Genes expressed in the brain during embryonic and fetal development can be different than those expressed in the adult brain. Understanding the interactions of different proteins in the developing brain is important to understanding the etiology of mental retardation (MR), which affects approximately 1-3% of the population (Chelly and Mandel 2001) and brain development.

The angiotensin II type receptor (AGTR2) is a seven transmembrane receptor consisting of 363 amino acids (Mukoyama et al. 1993). The AGTR2 gene is located on human chromosome Xq23 and consists of 3 exons (Gard 2002). It is expressed at high levels in fetal brain (Nuyt et al. 1999), but is predominately expressed in the cerebellum of the adult brain, though it is up-regulated in some cases of neurological disease (von Bohlen und Halbach and Albrecht 2006). Angiotensin II has been shown to affect not only physiological behaviors related to water intake, but also affecting cognition and emotional centers (Gard 2002).

Several mutations in AGTR2 have been characterized in humans. Specifically, a G21V mutation in the N-terminal, an A324G and I337V mutations in the C-terminal and a FSPhe[133] deletion and I53F mutation in the transmembrane domain have been described in individuals with MR(Vervoort et al. 2002; Ylisaukko-ojo T 2004). Also,

several proteins (Erb3, PLZF, ATIP, NHE6) have been found to interact with

AGTR2 through in-vivo and in-vitro studies (Knowle et al. 2000; Senbonmatsu et al.

2003; Nouet et al. 2004; Pulakat et al. 2005).

The amino terminal of AGTR2 has been shown to be necessary for the binding

of angiotensin II (Yee et al. 1998). The second intracellular loop of AGTR2 is

necessary for G-protein signaling (Moore et al. 2002). Studies using *Xenopus* oocytes

showed that the C-terminus of the 3rd intracellular loop of AGTR2 is necessary to

lower cGMP levels mediated by AGTR2 and that the C-terminal tail is necessary for

negative regulation of cGMP (Pulakat et al. 2005). Previous yeast two-hybrid

studies have found that the 3rd intracellular loop of AGTR2 interacts with v-erb-b2

erythroblastic leukemia viral oncogene homologue, (ERBB3) (Knowle et al. 2000),

and solute carrier family 9 Na/H exchanger isoform 6, (NHE6) (Pulakat et al. 2005).

The C-terminal domain has been found to interact with promyelocytic leukemia zinc

finger protein (PLZF) (Senbonmatsu et al. 2003) and AGTR2 interacting protein,

(ATIP) (Nouet et al. 2004).

In light of these findings, our goal is to identify proteins that interact with

AGTR2 in the developing brain and to further understand AGTR2 mediated

signaling in developing brain. Using a yeast two hybrid system, individual constructs

of either the amino or carboxy terminal of AGTR2 were made and screened against

a human fetal brain cDNA library. Here we describe the interaction between the

amino terminal of AGTR2 and three proteins: ASMTL, GNB2L1 and NGLY1.

Materials and Methods

Cloning vector and Yeast Strains: The *Saccharomyces cerevisiae* strain AH109 (Ade-,

Met+, Trp-, Leu-, His-) was used from the MATCHMAKER Gal4 2-Hybrid System

Three (Clontech). The plasmid pGBKT7 (Clontech) two-hybrid bait vector was

used to express a protein of interest in fusion with the GAL4 binding domain (BD)

and the interacting protein. It contains a kanamycin resistance gene for selection in

E. coli, and when transformed into yeast it is prototrophic for tryptophan. The

plasmid pACT2, a yeast two-hybrid prey vector (CLONTECH) was used to

construct translational fusions of the GAL4 activation domain (AD) and the protein

of interest. It contains an ampicillin resistance gene for selection in *E. coli*, and is

prototrophic for leucine when transformed into the AH109 strain.

 Construction of bait vectors: Primers were designed with an EcoRI adapter

sequence to make a PCR product of the first 45 amino acids of AGTR2 and a

separate primer set for the last 52 amino acids of AGTR2. The amplicon was ligated

into the PCR2.1 vector (Invitrogen). Positive clones were selected and cultured in

LB with 20ng/ml of ampicillin. Plasmid DNA from selected clones was isolated

with Qiagen Mini-prep kits according to manufacturer instructions (Qiagen*).*

Plasmids were sequenced using M13 primers, F- 5' CTGGCCGTCGTTTTAC 3'

and R- 5' GTCATAGCTGTTTCCTG 3' and DYEnamic Dye Terminator Cycle

sequencing Kit (GE Healthcare) using the automated MegaBACE 1000 DNA

Analysis system (GE Healthcare). Sequences were analyzed using the DNASTAR

program (Madison, WI). Plasmid DNA was digested with EcoRI (New England

Biolabs), electrophoresed and the desired insert was gel isolated and ligated into an

EcoRI digested pGBKT7 plasmid. Ligation was achieved using the Ligate-IT Rapid

Ligation Kit (USB) according to manufacturer instructions. Plasmid DNA was

isolated from positive clones. The DNA was sequenced to verify that they were in-

frame with the Gal4 binding domain of pGBKT7. The bait constructs containing

AGTR2 gene inserts were transformed using the LiCl method into yeast strain

AH109 (Clontech) according to manufacturer's instructions. After transformation,

yeast was plated on SD media without tryptophan which selects for the pGBKT7

plasmid. To verify that the desired proteins were being produced, proteins from

the transformed yeast of each construct were harvested and purified according to

manufacturer instructions (Clontech 1999). Proteins were electrophoresed on a

12% SDS-Page acrylamide gel, transferred to supported nitrocellulose and then

hybridized with the Gal4 binding domain antibody (Santa Cruz Biotechnology).

Each construct was also tested for auto-activation by transforming the plasmid DNA

into AH109 yeast with an empty activation domain vector, plating on SD media

lacking leucine, tryptophan, adenine and histidine and containing α-galactosidase (-

AHLT αgal) and verifying there was no positive interaction. A positive interaction is

defined as colonies that can grow on –AHLT αgal media and turn blue. Neither

construct grew on selective media when transformed with an empty activation

domain vector.

Amplification of fetal brain library: A human fetal brain library consisting of

cDNA from 4-5 fetuses of 20-25 weeks gestational age, was purchased from

CLONTECH. This library contains cDNA fragments of 400 to 4500 bp inserted

into the pACT2 plasmid with EcoRI and XhoI restriction sites in frame with the

GAL4 activation domain (AD). pACT2 has the selection marker –*leu* for selection in

yeast and is ampicillin resistant for selection in *E. coli*. The library was amplified to 3

x 10^6 coverage according to manufacturer instructions (Clontech 1999). The

collected amplified library plasmid DNA was purified using the Qiagen Mega-Prep

kit according to manufacturer specifications (Qiagen*).*

Yeast transformation and screening: *Saccharomyces cerevisiae* strain AH109 was cultured

in Yeast extract Peptone Dextrose with 0.03% adenine hemisulfate media (YPDA)

until reaching log phase. One microgram of each the bait plasmid and the library

plasmid were co-transformed into the yeast using the LiCL method with the

Yeastmaker™ Yeast Transformation Kit (CLONTECH).   Transformed yeast was

collected and then cultured in YPDA for 1-3 hours prior to plating on –LT and –

AHLTα-gal media plates. Plates were then incubated at 30º C for 5 days, and then –

LT plates were counted and co-transformation efficiency was calculated using the

following formula (Clontech 1999):

Count the colonies (cfu) formed on a diluted –LT SD plate

$$\frac{\text{CFU x total suspension volume (μl)}}{\text{Volume plated (μl) x dilution factor x μg library plasmid}} = \text{cfu/μg DNA}$$

Transformation efficiency is then used to calculate the number of clones screened using the following formula: cfu/μg x μg of library plasmid used = # of library clones screened (Clontech 1999). Colonies growing on –AHLTα-gal and turning blue were selected and re-plated in a grid pattern on –AHLTα-gal plates and incubated at 30ºC for 5 days with a positive control reference on each plate. Colonies that grew and were blue on the second plating were considered positive and were selected for follow-up studies. The selected library plasmids were isolated using the Zymoprep II yeast plasmid isolation kit (ZymoResearch). Isolated plasmids were amplified with pACT2 specific primers: F- CTATTCGATGATG-AAGATACCCCACCAAACCC and R- GTGAACTTGCGGGGTTTTTCAG-TATC with the following PCR conditions: 95ºC for 5 min., 95ºC for 30 sec., 64ºC for 30 sec., 72ºC for 45 sec. for 30 cycles followed by a 7 min. extension at 72ºC. Amplicons were purified and then sequenced as previously described. Sequences were analyzed using BLASTN and BLASTX algorithms from the NCBI website (http://www.ncbi.nlm.nih.gov/BLAST). Clones containing sequence of only a 3' UTR were discarded. Isolated clones with sequence matching a coding region of a gene were selected for further analysis. Yeast plasmid DNA from clones selected for further analysis was amplified by transforming into competent *E. coli* and selecting for ampicillin resistance. Plasmid DNA was purified from bacterial colonies as previously described. The plasmid DNA was then co-transformed with the bait vector plasmid DNA into AH109 yeast and plated on –LT and –AHLTα-gal

media. Clones that were positive for this test were co-transformed into AH109 yeast

with the empty bait vector pGBKT7 and plated on –LT and –AHLT α-gal media.

Clones that grew with the empty vector on –AHLT α-gal were considered false

positives and discarded.

 Co-immunoprecipitation   Co-immunoprecipitation was performed using the

Matchmaker™ CO-IP kit (CLONTECH). The pACT2 vector does not contain a T7

promoter sequence and this was added to the selected prey plasmids via PCR with

the following primers: F- 5'AAAATTGTAATACGACTCACTATAGGGCGACC-

CGCCACCATG 3' and R- 5' – ACTTGCGGGGTTTTTCAGTATCTACGAT 3'

with PCR conditions as recommended by the manufacturer (Clontech 2006) as

follows: 94ºC for 1 min., followed by 2 cycles of 94ºC for 15sec., 72ºC for 5 min.,

followed by 2 cycles of 94ºC for 15 sec. 70ºC for 5 min., followed by 94ºC for 15

sec., 68ºC for 5 min. for 21 cycles, followed by a 7 min. extension at 68ºC.   The bait

plasmid and positive clone prey plasmids were translated using the Promega TnT

Coupled Reticulocyte System (Promega) and ^{35}S-methionine according to

manufacturer instructions. In brief, after the initial T7 translation proteins from the

candidate clones were combined with protein of bait plasmid and incubated with

either the c-Myc or HA antibody and then co-immunoprecipitated with Protein A

beads according to manufacturer instructions (Clontech 2006). This consisted of

adding 10 µl of combined lysate to 3µl of prepared Protein A beads and rotating at

low speed for at least 1 hour at room temperature. After rotating, beads were

washed six times with manufacturer provided wash solution and then resuspended in

20μl of 0.1% SDS-BPB loading dye.   Protein beads were denatured at 95ºC for 5

minutes, electrophoresed on a 15% SDS polyacrylamide gel and then electroblotted

on supported nitrocellulose.   Dried nitrocellulose membranes were imaged

radiographically.

Quantitative RT-PCR RNA from transformed human lymphocyte cell lines was

extracted with the RNeasy RNA extraction kit (Qiagen). Samples were further

treated with Turbo DNase-*free* (Ambion). Primers were designed using Primer Bank

(http://pga.mgh.harvard.edu/primerbank/index.html). The list of primers is

detailed in Table 2.1.

Table 2.1
Primers for Quantitative RT-PCR of AGTR2 Interactors

Primer Name	Primer Sequence – 5' to 3'	Annealing Temp. ºC
ASMTL	F- CAACCGGCTGTACCAGAAAGAC R- GATCGTGTCCGCTCCAATG	61
ASMTL2	F- CAACCGGCTATACCAGAAAGAC R- GATCGTGTCCGCTCCAATG	60
GNB2L1	F- GACCATCATCATGTGGAAACTGA R- CCGTTGTGAGATCCCAGAGG	60
GAPDH	F- GAAGGTGAAGGTCGGAGTC R- GAAGATGGTGATGGGATTTC	61
NGLY1	F- GACTGGCACATGGTATATTTGGC R- TGCTGTATCAGATCGCAATTTCC	55
WDR1	F- GGAGCACCTGTTGAAGTATGAG R- GAAGAGCCACTATCCCAGAGG	55

Quantitative RT-PCR was carried out using I-Script One-Step RT-PCR kit with Sybr

Green (Biorad) in a total volume of 25 μl on the Biorad I-cycler (Biorad). All

samples were analyzed in triplicate using 5 ng total RNA and analyzed using the standard curve method (Larionov et al. 2005).

<u>Genomic PCR</u> Human DNA isolated from lymphocytes was amplified as previously described in Chapter One. The following primers were used: ASMTLex13F- 5' TCTCCCATCCCTATCCCTAGA 3' and ASMTLex13R- 5' TGACGGAGT-GTTCAATGGAG 3'. The following PCR conditions were used: 95ºC for 5 min., followed by 95ºC for 30 sec., 60ºC for 30 sec., 72ºC for 30 sec. for 30 cycles followed by a 7 min. 72ºC extension. This produces a 400 bp amplicon. For densitometry analysis 100ng of each patient sample was used in the PCR. After gel electrophoresis on a 1.8% agarose gel, samples were analyzed using the densitometry program of the Alpha-Imager (AlphaInnotech).   Rf values of each sample were then compared to quantitate gene dosage.

<div align="center">Results</div>

<u>Identification of candidate interacting proteins</u>

Proteins from the C-terminal and N-terminal constructs, the empty bait vector pGBKT7 and AH109 yeast were isolated and analyzed by Western blot. An antibody to the Gal4 BD domain was hybridized to the blot and confirmed that both constructs were producing the expected protein. Western blot analysis showing the appropriate sizes for each construct is shown in Figure 2.1.
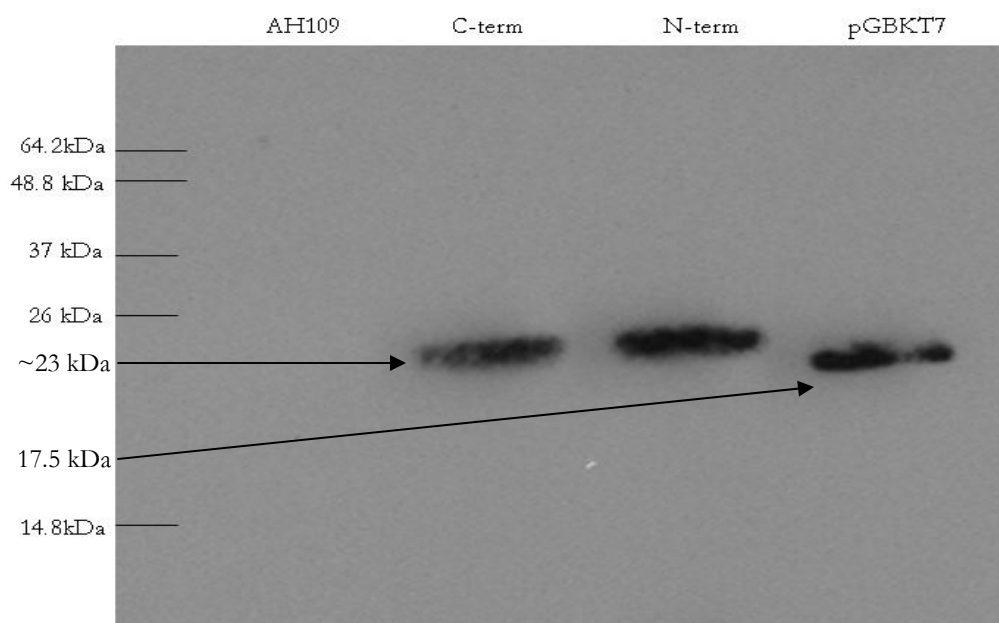
<u>Figure 2.1</u>– Western blot using Gal4BD antibody of yeast transformed with no construct (AH109), pGBKT7 with the AGTR2 C-terminal, pGBKT7 with the AGTR2 N-terminal, and pGBKT7 alone (pGBKT7). AGTR2 constructs are expected to be ~5kD larger than the empty vector.

The C-terminal intracellular domain of AGTR2 construct was screened against the human fetal brain library. A total of 2.11×10^6 clones were screened. No positively interacting clones were identified.

Screenings of the N-terminal extra-cellular domain totaling 944,700 clones resulted in 376 positive clones. Positive clones were then restreaked on –AHLT α-gal plates. Of these, 108 clones were selected for sequencing. Sequences were analyzed using BLASTN and BLASTX (http://www.ncbi.nlm.nih.gov/BLAST/) to identify clones with inserts in frame and coded for a protein. Of the 108 clones sequenced, 39 were selected for further testing as they fit this criteria. Further

testing included re-interacting the selected prey plasmid with the N-terminal

construct via yeast transformation and also interacting it with the empty pGBKT7

plasmids. Library plasmids that failed to re-interact with N-terminal construct or

interacted with the empty pGBKT7 plasmid were considered false positives. After

this screening, 19 clones remained, representing 7 genes, which are detailed in table

2.2.

Table 2.2
Candidate Gene Results from Screening of AGTR2 N-term

Gene symbol	Gene ID	Number of clones	HA Co-IP	C-myc Co-IP	Protein size
Asmtl	NM_004192	1	yes	yes	15 kd
Aplp1	NM_005166	12	yes	yes	8 kd
Chrom 12p		1	No translation	N/A	N/A
Chrom 1		1	No translation	N/A	N/A
Gnb2L1	NM_006098	2	yes	yes	20 kd
Ngly-1	NM_006098	1	yes	yes	10 kd
Wdr1	NM_017491	1	yes	yes	20 kd

Confirmation of AGTR2 interacting proteins

Clones listed in Table 2.2 were further analyzed by co-immunoprecipitation

after T7 translation. Clones Chrom12p and Chrom1 were eliminated as they failed

to translate. The other five interaction candidates (ASMTL, APLP1, GNB2L1,

NGLY-1 and WDR1) were found to make a specific protein in a T7 translation

assay.   These clones are shown on selective yeast media with positive and negative

controls in Figure 2.2


-LT plate

-AHLT α-gal plate
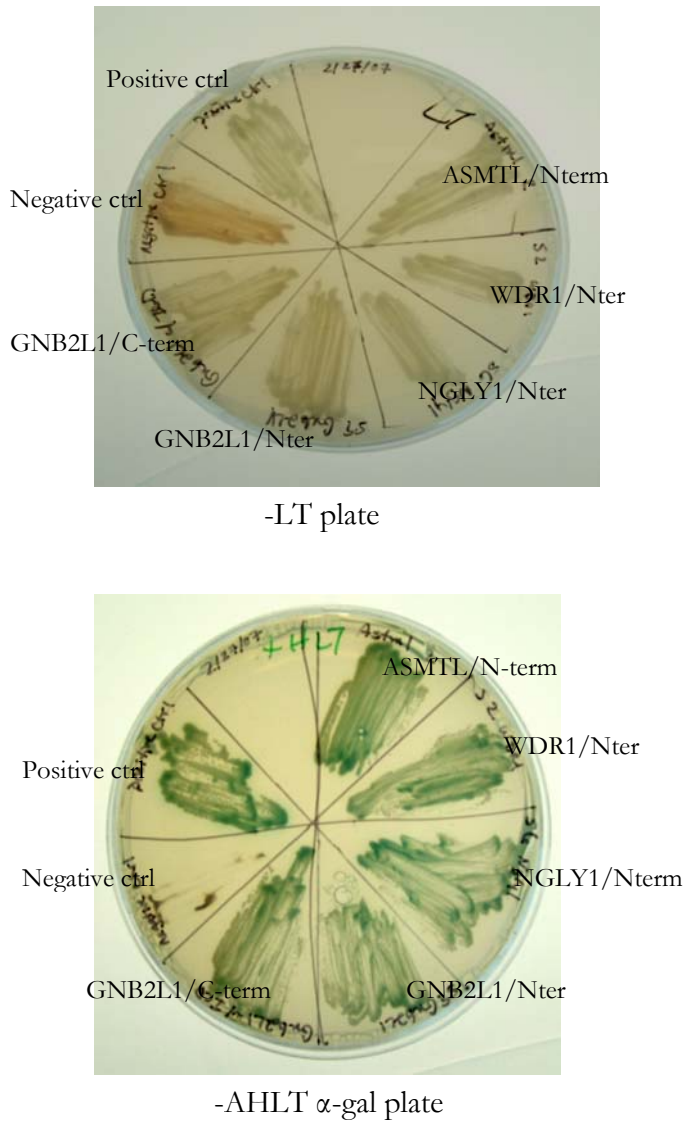
Figure 2.2 Positive clones on non selective (-LT) and selective (-AHLT) media.
Positive clones turn blue in the presence of alpha-galactosidase. All clones
containing both AD and BD plasmids grow on –LT media. Only clones with
interacting proteins grow on –AHLTαgal media and turn blue.

The positive control consisted of the pVA3-1 (containing the Gal4BD and p53T antigen) and pTD1-1 (containing the Gal4AD and SV40 large T antigen). This control grows on –AHLTαgal media and demonstrates strong β-Galactosidase activity. The negative control consisted of pLAM5' (containing the Gal4BD and human β-lamin) and pTD1-1. This control grows on –LT media, but will not grow on –AHLTαgal media.

Of these clones, three were verified by co-immunoprecipitation (Figures 2.3 and 2.5). APLP1 and WDR1 were also found to co-immunoprecipitate with the pGBKT7 murine p53 control construct (figure 2.4) and thus were considered false positives. Co-immunoprecipitation was confirmed using both the c-Myc antibody, which is specific for the bait plasmid, and the HA antibody, which is specific for the library prey plasmid. Three proteins, ASTML, GNB2L1 and NGLY1, were identified as positive interactors.
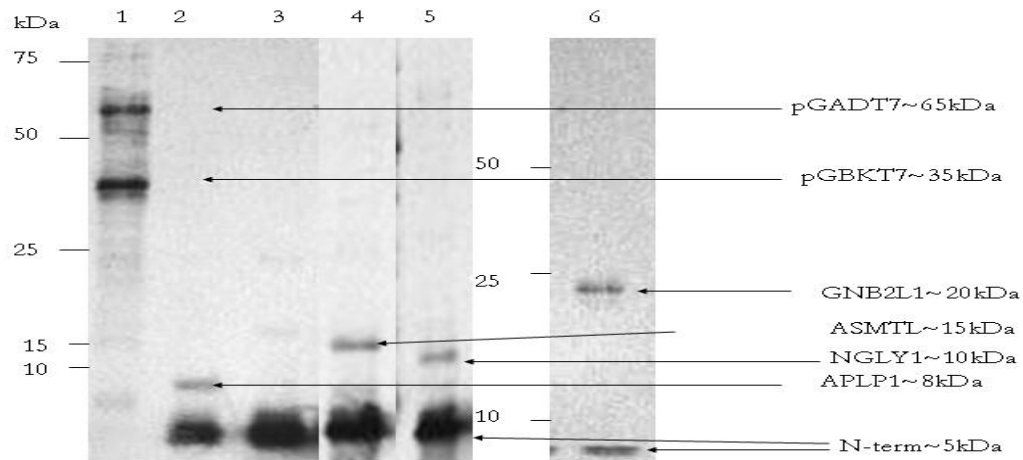
Figure 2.3: CO-IP with c-Myc ab. 1= pGADT7 SV40 and pGBKT7 Murine p53 controls, 2 = APLP1 and ECD, 3 = ECD alone, 4 = NGLY1 and ECD 5 = Asmtl with ECD, 6 = GNB2L1 and ECD
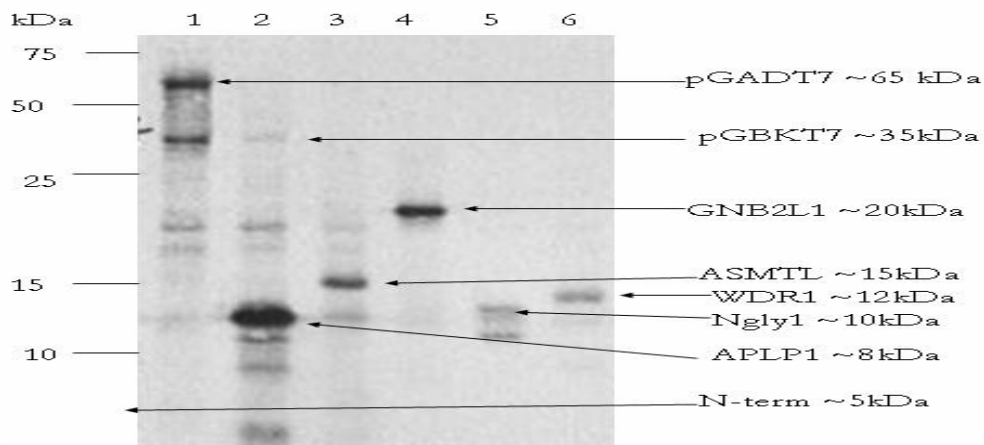
Figure 2.4 CO-IP of candidate proteins and control with HA antibody. 1 = pGADT7 SV40 and pGBKT7 Murine p53 controls, 2 = APLP1 and pGBKT7 control, 3 = ASTML and pGBKT7 control 4 = GNB2L1 and pGBKT7 control 5 = NGLY1 and pGBKT7 control 6 = WDR1 and pGBKT7 control. In lane 2 a band corresponding to the pGBKT7 control is seen, indicating that APLP1 is a false=positive.
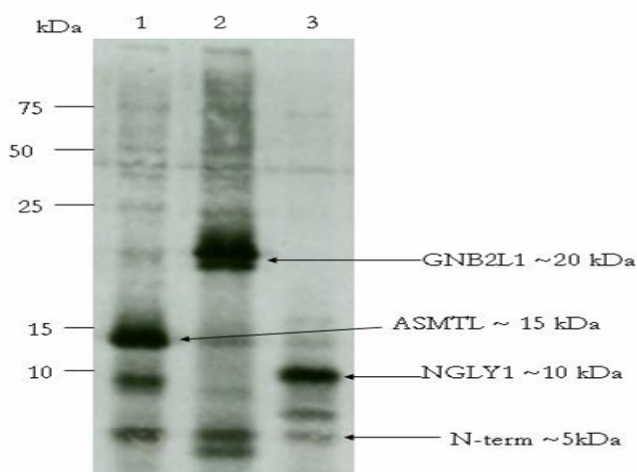
Figure 2.5: CO-IP of candidate proteins and AGTR2 N-terminal with HA antibody. 1 = ASMTL and ECD, 2 = GNB2L1 and ECD, 3 = NGLY1 and ECD. The HA antibody did not give as clean a result as the c-Myc antibody, causing extra bands on the image.

Evaluation of G21V mutation with candidate AGTR2 interactors

An N-terminal extracellular domain construct containing the G21Vmutation in the pGBKT7 vector was interacted individually with APLP1, ASMTL, GNB2L1, NGLY1 and WDR1. This construct interacted with all five of these clones.

Analysis of Candidate Protein Specificity

GNB2L1 has previously been shown to interact with the angiotensin II receptor-associated protein (Agtrap) which in turn interacts specifically with the carboxy terminal of AGTR1 (Wang et al. 2002). To test the specificity of GNB2L1 binding to AGTR2, the positive clone containing GNB2L1 was also co-transformed with the carboxy terminal of AGTR2 both in AH109 yeast and by co-immunoprecipitation. GNB2L1 was found to positively interact with the AGTR2 C-

terminal in yeast, (see Figure 2.2) and by co-immunoprecipitation (Figure 2.5, lane 1).

NGLY1 and ASMTL were also found to interact with the C-terminal of AGTR2 via

co-immunoprecipitation. When co-transformed with the C-terminal construct in

AH109 yeast, ASMTL did not interact as strongly with the C-terminal construct as

with N-terminal construct, as indicated by α-galactosidase activity. Ngly-1 was found

to only interact with the N-terminal construct in AH109 yeast as it failed to have any

growth on –AHLTαgal media when co-transformed with the C-terminal construct.
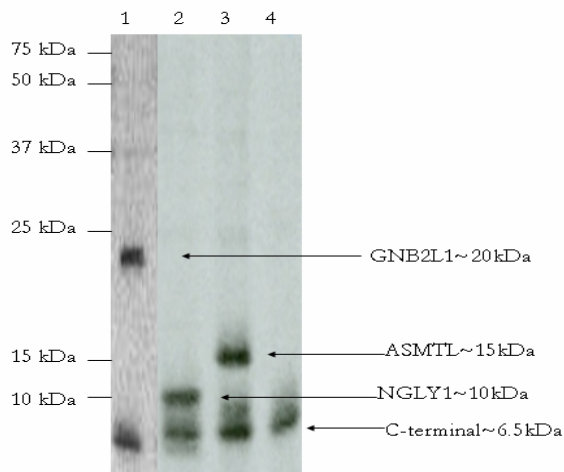
Figure 2.6   CO-IP of AGTR2 C-terminal and positive interactors with c-Myc antibody. 1 = GNB2L1 and C-term, 2 = NGLY1 and C-term, 3 = ASMTL and C-term, 4 = C-term alone.

Expression of AGTR2-interactive genes in patients with *AGTR2* gene mutations

To examine if the *AGTR2* mutations affected the expression of the interacting

partners identified in our study, quantitative RT-PCR was performed using total

RNA from transformed leukocytes. Samples were collected from the patient with no

AGTR2 expression (CMS0813), her parents (CMS5065 and CMS0814), a patient

with the G21V mutation (CMS5103) and two patients with the FS at F^{132} mutation

(CMS0690 and CMS4481). Expression of ASTML, GNB2L1 and NGLY1 was

examined. The results are shown in Figures 2.6, 2.7 and 2.8.
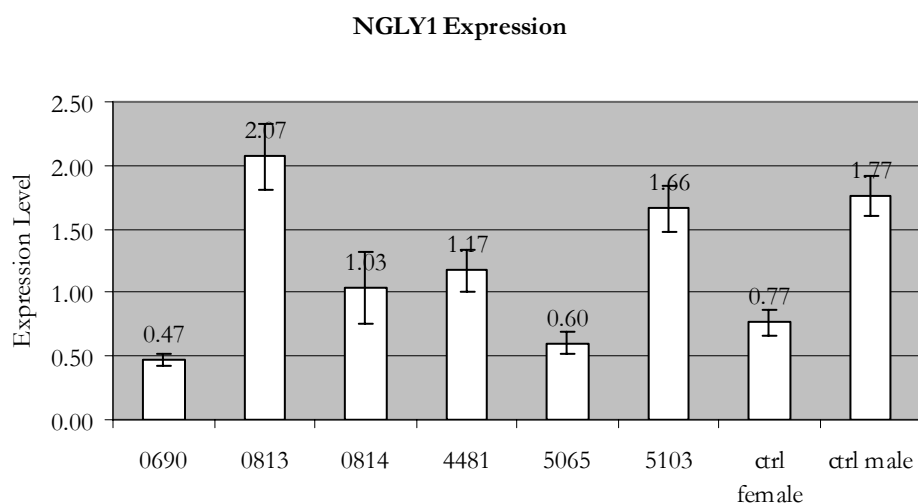
NGLY1 Expression

Figure 2.7 Expression of *NGLY1* in human transformed lymphocytes. 0690 – patient with 395/402Del T deletion, 0813 patient with no AGTR2 expression, 0814 – mother of 0813, 5065 – father of 0813, 5103 – patient with G21V mutation, control female and control male. Error bars show standard deviation. Expression is normalized to GAPDH.
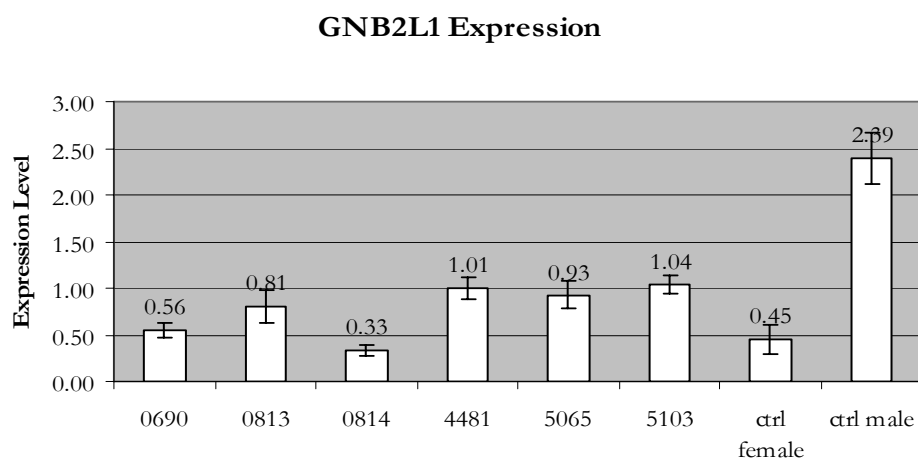
GNB2L1 Expression

Figure 2.8 Expression of *GNB2L1* in human transformed lymphocytes. 0690 – patient with 395/402Del T deletion, 0813 patient with no AGTR2 expression, 0814 – mother of 0813, 4481 – patient with 395/402Del T, 5065 – father of 0813, 5103 – patient with G21V mutation, control female and control male. Error bars show standard deviation. Expression is normalized to GAPDH.
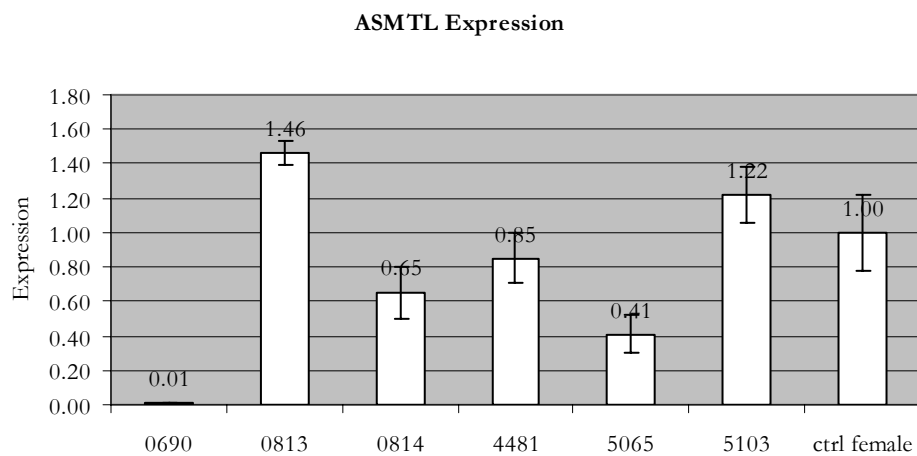
ASMTL Expression

Figure 2.9 Expression of *ASMTL* in human transformed lymphocytes.   0690 – patient with 395/402Del T deletion, 0813 patient with no AGTR2 expression, 0814 – mother of 0813, 5065 – father of 0813, 5103 – patient with G21V mutation and a control female. Errors bars show standard deviation. Expression is normalized to GAPDH.

Quantitative RT-PCR indicated that one patient (CMS0690) with the FS at F^{132} mutation had no expression of *ASTML*. However, the other FS at F^{132} mutation patient had expression in the normal range (Figure 2.8). As the *ASMTL* gene is in the pseudo-autosomal region of the X and Y chromosome, PCR using densitometry was used to ascertain whether the patient had two copies of *ASMTL*. PCR of genomic DNA with densitometry indicated that patient CMS0690 has an intact *ASMTL* gene on both the X and Y chromosomes (data not shown). No conclusions were drawn regarding the expression of both the *NGLY1* and *GNB2L1* genes, as there was significant variability between all subjects tested (Figures 2.6 and 2.7).

When the RNA expression of GNB2L1 from brains of *Agtr2$^{-/y}$* mouse embryos was compared with that of normal ones using quantitative RT-PCR, expression was 1.5 fold lower (p = 0.1) in *Agtr2$^{-/y}$* mouse brains (see Chapter One, page 45). When examining the same expression in P1 *Agtr2$^{-/y}$* mice, *Gnb2l1* was slightly higher, but not significantly (p = 0.6). The two microarray probes representing *Gnb2l1* showed a 1.3 and 1.2 fold decrease in expression in the *Agtr2$^{-/y}$* E15 brains, but no significant change at P1. No mouse homologue is currently known for ASTML. Microarray analysis revealed little difference in expression between *Agtr2$^{-/y}$* brains for Ngly1 at either developmental stage.

<u>Discussion</u>

This study identified three proteins, GNB2L1, NGLY1 and ASMTL, that interact with AGTR2. To identify AGTR2 interacting proteins, a human fetal brain library was used in a yeast two-hybrid screening system. These interactions were observed in-vivo (yeast 2-hybrid) and in-vitro (co-immunoprecipitation).

The AGTR2 N-terminal extracellular domain interacted with amino acids 119-317 of GNB2L1. This domain, which contains almost the entire coding sequence, consists of exons 2 through 8 of GNB2L1 (Figure 3.12). Quantitative RT-PCR showed that GNB2L1 is down-regulated in $Agtr2^{-/y}$ E15 mouse brains, but not in P1 $Agtr2^{-/y}$ brains. This may suggest a specific function for AGTR2/GNB2L1 binding that is unique to the earlier developmental period.

GNB2L1 is a seven bladed beta-propeller protein made of 316 a.a., containing seven WD40 repeats and acts as an intracellular adaptor protein (Sklan et al. 2006). The $GNB2L1$ gene is located at 5q35.3, and consists of eight exons that code for a cDNA transcript that is 1142bp in length (Wang et al. 2003). It belongs to the family of receptor for activated protein C (RACK) proteins and also belongs to the family of WD40 repeat proteins (Wang et al. 2003). It is expressed highly in many tissues, expressing the same size transcript (Wang et al. 2003).

Both AGTR2 and GNB2L1 are expressed at different levels at different stages of development in the embryonic and fetal brain, but in the same areas. GNB2L1 (RACK1) and AGTR2 are first expressed at mouse embryonic day

11.5(Nuyt et al. 1999; Ashique et al. 2006). GNB2L1 is expressed in a gradient throughout the developing brain and is highest in the telencephalic areas (Ashique et al. 2006). AGTR2 is expressed at moderate to low levels in the telechephalon late in fetal development, but at higher levels in developing brain areas concerned with motor functions (Nuyt et al. 1999). Western blot comparison of hippocampal lysates from E13.5, E18.5 and P21 mice probed with anti-RACK1 antibody show a gradual decrease of RACK1 expression in the hippocampus through development (Ashique et al. 2006). In postnatal and adult brains both GNB2L1 and AGTR2 are highly expressed in the cerebellum and both are expressed in the hippocampus(Ashique et al. 2006; von Bohlen und Halbach and Albrecht 2006). This may indicate a role for an interaction of AGTR2 and GNB2L1 in the development of the hippocampus. At the cellular level, GNB2L1 and AGTR2 are expressed in neural cells but not glial cells (Gendron et al. 2003; Ashique et al. 2006). Together these findings support a likely role for the interaction of GNB2L1 and AGTR2 in brain development and function.

GNB2L1 is a scaffolding protein that has many functions including affecting other scaffolding proteins, cell adhesion, NMDA activation and dopamine transport (Sklan et al. 2006). NMDA receptors are important to synaptic plasticity, learning and memory and neuronal development (Dang et al. 2006). GNB2L1 has been shown to inhibit the function of NMDA receptors by binding Fyn, the substrate for the NR2B subunit of NMDA receptors (Yaka et al. 2002).

AGTR2 has previously been shown to have effects on neurite outgrowth and cell differentiation probably through rearrangements of the cytoskeleton (Gendron et al. 2003). Recently it has been demonstrated that GNB2L1 binds to human angiotensin II receptor-associated protein (AGTRAP) which in turn interacts with the C-terminal of AGTR1 acting as an inhibitor of AGTR1 signaling (Wang et al. 2002). The study described here demonstrated that GNB2L1 interacts with the AGTR2 receptor at both the C-terminal and N-terminal in yeast 2-hybrid interactions and co-immunoprecipitation.

AGTR1 and AGTR2 counter-balance the actions of each other physiologically (von Bohlen und Halbach and Albrecht 2006). AGTR2 has been shown to be a direct antagonist of AGTR1 in COS-7 and rat fetal fibroblasts (AbdAlla et al. 2001). It is possible that the GNB2L1 /AGTRAP complex could be a mediating complex for AGTR2 and AGTR1 in some tissues. Such speculation would require additional studies.

The AGTR2-interacting protein N-glycanase 1, (NGLY1), is a 654 amino acid protein that is thought to participate in the degrading of misfolded glycoproteins by the proteasome (Suzuki et al. 2003). The *NGLY1* gene is located on human chromosome 3p24.2, is 64,226 bp in length consisting of 11 exons. It consists of a PUB, transglutaminase and PAW domains (Allen et al. 2006). It is primarily a cytosolic protein (Park et al. 2001) and is expressed in the heart, brain, liver, kidney and testis and is highly conserved in eukaryotes (Suzuki et al. 2003). This screening

found that the amino terminal of AGTR2 interacts with the last 85 amino acids of NGLY1 in its C-terminal, the PAW domain (Figure 2.9).

Mouse Ngly1 has also been shown to interact with mouse Hr23b, (the mouse homologue of yeast Rad23p) which links Ngly1 to the proteasome (Park et al. 2001). The same study also found that mouse Ngly1 interacted with mouse S4, which is a 19s proteasome subunit, and required the N-terminal domain of Ngly1 for the interaction. The N-terminal domain is a PUB domain that is unique to mammals (Park et al. 2001; Allen et al. 2006). Park and co-workers (2001) proposed that Ngly1 may recruit proteins interacting with the ubiquitin proteasome and link them to the 26S proteasome for degradation of unfolded glycoproteins. Li and associates confirmed this hypothesis by finding that Ngly1 forms a complex with p97, Amfr, mY33K and mHr23b to combine ubiquination and deglycosylation actions that send misfolded glycoproteins to the proteasome (Li et al. 2005; Li et al. 2006).

AGTR2 is a glycosylated protein whose N-linked oligosaccharide side chains vary according to the tissue in which it is expressed (Servant et al. 1996). Some membrane proteins have to be N-glycosylated for cell surface expression (Servant et al. 1996). While the N-terminal of AGTR2 is necessary for the binding of angiotensin II (Servant et al. 1997), glycosylation is not necessary for cell surface expression or angiotensin II binding (Servant et al. 1996). If deglycosylation does not affect these processes, does NGLY1 bind with AGTR2 as part of the process of apoptosis through the proteasome? Our microarray analysis of mouse E15 and P1

brains from *Agtr2^(-/y)* and control mice (see Chapter 1) found several genes involved in the ubiquitin/proteasome pathway dysregulated, providing evidence that may suggest that AGTR2 may also be involved with the proteasome.

ASMTL is a 629 amino acid protein that is not well characterized. This gene maps to the pseudo-autosomal region Xp22.3 and Yp11.3 (Ried et al. 1998). The amino terminal of AGTR2 interacted with amino acids 487- 621 the methyl-transferase domain of ASMTL (Figure 2.8). This domain catalyzes the reaction of S-adenosyl-L-methionine and N-acetylserotonin to S-adenyl-L-homocysteine and melatonin. ASMTL is widely expressed in all tissues except adipose or nerve tissue (UniGene/database). RNA expression of this gene was found to be absent in one patient with a FS^{132} mutation in AGTR2, but not in his affected maternal cousin with the same mutation. Other patients with AGTR2 mutations had expression within the range of normal controls (Figures 2.8).

Further study is needed to describe the function of the ASMTL gene with AGTR2. Co-localization studies in cell lines could further illuminate where both genes interact in the cell. It would be also interesting to investigate whether the interaction of ASMTL and AGTR2 is unique to the developing brain.

This study did not find any interaction of the AGTR2 C-terminal with the fetal brain library. While other studies have found this domain to interact with specific proteins, none of those studies utilized a fetal brain library. Interactions with the C-terminal domain were found in-vitro however, and this may due to co-

immunoprecipitation being a more sensitive assay than in-vivo yeast 2-hybrid

screening. Even though protein production of the C-terminal construct was verified

by western blot, technical problems cannot be ruled-out.
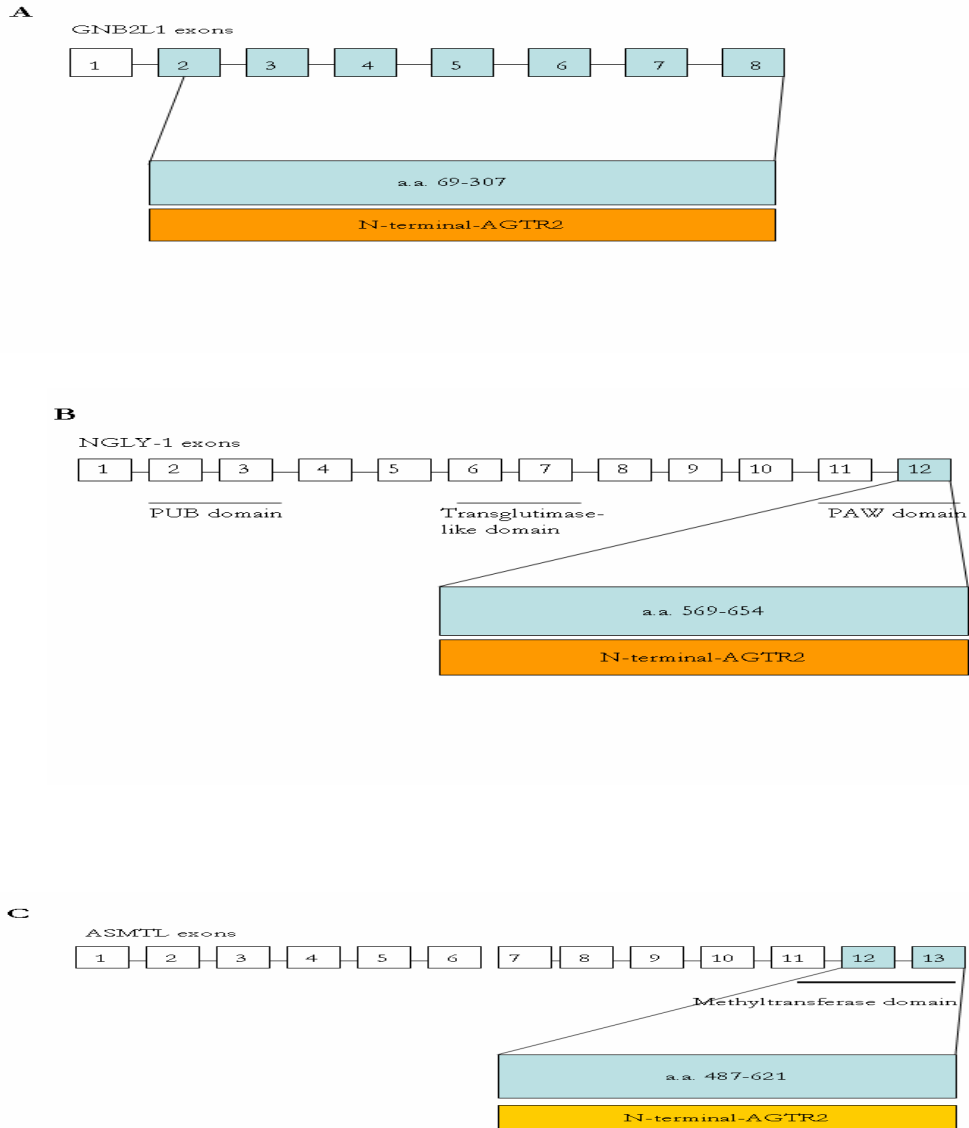
Figure 2.10 Graphical representation of the portion of each positive clone that interacts with the amino terminal of AGTR2. Most of the ORF of GNB2L1 was present in the prey construct. Only the PAW domain of NGLY1 interacts with AGTR2 in this study. The methyltransferase domain of ASMTL interacts with AGTR2.

With the exception of one patient with no ASMTL expression, no significant differences were noted in the expression of candidate genes in the AGTR2 mutation patients. This may be explained by the RNA being collected from leukocytes rather than brain tissue, or that these protein interactions are only seen during the fetal period. Mutations in AGTR2 may also have no effect on the expression of these genes.

In summary, this study has characterized three proteins expressed in fetal brain that interact with AGTR2. GNB2L1 is a scaffolding protein, highly expressed throughout brain development and has previously been shown to interact with many other proteins. Pathway Studio software was utilized to identify targets common to AGTR2 function. GNB2L1 has many cellular targets in common to both AGTR1 and AGTR2 (Figure 2.10). In particular, GNB2L1 binds PTPN11 (aka SHP-2) (Kiely et al. 2005) which is down-regulated by AGTR2 (Elbaz et al. 2000) and AGTR1 (Marrero et al. 1998). SHP-2 has been shown to interact with ATIP after AGTR2 stimulation, which induces MMS2 expression. MMS2 plays an important role in neural differentiation (Li et al. 2007). The interaction of AGTR2 and SRC has also been shown to influence neural differentiation (Li et al. 2007),
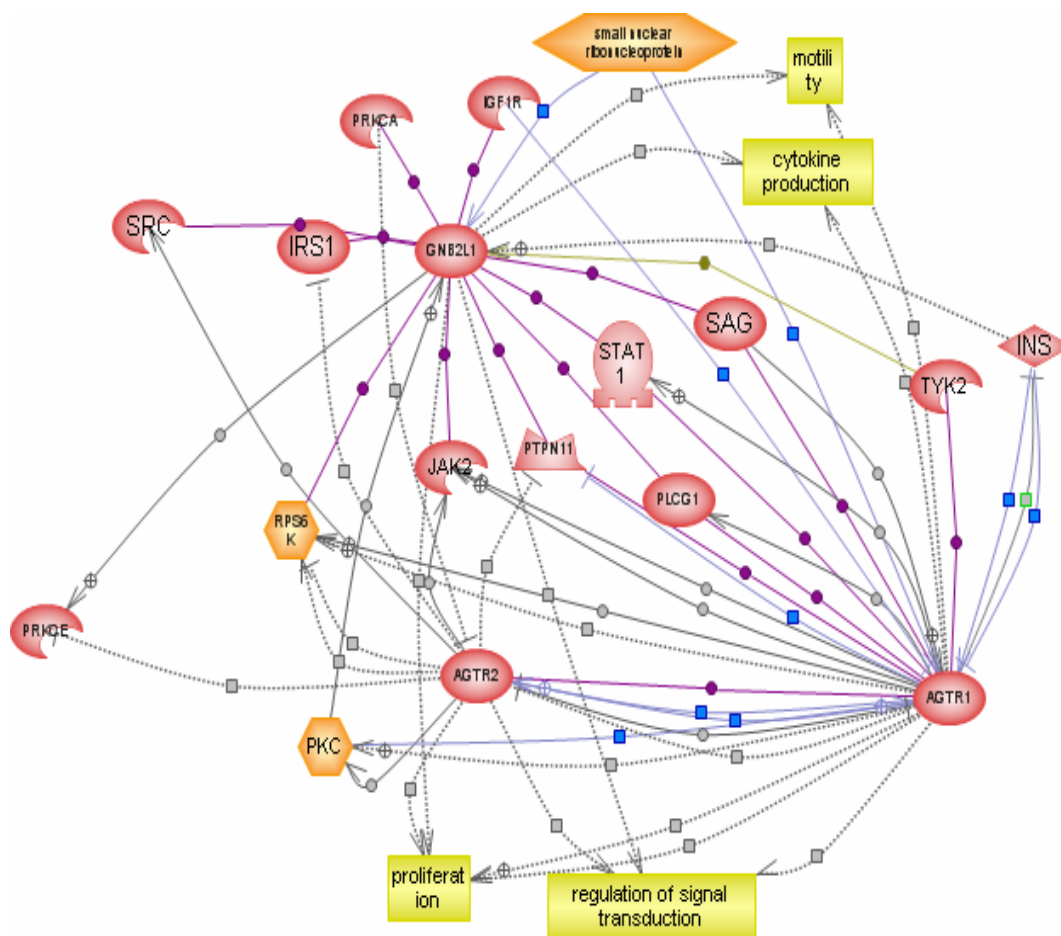
Figure 2.11 Pathway Studio (Ariadne Genomics, Rockville, MD) demonstration of common targets of AGTR1, AGTR2 and GNB2L1. Pink shapes = proteins, orange octagons = functional groups, yellow squares = cellular functions, purple lines = binding, blue lines = expression, gold lines = protein modification, grey lines = regulation. Direction of arrows indicates up-regulation. Straight line instead of an arrow indicates inhibition. Small squares on lines are references than can be accessed via the Pathway Studio program.

and SRC is shown to be bound by GNB2L1. Also, GNB2L1 and AGTR1 are involved in the insulin pathway through insulin II (INS) and the insulin growth factor one receptor (IGF1R). AGTR2 and GNB2L1 are connected in the insulin pathway through insulin receptor substrate one (IRS1).

NGLY1 cleaves oligosaccharides and participates in the proteasome. Perhaps it is involved with AGTR2 in apoptosis via the ubiquitin-proteasome system. ASMTL has an unknown function, but has a methyltransferase domain that interacts with AGTR2.

As AGTR2 is expressed in different brain areas depending on developmental stage, it would be interesting to investigate the expression pattern of NGLY-1 and ASMTL in the developing brain also. These newly identified AGTR2 interactors add to the complex picture of AGTR2 function in the developing brain.

CHARACTERIZATION OF THE AGTR2 INTERACTING PROTEIN (ATIP)

Several previous studies have identified different AGTR2 regions responsible for the interaction with other proteins involved in AGTR2 activation and regulation. The cytoplasmic intracellular domain of AGTR2 has been shown to contain a binding domain for ERBB3 (Knowle et al. 2000), PLZF (Senbonmatsu et al. 2003) and NHE6 (Pulakat et al. 2005). In an effort to better the signaling mechanisms of AGTR2, Nouet and colleagues (Nouet et al. 2004) identified a novel interacting protein called the AGTR2 Interacting Protein (ATIP) that interacted with the C-terminus of AGTR2. Subsequently the human homologue was isolated from a human lung cDNA library and mapped to 8p21.3 (Nouet et al. 2004). Northern analysis probed with the 354bp cDNA identified as the ATIP interacting domain (ATIP-ID) revealed a 1.9 kb transcript in all tissues (spleen, thymus, prostate, testis, ovary, small intestine and colon) tested. It was determined that ATIP had four transcripts with varying lengths in the N-terminal domain, but all containing the ATIP-ID and C-terminal domain. Functional studies revealed that the binding of ATIP to the AGTR2 cytoplasmic tail inhibited cell proliferation (Nouet et al. 2004). This gene was found to be identical to the already annotated gene Mitochondrial Suppressor Gene One (MTSG1).

Subsequently, Wruck and co-workers (Wruck et al. 2005) identified the ATIP mouse homologue, termed ATB50, in a yeast two-hybrid screen with the C-terminus of AGTR2. The protein had 440 amino acids. These authors found this

protein and AGTR2 are co-expressed in mouse tissue. In addition, in-situ hybridization of AGTR2 knockout mouse tissues revealed the expression of ATBP50 was less than 10% of that of normal animals (Wruck et al. 2005). Studies in COS-7 cells with fluorescent markers showed that ATBP50 proteins localized to the golgi matrix. Using siRNA they found that the ATBP50 isoform is necessary for surface expression of AGTR2.

The Wruck group (2005) also found that the ATBP50 isoform is the result of alternative splicing, as all three isoforms they identified had exons 7 to 15, but ATBP50 uniquely contained exon 6. The other two isoforms identified, ATPBP60 and ATPBP135 were not found to be expressed in the brain and spleen nor did they interact with AGTR2, as ATBP50 did. These authors also found that stimulating PC12W cells with angiotensin II causes a strong expression of ATBP50 (Wruck et al. 2005).

Di Benedetto and colleagues described the genomic structure and expression patterns of the human ATIP (Di Benedetto et al. 2006). The ATIP gene spans 112 kb consisting of 17 exons and maps to chromosome 8p21. Five transcripts: ATIP1, ATIP2, ATIP3a, ATIP3b and ATIP4 were identified. The ATIP1 isoform is the most predominately expressed isoform in adult brain and is a 436 amino acid protein. ATIP2 is a 770 amino acid protein found to be expressed at very low levels in all tissues examined. The isoforms ATIP3a and ATIP3b are large transcripts and are expressed in many tissues, but at low levels in the adult brain.

ATIP3a and ATIP3b consist of 1270 and 1216 amino acid proteins respectively.

ATIP4, the only form expressed in fetal brain, is a 517 amino acid protein. It is also

expressed at relatively high levels in the cerebellum in the adult brain. The genomic

structure of each isoform is summarized in Figure 3.1.
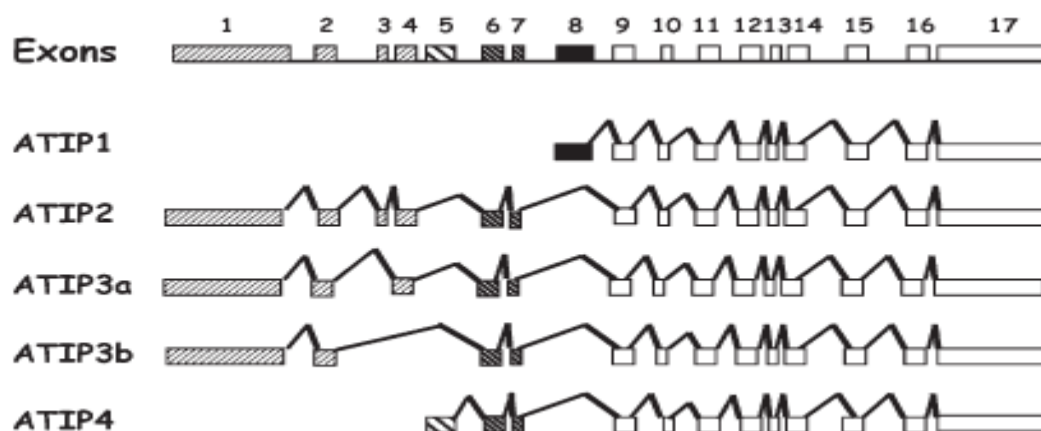
Figure 3.1 Exon structure of ATIP isoforms. White boxes indicate exons common
to all transcripts. Black box indicates ATIP1 specific exon. Hatched boxes indicate
Exons used by ATIP3 and/or ATIP 4 transcripts. Note that exon five is unique to
ATIP4. (Figure used by permission from Di Benedetto et al. 2006 figure 1A).

In this study the potential for ATIP to be a causal gene for MR was explored.

The ATIP4 isoform was of particular interest as it is the only isoform expressed in

the fetal brain, having the potential to interact with AGTR2 and affect brain

development. Brain expression was elucidated through the use of Northern blots of

sections of adult brain. A mutation screening of ATIP in patients with MR was also

undertaken.

The seventeen exons of ATIP were analyzed in 80 patients. Particular

attention was given to the screening of exon 5 because of its unique expression in

fetal brain. Exon 5 was screened in 500 patients with MR. We found no significant mutations in any of the patients screened.

<div align="center">Methods</div>

Northern blots and probes The ATIP-ID 354 bp probe was made by amplifying human cDNA with the following primers: F- 5' CAGGCTGAAAAAA-CAGAACGA 3'and R- 5' TTTTTCATTTAAAGCATCATT 3'. PCR conditions were as follows: Denaturation at 95ºC for 5min. then 95ºC for 30 sec., 55ºC for 30 sec., 72ºC for 30 sec. for 30 cycles followed by a 7 min. extension at 72ºC. The 354 bp ^{32}P labeled product was hybridized to Northern blots containing poly A+ RNAs from different human brain sections (from individuals of ages 16-75 years) (Clontech) using ExpressHybe (Clontech) at 65ºC for 1 hour after pre-hybridizing at 65ºC for 2 hours. The filters were washed with of 2X SSC-0.05% SDS solution at 65ºC for 40 minutes and then with 0.1X SSC-0.1% SDS solution at room temperature for 20 minutes. The filters were exposed to Biomax film (Kodak) 24 hours and for 5 days at -80ºC.

Mutation screening   Mutation analysis was performed using Denaturing High Pressure Liquid Chromatography (DHPLC) or Incorporation-PCR Single-Strand Conformation Polymorphism (IPS).   Amplicons were amplified with the primers listed in Table 3.1 (primer sequences were provided by Dr. C. Nahmias) by using 1 ng of genomic DNA with 1X PCR buffer, 125 μM dNTPS, 1 μCi of αP^{33} dCTP (3,000Ci/mmol), 0.5 μM of each primer and 1U of GO Taq™ polymerase

(Promega) in a 10μl reaction. PCR conditions were as follows: 95ºC for 5 min. followed by 95ºC for 30 sec., appropriate annealing temperature for 30 sec., 72ºC for 30 sec. for 30 cycles followed by a 7 minute extension at 72ºC. Ten microliters of formamide/NaOH BPB buffer was added to each sample and then they were denatured at 95ºC for 5' and placed on ice. Samples were loaded on a 6% MDE gel (FMC) and run at constant power of 8W from 16-20 hours. Gels were dried and visualized with X-Ray Biomax film (Kodak) at room temperature. Samples that demonstrated a banding pattern or shift that differed from normal controls were selected for sequence analysis.

Amplicons selected for DHPLC were amplified using 20 ng of human genomic DNA, 1X PCR buffer, 250μM dNTPs, 1.0 μM of each primer and 1U of GO Taq™ polymerase (Promega) in a 20 μl reaction. Five μl of each PCR mix was run on a 1.8% agarose gel to verify the amplicon. Samples were then pooled in groups of four. Pooled samples were heteroduplexed by heating to 94ºC for seven minutes and then 55ºC for four minutes. DHPLC conditions based on the melting temperature of each amplicon were selected using the Wavemaker program (Transgenomics). Chromatography using the appropriate temperatures was performed and their denaturing profiles were inspected visually.

Samples that showed a profile differing from normal controls were selected for further analysis. The four individuals from the abnormal pooled sample were PCR

amplified and then subjected separately to DHPLC analysis. The individual sample

that differed from the normal control was selected for sequence analysis.

Samples selected for sequencing from either IPS or DHPLC were amplified

by using 100 ng DNA genomic DNA, 1 X PCR buffer, 0.5 μM of dNTPs, 1.0 μM

of each primer and 2U of GO Taq™ polymerase in a 50 μl reaction. PCR products

were purified and both strands were sequenced using the DYEnamic ET Dye

Terminator Cycle Sequencing Kit (GE Healthcare) and the automated MegaBACE

1000 DNA analysis system (GE Healthcare). Sequences were analyzed using the

DNASTAR program (Madison, WI USA).

Table 3.1
Primers for ATIP Gene Screening

Exon	Primer sequence 5' – 3'	annealing temperature °C	product size (bp)
Exon 1.1	F: GACAGACCATTTTGCCCACCCTCTC R : CAACTGTGTTGCAGATATTTGGGC	64	444
Exon 1.2	F : GTAAGCAGGTGTTAGATATGC R : GGCTTCTGATGGTGTGACTTGAGG	55	443
Exon 1.3	F : CATCTTCCCATTCTGATAAGACGC R : CATCAATAAGACAATAGGAC	55	417
Exon 1.4	F : GCTCATACAGGCACAAGGAAATGG R : GTCTGGTATGTTTTTAAGCCCTCG	55	413
Exon 1.5	F : GTTTCACCGATTGAAGCGACGG R : GAATGAGTTGTAACATGCACAGCC	64	458
Exon 1.6	F : TAACAAGACACATAAGCAGCAG R : GCTAACACATCTCAGTTTTCTCC	55	446
Exon 2	F : GGGGCCCATTCAGTCAGTTG R : GACCTATAATCATGACTGTCC	55	356

Table 3.1 (continued)

Exon 3	F: GATAGCCTATTGTCCTAATGG R: GCAAGAGAGCAGAAATGATGAGGC	55	224
Exon 4	F : CTTAAAAAGTGCCAGCTTTCGGG R : CATTAGTTTTTCTTGTAATGACTG	55	290
Exon 5	F : CATGTTGACTTGGCCACCGTTTC R : AAATTTAAGCATGCTTACAAAG	53	585
Exon 6	F : GGACAAAGGAATAAATGTGG R : CAAGCCAAGGACTTTAAGCG	55	269
Exon 7	F :CCGGGAACCTGAAATGTAGCG R : GGAAATTCTACTTATAAGCACACC	62	267
Exon 8	F : GAGACCACCCACTTTCTCCTCCCC R : GCAAATTAATGAAGACATCCCCC	57+DMSO	539
Exon 9	F: GTTTTTGAATCCTTGTGGTGG R: GCGTGTGAGCAAGTCCTCCCCG	56	364
Exon 10	F : GCCTAAATGATTCATATCTTGGC R : AACAGCTCCCAGCATGCAACTCC	56	298
Exon 11	F : GTATGCTTCAGGTGTCATCACAGC R :CCTATTAGACTAAAAAAGAGAAGCTC	57	408
Exon 12	F : GCCTTTAAACTAGAGCCCACGC R : CCACAGGGCATTCGCTGAAGCAGG	59+DMSO	336
Exon 13	F : GGCTTCATCATCAACCCC R : CGTACACAGAAACATTAAAACC	57+DMSO	259
Exon 14	F : CGTATGCTGAGTTTCTGGGGTT R : TGTTATTTCTCTGGCTGCTG	59+DMSO	248
Exon 15	F : CGCTTGCTACTTGTCTAATGTC R : ATAAATATGGAACAAACTTGGA	56	387
Exon 16	F : TTTTTCAGTATGTTTGTTAGTGT R : GCAGGGGTAGAGCGTGTCCAGA	57	340
Exon 17	F : GCCAAATACCTGTGACCTTGTGC R : CCCACGTTCCTCCTTGGGG	60	438

<u>Characterization of a heterozygous deletion</u> Sequencing of both DNA strands of a

patient with an alternatively migrating fragment of exon 14 produced very poor

sequence results. This was thought to be due to a deletion. To confirm the deletion,

sequencing of both strands was undertaken. To separate the leading and lagging

strands, the exon 14 amplicon was subcloned into the pCR2.1 vector in the TA

Cloning Kit (Invitrogen) as described in Chapter 2. Ten clones containing inserts

were selected and DNA was prepared. Purified plasmid DNA from these clones was

sequenced as described previously using the following primers: M13F 5'

CTGGCCGTCG-TTTTAC 3' and M13R 5' GTCATAGCTGTTTCCTG 3'.

Sequences were analyzed with DNASTAR (Madison WI, USA). This technique

allows for clean sequencing by separating the leading and lagging strands.

<u>Mutation screen via restriction enzyme digest</u> To screen for a possible polymorphic

variant in exon 14, 120 normal controls and the patient with a 4 bp intronic deletion

were amplified with exon 14 primers in a 25 µl PCR reaction as previously described.

Ten microliters of the 238 bp product were then digested with 2 U of Hpa I

restriction endonuclease (New England Biolabs) and 1 X buffer in a 20 µl reaction

and incubated at 37ºC for at least 4 hours. The digest was run on a 3% NuSieve

agarose gel and visualized with ethidium bromide on a UV illuminator. The deletion

destroys the Hpa I site and thus a deletion has a 238 bp band instead of 219bp and

19 bp band. Heterozygotes would have a 238 bp, 219bp and 19 bp bands.

<div align="center">Results</div>

<u>Expression of the ATIP gene in brain</u>

Expression of ATIP has been shown in human brain (Di Benedetto et al.

2006). To monitor the expression pattern in brain regions in humans, a Northern

blot containing RNAs from the different regions of the adult human brain was used.

A cDNA probe containing the ATIP-ID coding region was hybridized to human

adult brain Northern blots (Clontech). The ATIP-ID was found to be expressed in

all brain tissues. A transcript of 4.4 kb was found in all tissues examined. A

relatively weakly expressed transcript of 7.4 kb was also seen (Figure 3.1).

Expression appeared to be highest in the corpus callosum, cerebellum and thalamus

(Figure 3.1).

PCR of a human fetal brain library with ATIP-ID primers found that this

domain was not expressed in the library made from 20-25 week human fetal brain.

However, the unique transcript, containing exon 5, was expressed (data not shown).

Mutation screening and detection of nucleotide variants in the ATIP gene

The ATIP gene contains 17 exons.   All exons were screened in female

patients with MR. These patients previously tested negative for the MR causing

FMR1 gene expansion.   Two normal controls and 80 or 160 patients were screened

using either IPS or dHPLC (Table 3.2). Patients with alternatively migrating

fragments were selected for sequencing. Six patients were found to have a

c.1791A>C (p.K435T) alteration in exon one. This alteration was also found in 8 of

90 normal male controls. One patient carried a heterozygous deletion of five

nucleotides (ivs13-22del5). Subsequently, this patient was found to have San Fillipo

syndrome through biochemical testing and thus this deletion is unlikely to be MR
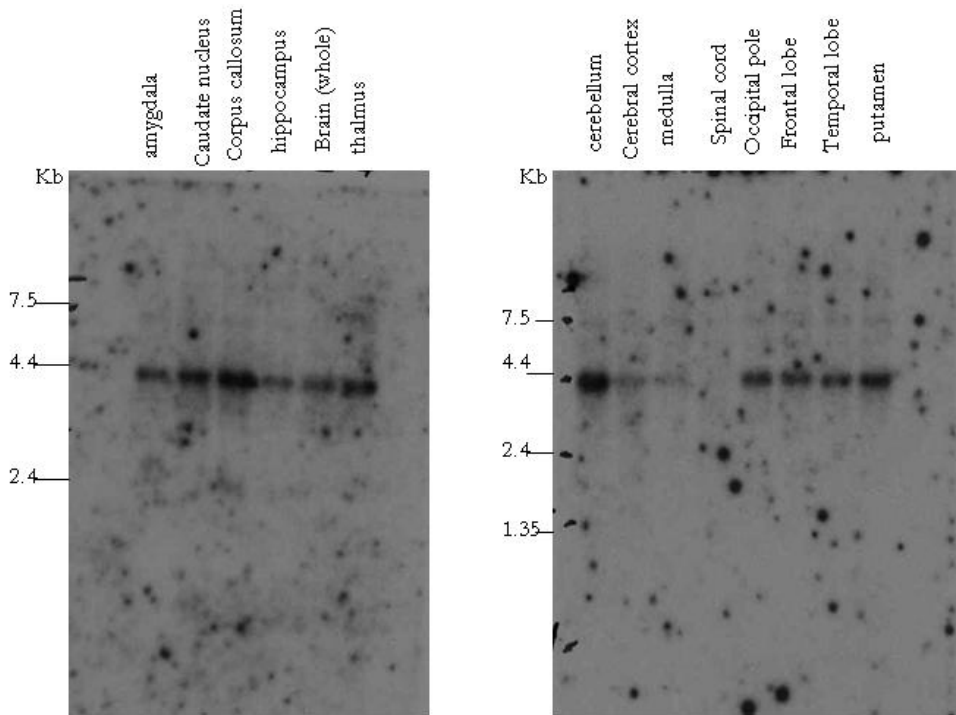
Figure 3.2 Expression of ATIP isoform in the human brain. Northern blots (Clontech) containing RNA from different human adult brain sections were hybridized with a 354 bp ATIP cDNA probe.

causing in this patient. This patient's deletion was elucidated by subcloning the exon 14 amplicon and then sequencing a number of insert-containing plasmids. By this technique the leading and lagging strands were separated and single-strand sequencing was accomplished. The sequence chromatogram of this patient's normal and deleted exon 14 are shown in Figure 3.3. A summary of the mutation screening is detailed in Table 3.2.
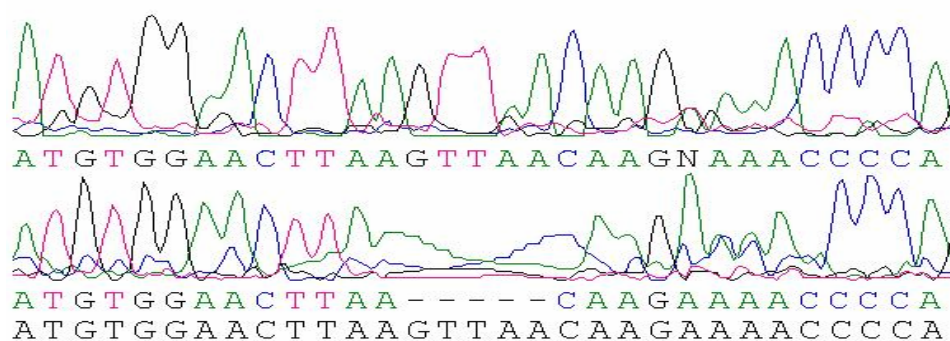
Figure 3.3 Electropherogram of aligned exon 14 from patient with a 5 bp deletion. The normal strand is on the top row, the deleted strand in on the second row and the ATIP exon 14 sequence is on the lower row.

Table 3.2
Mutation Screen Summary for ATIP

Exon	Number of Patients Screened	Nucleotide Change	Amino Acid Change	Number of Patients with a shift	Number of controls with a change	Screening Method
1	80	c.1791A>C	p.K453T	6	8 of 90	DHPLC
2	80	none		0		DHPLC
3	80	none		7*		IPS
4	80	none		0		IPS
5	160	none		0		DHPLC
6	160	none		0		DHPLC
7	160	none		1*		DHPLC
8	160	none		0		IPS
9	80	none		0		DHPLC
10	80	none		2*		IPS
11	80	none		1*		IPS
12	80	none		0		IPS
13	80	none		1*		IPS
14	80	IVS13-22del5	No	1	0 of 120	IPS
15	80	none		0		IPS
16	80	none		0		DHPLC
17	80	none		0		DHPLC

*No nucleotide changes were found in these samples.

Discussion

Northern blots of adult brain tissues probed with the ATIP-ID cDNA found

a 4.4 kb transcript and a weakly expressed 7.4 kb transcript. Expression was

comparatively higher in the corpus callosum, cerebellum and thalamus. Expression

was noticeably absent from the spinal cord. No expression of the ATIP-ID was

detected in the human fetal brain library. However, the fetal brain library did

contain cDNA from exon 5, which is specific to the fetal brain isoform of ATIP.

No significant alterations in an initial screen of our MR population were found.

Interestingly, the *Atip* gene was not found to be dysregulated at either

developmental stage in *Agtr2*$^{-/y}$ mice. Microarray analysis of *Agtr2*$^{-/y}$ mice (see

Chapter One) revealed no significant difference in the expression of *Atip* (alias

Mtus1) from normal controls.

The initial discovery of ATIP was found through a yeast 2-hybrid screen

using the last 52 amino acids of AGTR2 as bait against a mouse fetal cDNA library.

The cDNA region that encoded the 118 amino acids found to interact with AGTR2

was designated the ATIP-ID

The ATIP4 isoform containing exon 5 is the only isoform of ATIP found to

be expressed in fetal brain. This isoform is also expressed in the adult brain,

predominately in the cerebellum, but is not found in any other tissues (Di Benedetto

et al. 2006). Previous analysis of the same adult brain blots used in this study with

AGTR2 cDNA as a probe, found expression only in the cerebellum (Vervoort et al.

2002).   This is also consistent with the high expression of the ATIP-ID found in the cerebellum on this study's northern blots (Figure 3.1). It might be possible that the interaction of ATIP and AGTR2 is limited to the cerebellum.

Using the C-terminal of mouse Agtr2, Wruck and colleagues, (2005) found a full-length cDNA designated ATBP50, a gene analogous to human *ATIP*. ATBP60 and ATBP135 were two other ATB isoforms and were found not to interact with AGTR2. While all three isoforms contained exons 7 to 15, *Atbp50* uniquely included exon six, which is analogous to human *ATIP* exon eight. Di Benedetto and co-workers discovered that ATIP exon 5 (isoform ATIP4) has a 90% homology to ATBP60 and ATIP1 unique exon 8 has an 87% homology to ATBP50 (Di Benedetto et al. 2006). It is interesting to note that the only described mouse isoform able to interact with AGTR2, ATBP50, is analogous to adult brain ATIP1. The mouse isoform analogous to fetal brain expressed ATIP4 (ATBP60), was not shown to interact with AGTR2 (Wruck et al. 2005).

Co-expression of *Atbp* and *Agtr2* in tissues of *Agtr2$^{-/y}$* mice was examined by Wruck and colleagues (Wruck et al. 2005) via is-situ hybridization and quantitative RT-PCR.   Using a probe common to all three isoforms, they examined co-expression of *Atbp* and *Agtr2* in adrenals, kidney, lung, heart and brain from adult control and *Agtr2$^{-/y}$* mice.   They found expression patterns of both genes to be similar in all tissues examined. Using uterine tissue from control and *Agtr2$^{-/y}$* animals, they also found that the expression of *Atbp* was less than 10% of normal in *Agtr2$^{-/y}$*

mice. The microarray results seen in our study were from brains of control and

Agtr2$^{-/y}$ E15 and P1 mice and no difference was seen between the two groups. This

may be explained by the ATBP50 isoform not being expressed in fetal brain.

The mutation screen of the patient cohort analyzed in this study did not find

any disease causing mutations. ATIP exon 5 specific to the isoform expressed in

fetal brain, was screened for a larger cohort of 500 patients with MR. Mental

retardation is a heterogeneous disorder that is likely caused by many factors.

Mutations in causal genes of MR are rare and are often found at a low frequency.

Thus a larger number of patient samples would need to be screened before ruling

out *ATIP* as a gene involved in MR. Further investigation of the function of the

ATIP isoform specific to fetal brain may also be pursued to further clarify its role in

developing brain.

CONCLUSIONS

The functions of AGTR2, a receptor for angiotensin II, are still not fully understood. While better characterized for its role in blood pressure regulation and fluid homeostasis, the brain functions of AGTR2 are just beginning to be explored. The fact that AGTR2 is expressed at higher levels, and in different areas, in the fetal brain as compared to the adult brain, point to its function in brain development. The purpose of this study was to further elucidate the function of AGTR2 in the developing brain.

In Chapter One we explored the differences in gene expression between E15 and P1 *Agtr2*$^{-/y}$ and control mouse brains. Abnormal dendritic spine morphology and cell number had previously been observed in *Agtr2*$^{-/y}$ mice. RNA from eight knockout and six control E15 brain samples was hybridized to 16 Agilent Whole Mouse Genome 44K arrays. Data from these arrays was used to produce a list of 52 up-regulated and 10 down-regulated genes in E15 *Agtr2*$^{-/y}$ mouse brains. RNA from four *Agtr2*$^{-/y}$ and four control P1 brain samples were also hybridized to eight arrays. Data from this experiment produced a final list of 50 up-regulated and 12 down-regulated genes in P1 *Agtr2*$^{-/y}$ mouse brains. Results were verified via quantitative RT-PCR.

The gene expression profiling analysis in the study revealed a number of genes involved in microtubule regulation, protein binding, cell adhesion, transcription, DNA binding and kinases up-regulated in developing brain.

Transferases, as well as a large number of transcription factors, were up-regulated in E15 *Agtr2*^{-/y} mouse brains. Unique to the P1 *Agtr2*^{-/y} mouse brains were genes involved in glutamate metabolism, cell cycle control and RNA metabolism. Our findings add strength to the hypothesis that AGTR2 contributes to the developing brain by influencing cell morphology and synaptic connectivity.

In Chapter 2, three AGTR2 interacting proteins, GNB2L1, NGLY1 and ASMTL were identified. These proteins were found by screening a human fetal brain library with the N-terminal domain of AGTR2. These interactors were also verified by co-immunoprecipitation. A weak interaction was also noted for GNB2L1 and ASMTL with the C-terminal of AGTR2. The interaction of NGLY1 was specific to the N-terminal of AGTR2. GNB2L1 is a scaffolding protein with many functions, and has been shown to be involved in the signaling cascade in the central nervous system. GNB2L1 may interact with AGTR2 as part of a gene network that contributes to neuronal differentiation. ASMTL gene function is largely unknown. NGLY1 participates in degradation of misfolded glycoproteins by the proteasome. A role for AGTR2 in apoptosis has been described. We hypothesize that NGLY1 in association with AGTR2 may be involved in apoptosis through the ubiquitin-proteasome.

In Chapter 3, a partial characterization of a previously identified AGTR2 interacting protein, ATIP, has been discussed. This gene was explored as a potential MR candidate gene as it has been shown previously to interact with AGTR2 and is

expressed in the brain. Northern blot analysis of adult human brain tissue found that the region encoding the ATIP interacting domain (ATIP-ID) is expressed in all brain tissues.   The expression of the *Atip* gene was not dysregulated at either developmental stage of the *Agtr2*$^{-/y}$ mice, possibly indicating that the interaction of the ATIP isoform with AGTR2 is likely not to be crucial to brain development.

Furthermore, in a human mutation screening we did not identify any MR disease causing mutations in 80 patients analyzed. Further investigation of the function of brain specific isoforms of ATIP my further clarify its role in brain function.

APPENDIX

Mapping of X;7 Translocation in a Female Patient with MR and No AGTR2
Expression

Introduction

A female patient with moderate to severe mental retardation (IQ 44) was

previously found to have a de novo t(X;7)(q24;q22) translocation. The patient has

totally skewed X inactivation in favor of the translocated X chromosome, as

compared to random X-inactivation in her mother with two normal copies of the X

chromosome. Because causative genes are present at long distances in several

disease-associated balanced translocations, expression studies of candidate genes for

the X breakpoint region were performed. This revealed that this patient had no

expression of AGTR2. A subsequent screening of affected males from 33 families

with possible X-linked mental retardation and 552 unrelated males with mental

retardation found nine patients with mutations in AGTR2 (Vervoort et al. 2002).

The X breakpoint region was mapped 150 kb proximal to the AGTR2 gene. The

AGTR2 gene was found not to be disrupted. It was hypothesized that the loss of

expression in the patient with the t(X;7) may result from separation of distant

regulatory elements. Through Fluorescent In-Situ Hybridization (FISH), pulsed-field

and southern blot analysis and Comparative Genomic Hybridization (CGH) it was

determined that the X breakpoint was in a region of a pseudogene near the DXZ4

locus (Vervoort et al., unpublished work). The CUTL1 gene was putatively

disrupted on chromosome 7, but it was determined that the patient had expression

of this gene from her normal chromosome 7. In this study the Xq24 and the 7q22

breakpoint were partially mapped.

<u>Materials and Methods</u>

Florescent-InSitu Hybridization (FISH) Lymphocytes from patients were

transformed with EBV and cultured until confluent. BAC clones were selected by

searching the breakpoint region using the NCBI MapViewer

(http://www.ncbi.nlm.nih.gov/mapview/).   BAC clones purchased from Chori or

Invitrogen were grown on LB media with chloramphenicol as described in previous

studies. Individual colonies were cultured in LB media with chloramphenicol and

the plasmid DNA isolated using Qiagen Mini-Prep columns as previously described

in Chapter 2. DNA was labeled by incorporation of digoxigenin-11-dUTP

(Boehringer Mannheim) by nick translation using DNA polymerase I (Life

Technologies). Metaphase chromosome spreads were obtained from harvested

patient lymphoblast cell lines and FISH was performed using standard methods

(Vervoort et al. 2002). The labeled probes were visualized with rhodamine-labeled

anti-digoxigenin and the chromosomes were counterstained with DAPI. Images

were examined under a Zeiss Axiphot fluorescent microscope.

Pulsed-Field and Southern Blot Hybridization (Pulsed-field gel Southern blots

were made by V. Vervoort). Total genomic DNA (100ng) was digested with EcoRI

(New England Biolabs) and electrophoresed on a 0.8% agarose gel. The gel was

denatured and transferred to a Hybond (GE Healthcare) charged nylon membrane

using alkaline 3M NaCL 0.4M NaOH transfer method. After transfer was complete,

membrane was baked at 65ºC for one hour and pre-hybridized with hybridization

solution (4x SSPE, 2X Denhardt's solution, 0.5% SDS, 6% polyethyleneglycol, 40

mg/ml denatured salmon sperm DNA) at 65ºC for at least 2 hours. Fresh

hybridization solution was then added. DNA probes were labeled with ^{32}P d-CTP

using the Redi-Prime Random Labeling kit (Invitrogen) according to manufacturer

instructions, and then hybridized overnight at 65ºC. Filters were then washed with

5X SSC 0.1% SDS for one min. at 65ºC, 2X SSC 0.1% SDS for 15 min. at 65º C

and then for 15 min. at room temperature; and with 1X SSC, 0.1% SDS for 15 min.

at room temperature. Filters were exposed to Biomax (Kodak) film at -80ºC for at

least 24 hours. Primers used for amplifying specific probes are listed in Table A.1.

(Primers designed by V. Vervoort)

Table A.1
Primer sequences for Probes

Name	Sequence 5' to 3'	Annealing Temp. ºC	Size (bp)
Probe 7	F-CTCTCACCTGGTCCCCTTATCTCT R-GTATGGCCCTGTGGTGGTGTG	68	1171
Probe 8	F-TTTCCCCATCCCATCTCCACTTGA R-ATCGCTGCCGCCTCCTTCTTCTG	62	657
Probe 8B	F-CCTCCCCCAACTCTCCCCTTAGC R-CTCATATCCGGGACTTGCTGCTCT	55	715
Probe DXZ4	F-ACCGGCAAGGGGCTGGGGGAAGAG R-TGAAGGCGCACGTGGGCAAGAAGT	68	2334

Comparative Genomic Hybridization Analysis CGH was carried out using an

Agilent 44K Human Genome Chip (Agilent). Patient and control DNA were first

quantified to be of equal concentration and then digested with RsaI, labeled with either dUTP Cy5 or dUTP Cy3 (Perkin Elmer) and hybridized according to manufacturer protocol. In brief, each CGH slide was hybridized with two DNA samples: a control and the patient. The control was labeled with either dUTP Cy5 or dUTP Cy3 and the patient is labeled with the other. Another slide was also used utilizing a dye-swap strategy. The labeled samples were combined with manufacturer provided hybridization solution, spread on the CGH slide, sandwiched with a gasket slide and hybridized in a 65°C oven with rotation for 17 hours. Slide assemblies were then unassembled, washed briefly in SSC washes (Agilent part number 5188-5221 and part number 5188-5222), washed briefly in acetonitrile and also in proprietary ozone scavenging solution (Agilent part number 5185-5979). Slides were read on a GenePix 4000B scanner and data was extracted and normalized using Feature Extraction 8.0 software (Agilent). Analysis of results was performed using CGH Analytics software (Agilent).

RNA Extraction RNA was extracted from EBV transformed leukocytes using the Qiagen RNeasy kit (Qiagen) according to manufacturer instructions. Samples were then DNased using the Ambion Turbo DNase-free kit (Ambion Inc.). Samples were analyzed on the Agilent 2100 expert bioanalyzer (Agilent) for purity and concentration as described in Chapter 1.

Quantitative RT-PCR Primers were designed using the Primer3 program from MIT (http://frodo.wi.mit.edu/cgi-bin/primer3/primer3_www.cgi) (Rozen and

Skaletsky 2000). Biorad I-Script 1 step RT-PCR with SYBR green (Biorad) was used according to manufacturer instructions with 5 ng of RNA per sample used. Samples were run in triplicate on a Biorad i-cycler and analyzed using a standard curve method (Larionov et al. 2005)using GAPDH as a control as described in Chapter One. The primers for RT-PCR are listed in Table A.2.

Table A.2
Primers for Quantitative RT-PCR of CUTL1

Name	Primer Sequence	Annealing Temp. ºC	Product Size (bp)
Cutl1	F-CGGCAGAGGAAGTACCTGAG R-TTCTCGTGGAACTTGTGCAG	60	233 bp
GAPDH	F-GAAGGTGAAGGTCGGAGTC R-GAAGATGGTGATGGGATTTC	61	225 bp

Results

Comparative Genomic Hybridization (CGH) is a technique that allows for scanning an individual's whole genome at one time in order to find significant changes in gene dosage. To look for a possible small deletion on either chromosome 7 or X of patient CMS0813 with the (tX;7), an Agilent 44K Human genome chip (Agilent) was utilized. This chip has an average probe spatial resolution of 35 kb. No deletions or duplications were found.

Using FISH probes, the 7q22 breakpoint on the patient's translocated chromosome was narrowed to the CUTL1 gene (Figure A.1). This was accomplished by using probes in succession from the distal (area below the

breakpoint in the direction of the telomere) and from the proximal (area above the

breakpoint in the direction of the centromere) ends of the breakpoint region until a

probe is found that spans the breakpoint region. A schematic map of the probes for

the breakpoint region is shown in Figure A.1.
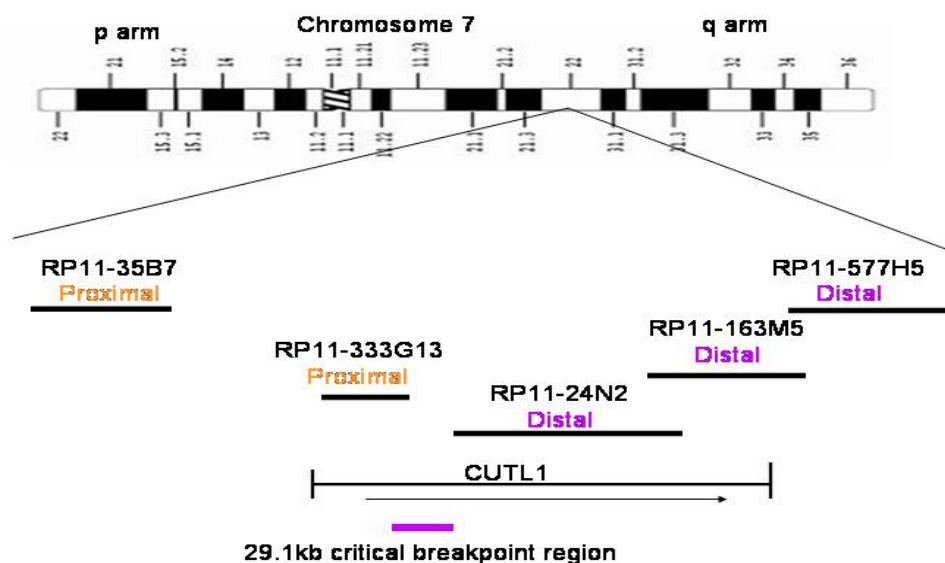
Figure A. 1 Map of FISH clones of 7q22 relative the CUTL1 gene on the translocated chromosome 7 of patient CMS0813.   The critical breakpoint region is located in the intronic region of the CUTL1 gene.

Since the CUTL1 gene appeared to be disrupted on the translocated chromosome 7

of patient CMS0813, a cDNA probe of CUTL1 was hybridized to the

EcoRI/EcoRV pulse-field blot to look for major shifts, but none were found. This

complemented the FISH data as the position of the FISH clones indicated that

majority of the CUTL1 coding region was distal to the breakpoint.

To further assess whether the patient's CUTL1 gene was affected by the breakpoint, quantitative RT- PCR analysis of the patient's and parents RNA was performed. This analysis showed the patient had expression of CUTL1 (Figure A.2). Expression was too variable among all samples analyzed including controls to accurately assess if the level of patient CMS0813's expression was affected by the disruption of CUTL1.
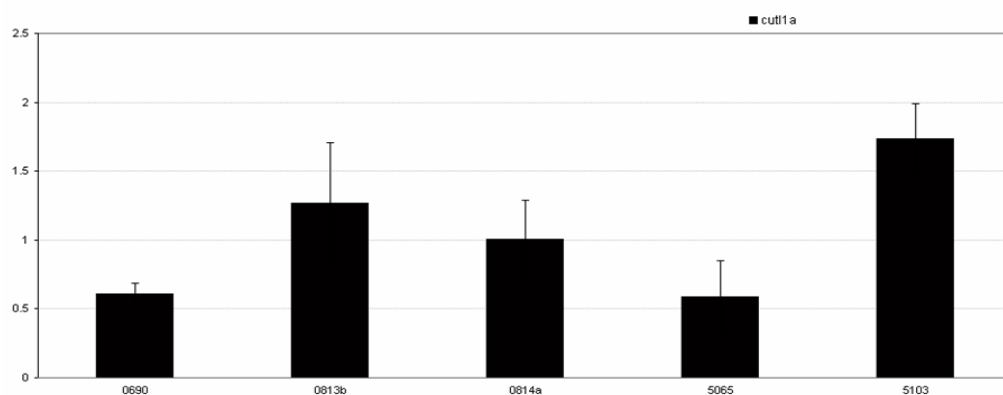
Figure A.2 Quantitative RT-PCR of CUTL1. CMS0690 = patient with truncated AGTR2 receptor, CMS0813 = patient with no functioning AGTR2, CMS0814 = control female, CMS5065 = control male, CMS5103 = patient with G21V mutation of AGTR2. All data normalized to GAPDH. Error bars indicate standard deviation.

A pulse field gel of the digested EcoR1 and EcoRV digest DNA of the translocation patient, her parents and controls was created in our laboratory previously. This blot was successively analyzed with several probes derived from the Xq breakpoint region. This analysis revealed a deleted and shifted region in the patient's chromosome X breakpoint area (Vervoort et. al., unpublished data). A probe made from microsatellite DXZ4 was found to be intact (Figure A.3), as well as

intronic probe number 7 (data not shown).   Probe number 8, a 657 bp region

upstream from DXZ4, was found to be deleted in the patient in both the EcoR1 and

EcoRV digest, as the patient had only her mother's allele (Figure A..4) Probe

number 8B was found to be shifted in the EcoR1 digest with the patient having her

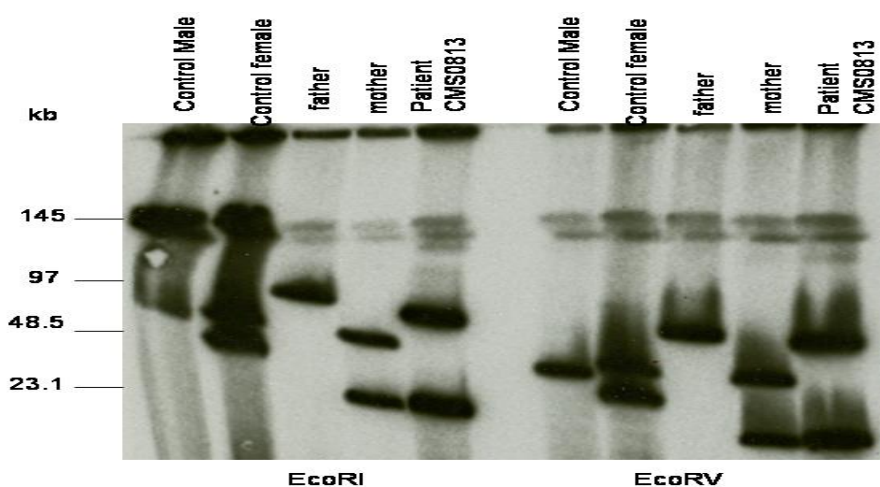mother's allele but missing her father's allele (Figure A.5).

Figure A.3 EcoRI and EcoRV digest pulse-field blot with probe DXZ4. Males have one band, females have two bands. Breakpoint patient CMS0813 has one allele from each parent with both digests indicating her DXZ4 region is intact.
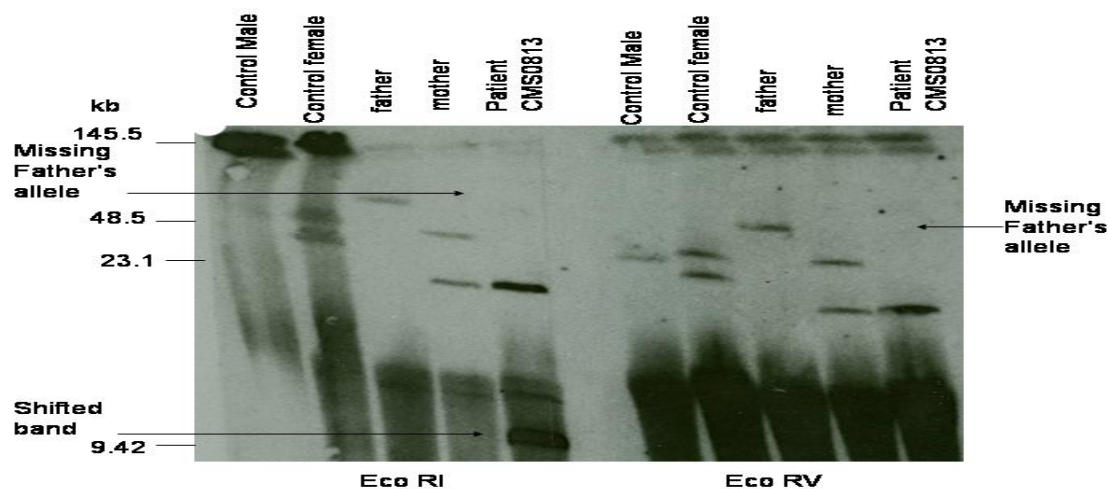
Figure A.4 EcoRI and EcoRV digest pulse-field blot with probe 8. This probe, proximal to probe DXZ4, patient CMS0813 has only her mother's allele, indicating a deletion of her father's allele.
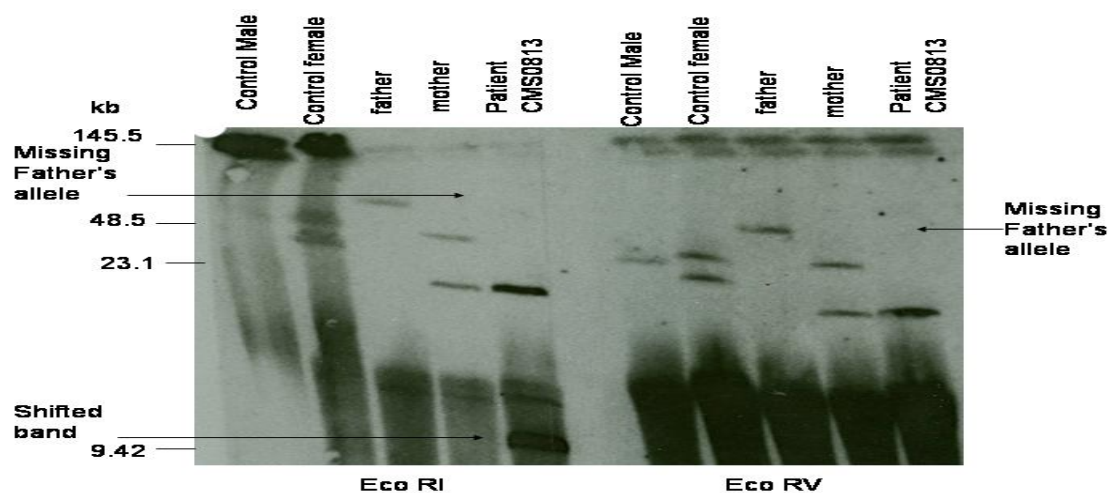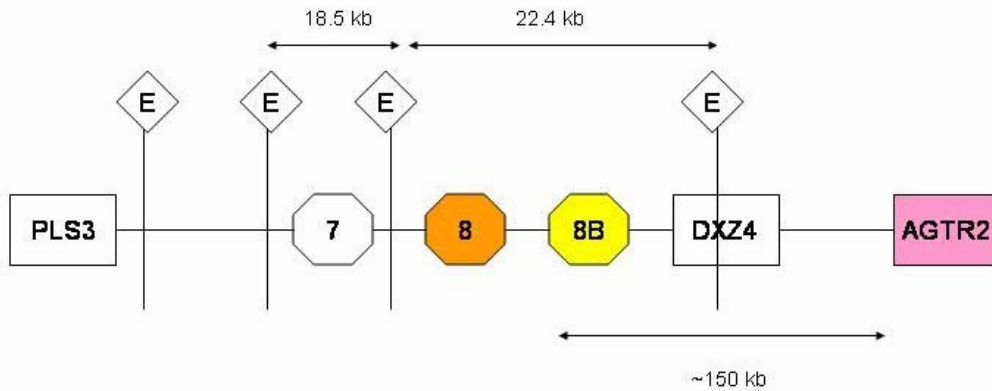

Figure A.5 EcoRI and EcoRV digest pulse-field blot with probe 8B. This probe, proximal to DXZ4 and distal to probe8, shows patient CMS0813 missing her father's allele in the EcoRV digest, but shows a lower, shifted band in the EcoRI digest

A map summarizing the position of these probes and their results can be seen in

Figure A.6.

<u>Figure A.6</u> Map of X breakpoint region for patient CMS0813. E's in diamonds
represent Eco RI cut sites. Orange probe 8 is deleted and yellow probe 8B detected
an alternatively migrating fragment.

Southern blot analysis was performed to better elucidate the size of the

shifted fragment in patient CMS0813 seen with probe 8B on the pulse-field gel

electrophoresis blot. The Southern blot analysis showed an approximately 10 kb

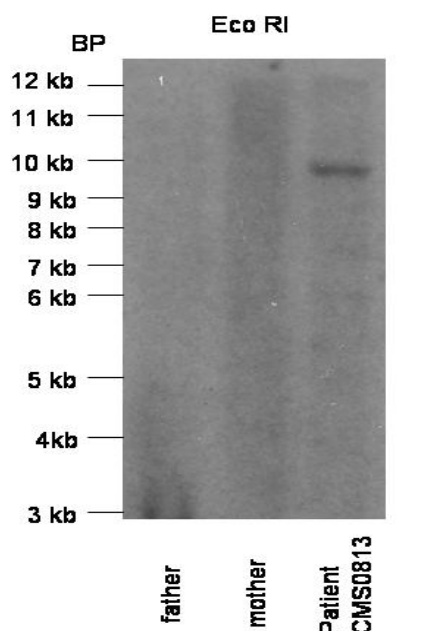band unique to the patient (Figure A.7).

Figure A.7   EcoRI Southern blot with probe 8B, showing 10 kb band unique to CMS0813. No bands were expected to be seen in the parental lanes. Further Southern blot analysis had narrowed the deleted region on the X chromosome in patient CMS 0813 to the 3 kb region between probe 8 and probe 8B (data not shown).

Sequence analysis of the probe 8 sequence with BLAST revealed this probe contained nucleotides 59 to 715 of a predicted gene, LOC728825 (XM_01128769), a pseudogene homologue of SUMO2 located on chromosome 17q25.1.   Some pseudogenes have been shown to produce active transcripts (Harrison et al. 2005). The cDNA of CMS0813, her parents and cDNA from a human fetal brain library was amplified using the probe 8 primers. All of the cDNA produced a 657 bp product and the genomic DNA produced a 657 bp and 700 bp band (figure A.8). This second band was produced on several attempts whether the DNA used was

from a male or female. It is most likely due to the primers amplifying both the

SUMO2 gene and its pseudogene LOC728825. However, the sequence homology

between this pseudogene and SUMO2 is too similar to determine if the pseudogene

produced the transcript.
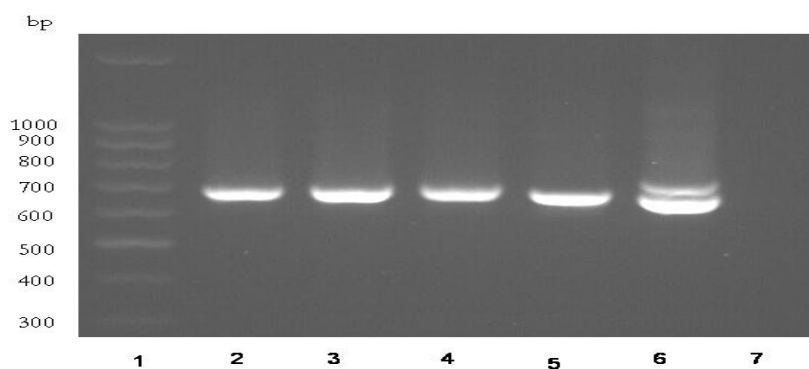
Figure A.8   cDNA PCR products of probe 8 primer. 1 – 100 bp ladder, 2 –
CMS0813, 3 – CMS0814 (mother), 4 – CMS5065 (father), 5 – fetal brain library, 6 –
genomic DNA from CMS5065 7 – water lane. The genomic samples produced two
bands, likely from the amplification of the SUMO2 gene and the pseudogene.

Previous works have demonstrated that breakpoints substantial distances

from disease causing genes can affect the expression of the primary gene (Pfeifer et

al. 1999; Crisponi et al. 2001).   This may also be the case in patient CMS0813. It

remains to be seen if the deleted pseudogene or a genomic element deleted in the

patient may act as a transcriptional regulator for AGTR2.

In conclusion, we were able to determine that the 7q22 breakpoint maps to the *CUTL1* gene.   Furthermore, the Xq24 breakpoint was narrowed to a 3 kb region that contains a pseudogene.

REFERENCES

AbdAlla S, Lother H, Abdel-tawab AM, Quitterer U (2001) The angiotensin II AT2 receptor is an AT1 receptor antagonist. J Biol Chem 276:39721-39726

Allen AM, Moeller I, Jenkins TA, Zhuo J, Aldred GP, Chai SY, Mendelsohn FA (1998) Angiotensin receptors in the nervous system. Brain Res Bull 47:17-28

Allen MD, Buchberger A, Bycroft M (2006) The PUB domain functions as a p97 binding module in human peptide N-glycanase. J Biol Chem 281:25502-25508

Ashique AM, Kharazia V, Yaka R, Phamluong K, Peterson AS, Ron D (2006) Localization of the scaffolding protein RACK1 in the developing and adult mouse brain. Brain Res 1069:31-38

Beaudry H, Gendron L, Guimond MO, Payet MD, Gallo-Payet N (2006) Involvement of protein kinase C alpha (PKC alpha) in the early action of angiotensin II type 2 (AT2) effects on neurite outgrowth in NG108-15 cells: AT2-receptor inhibits PKC alpha and p21ras activity. Endocrinology 147:4263-4272

Benjamini Y, Hochberg, Y (2000) On adaptive control of the false discovery rate in multiple testing with independent statistics. Journal of Educational and Behavioral Statistics: 60-83

Berry C, Touyz R, Dominiczak AF, Webb RC, Johns DG (2001) Angiotensin receptors: signaling, vascular pathophysiology, and interactions with ceramide. Am J Physiol Heart Circ Physiol 281:H2337-2365

Bienvenu T, Poirier K, Van Esch H, Hamel B, Moraine C, Fryns JP, Ropers HH, Beldjord C, Yntema HG, Chelly J (2003) Rare polymorphic variants of the AGTR2 gene in boys with non-specific mental retardation. J Med Genet 40:357-359

Bjorkblom B, Ostman N, Hongisto V, Komarovski V, Filen JJ, Nyman TA, Kallunki T, Courtney MJ, Coffey ET (2005) Constitutively active cytoplasmic c-Jun N-terminal kinase 1 is a dominant regulator of dendritic architecture: role of microtubule-associated protein 2 as an effector. J Neurosci 25:6350-6361

Bussolati B, Grange C, Bruno S, Buttiglieri S, Deregibus MC, Tei L, Aime S, Camussi G (2006) Neural-cell adhesion molecule (NCAM) expression by immature and tumor-derived endothelial cells favors cell organization into capillary-like structures. Exp Cell Res 312:913-924$Agtr2^{-/y}Agtr2^{-/y}$

Chelly J, Mandel JL (2001) Monogenic causes of X-linked mental retardation. Nat Rev Genet 2:669-680

Clapcote J, Roder J (2005) Simplex PCR assay for sex determination in mice. Biotechniques 38:702-706

Clontech (1999) MATCHMAKER GAL4 Two-Hybrid System 3 and Libraries User Manual.

Clontech (2006) Matchmaker CO-IP User Manual.

Crisponi L, Deiana M, Loi A, Chiappe F, Uda M, Amati P, Bisceglia L, Zelante L, Nagaraja R, Porcu S, Ristaldi MS, Marzella R, Rocchi M, Nicolino M, Lienhardt-Roussie A, Nivelon A, Verloes A, Schlessinger D, Gasparini P, Bonneau D, Cao A, Pilia G (2001) The putative forkhead transcription factor FOXL2 is mutated in blepharophimosis/ptosis/epicanthus inversus syndrome. Nat Genet 27:159-166

Csikos T, Chung O, Unger T (1998) Receptors and their classification: focus on angiotensin II and the AT2 receptor. J Hum Hypertens 12:311-318

Dang MT, Yokoi F, Yin HH, Lovinger DM, Wang Y, Li Y (2006) Disrupted motor learning and long-term synaptic plasticity in mice lacking NMDAR1 in the striatum. Proc Natl Acad Sci U S A 103:15254-15259

Dennis G, Jr., Sherman BT, Hosack DA, Yang J, Gao W, Lane HC, Lempicki RA (2003) DAVID: Database for Annotation, Visualization, and Integrated Discovery. Genome Biol 4:P3

Di Benedetto M, Bieche I, Deshayes F, Vacher S, Nouet S, Collura V, Seitz I, Louis S, Pineau P, Amsellem-Ouazana D, Couraud PO, Strosberg AD, Stoppa-Lyonnet D, Lidereau R, Nahmias C (2006) Structural organization and expression of human MTUS1, a candidate 8p22 tumor suppressor gene encoding a family of angiotensin II AT2 receptor-interacting proteins, ATIP. Gene 380:127-136

Driscoll WJ, Hill D, Smalstig A, Mueller GP (2006) Murine atrial HL-1 cells express highly active peptidylglycine alpha-amidating enzyme. Peptides 27:1547-1553

Duechler M, Shehata M, Schwarzmeier JD, Hoelbl A, Hilgarth M, Hubmann R (2005) Induction of apoptosis by proteasome inhibitors in B-CLL cells is associated with downregulation of CD23 and inactivation of Notch2. Leukemia 19:260-267

Elbaz N, Bedecs K, Masson M, Sutren M, Strosberg AD, Nahmias C (2000) Functional trans-inactivation of insulin receptor kinase by growth-inhibitory angiotensin II AT2 receptor. Mol Endocrinol 14:795-804

Eppig JT, Bult CJ KJ, Richardson JE, Blake JA, and the members of the Mouse Genome Database Group (2005) The Mouse Genome Database (MGD): from genes to mice-a commmunity resource for mouse biology. Nucleic Acids Res 33:D471-D475

Erdman J, Dahmlow S, Guse M, Hetzer R, Regitz-Zagrosek V (2004) The assertion that the G21V mutation in AGTR2 causes mental retardation is not supported by other studies. Hum Genet 114:396

Gard P (2002) The role of angiontensin II in cognition and behavior. European Journal of Pharmacol 438:1-14

Gendron L, Laflamme L, Rivard N, Asselin C, Payet MD, Gallo-Payet N (1999) Signals from the AT2 (angiotensin type 2) receptor of angiotensin II inhibit p21ras and activate MAPK (mitogen-activated protein kinase) to induce morphological neuronal differentiation in NG108-15 cells. Mol Endocrinol 13:1615-1626

Gendron L, Payet MD, Gallo-Payet N (2003) The angiotensin type 2 receptor of angiotensin II and neuronal differentiation: from observations to mechanisms. J of Mol Endocrin 31:359-372

Gendron L, Payet MD, Gallo-Payet N (2003) The angiotensin type 2 receptor of angiotensin II and neuronal differentiation: from observations to mechanisms. J Mol Endocrinol 31:359-372

Goto M, Mukoyama M, Suga S, Matsumoto T, Nakagawa M, Ishibashi R, Kasahara M, Sugawara A, Tanaka I, Nakao K (1997) Growth-dependent induction of angiotensin II type 2 receptor in rat mesangial cells. Hypertension 30:358-362

Grady EF, Sechi LA, Griffin CA, Schambelan M, Kalinyak JE (1991) Expression of AT2 receptors in the developing rat fetus. J Clin Invest 88:921-933

Harrison PM, Zheng D, Zhang Z, Carriero N, Gerstein M (2005) Transcribed processed pseudogenes in the human genome: an intermediate form of expressed retrosequence lacking protein-coding ability. Nucleic Acids Res 33:2374-2383

Hein L, Barsh G, Pratt R, Dzau V, Kobilka B (1995) Behavioral and cardiovascular effects of disruptin the angiotensin II type-2 receptor gene in mice. Nature 377:744-747

Hein L, Meinel L, Pratt RE, Dzau VJ, Kobilka BK (1997) Intracellular trafficking of angiotensin II and its AT1 and AT2 receptors: evidence for selective sorting of receptor and ligand. Mol Endocrinol 11:1266-1277

Ho HY, Rohatgi R, Lebensohn AM, Le M, Li J, Gygi SP, Kirschner MW (2004) Toca-1 mediates Cdc42-dependent actin nucleation by activating the N-WASP-WIP complex. Cell 118:203-216

Ichiki T, Labosky P, Shiota C, Okuyama S, Imagawa Y, Fogo A, Niimura F, Ichikawa I, Hogan B, Inagami T (1995) Effects on blood pressure and exploratory behavior of mice lacking angiotensin II type-2 receptor. Nature 377:748-750

Jang YJ, Kim YS, Kim WH (2006) Oncogenic effect of Polo-like kinase 1 expression in human gastric carcinomas. Int J Oncol 29:589-594

Janigro D (2006) The Cell Cycle in the Central Nervous System. Humana Press, Totowa, New Jersey

Johren O, Saavedra JM (1996) Gene expression of angiotensin II receptor subtypes in the cerebellar cortex of young rats. Neuroreport 7:1349-1352

Kiely PA, Leahy M, O'Gorman D, O'Connor R (2005) RACK1-mediated integration of adhesion and insulin-like growth factor I (IGF-I) signaling and cell migration are defective in cells expressing an IGF-I receptor mutated at tyrosines 1250 and 1251. J Biol Chem 280:7624-7633

Knowle D, Ahmed S, Pulakat L (2000) Identification of an interaction between the angiotensin II receptor sub-type AT2 and the Erb3 receptor, a member of the epidermal growth factor receptor family. Regul Pep 87:73-82

Koike G, Horiuchi M, Yamada T, Szpirer C, Jacob HJ, Dzau VJ (1994) Human type 2 angiotensin II receptor gene: cloned, mapped to the X chromosome, and its mRNA is expressed in the human lung. Biochem Biophys Res Commun 203:1842-1850

Larionov A, Krause A, Miller W (2005) A standard curve based method for relative real time PCR data processing. BMC Bioinformatics 6:62

Lavoie JL, Sigmund CD (2003) Minireview: overview of the renin-angiotensin system--an endocrine and paracrine system. Endocrinology 144:2179-2183

Leavitt BR, van Raamsdonk JM, Shehadeh J, Fernandes H, Murphy Z, Graham RK, Wellington CL, Raymond LA, Hayden MR (2006) Wild-type huntingtin protects neurons from excitotoxicity. J Neurochem 96:1121-1129

Li G, Zhao G, Zhou X, Schindelin H, Lennarz WJ (2006) The AAA ATPase p97 links peptide N-glycanase to the endoplasmic reticulum-associated E3 ligase autocrine motility factor receptor. Proc Natl Acad Sci U S A 103:8348-8353

Li G, Zhou X, Zhao G, Schindelin H, Lennarz WJ (2005) Multiple modes of interaction of the deglycosylation enzyme, mouse peptide N-glycanase, with the proteasome. Proc Natl Acad Sci U S A 102:15809-15814

Li JM, Mogi M, Tsukuda K, Tomochika H, Iwanami J, Min LJ, Nahmias C, Iwai M, Horiuchi M (2007) Angiotensin II-induced neural differentiation via angiotensin II type 2 (AT2) receptor-MMS2 cascade involving interaction between AT2 receptor-interacting protein and Src homology 2 domain-containing protein-tyrosine phosphatase 1. Mol Endocrinol 21:499-511

Lin JW, Wyszynski M, Madhavan R, Sealock R, Kim JU, Sheng M (1998) Yotiao, a novel protein of neuromuscular junction and brain that interacts with specific splice variants of NMDA receptor subunit NR1. J Neurosci 18:2017-2027

Luo JL, Kamata H, Karin M (2005) IKK/NF-kappaB signaling: balancing life and death--a new approach to cancer therapy. J Clin Invest 115:2625-2632

Marrero MB, Venema VJ, Ju H, Eaton DC, Venema RC (1998) Regulation of angiotensin II-induced JAK2 tyrosine phosphorylation: roles of SHP-1 and SHP-2. Am J Physiol 275:C1216-1223

Meffert S, Stoll M, Steckelings UM, Bottari SP, Unger T (1996) The angiotensin II AT2 receptor inhibits proliferation and promotes differentiation in PC12W cells. Mol Cell Endocrinol 122:59-67

Moore SA, Patel AS, Huang N, Lavin BC, Grammatopoulos TN, Andres RD, Weyhenmeyer JA (2002) Effects of mutations in the highly conserved DRY motif on binding affinity, expression, and G-protein recruitment of the human angiotensin II type-2 receptor. Brain Res Mol Brain Res 109:161-167

Mukoyama M, Nakajima M, Horiuchi M, Sasamura H, Pratt RE, Dzau VJ (1993) Expression cloning of type 2 angiotensin II receptor reveals a unique class of seven-transmembrane receptors. J Biol Chem 268:24539-24542

Nahmias C, Strosberg AD (1995) The angiotensin AT2 receptor: searching for signal-transduction pathways and physiological function. Trends Pharmacol Sci 16:223-225

Nishikata I, Sasaki H, Iga M, Tateno Y, Imayoshi S, Asou N, Nakamura T, Morishita K (2003) A novel EVI1 gene family, MEL1, lacking a PR domain (MEL1S) is expressed mainly in t(1;3)(p36;q21)-positive AML and blocks G-CSF-induced myeloid differentiation. Blood 102:3323-3332

Nouet S, Amzallag N, Li JM, Louis S, Seitz I, Cui TX, Alleaume AM, Di Benedetto M, Boden C, Masson M, Strosberg AD, Horiuchi M, Couraud PO, Nahmias C (2004) Trans-inactivation of receptor tyrosine kinases by novel angiotensin II AT2 receptor-interacting protein, ATIP. J Biol Chem 279:28989-28997

Nuyt AM, Lenkei Z, Palkovits M, Corvol P, Llorens-Cortes C (1999) Ontogeny of angiotensin II type 2 receptor mRNA expression in fetal and neonatal rat brain. J Comp Neurol 407:193-206

Okuyama S, Sakagawa T, Chaki S, Imagawa Y, Ichiki T, Inagami T (1999) Anxiety-like behavior in mice lacking the angiotensin II type-2 receptor. Brain Res 821:150-159

Park H, Suzuki T, Lennarz WJ (2001) Identification of proteins that interact with mammalian peptide:N-glycanase and implicate this hydrolase in the proteasome-dependent pathway for protein degradation. Proc Natl Acad Sci U S A 98:11163-11168

Pfeifer D, Kist R, Dewar K, Devon K, Lander ES, Birren B, Korniszewski L, Back E, Scherer G (1999) Campomelic dysplasia translocation breakpoints are scattered over 1 Mb proximal to SOX9: evidence for an extended control region. Am J Hum Genet 65:111-124

Pulakat L, Cooper S, Knowle D, Mandavia C, Bruhl S, Hetrick M, Gavini N (2005) Ligand-dependent complex formation between the Angiotensin II receptor subtype AT2 and Na+/H+ exchanger NHE6 in mammalian cells. Peptides 26:863-873

Pulakat L, Rahman S, Gray A, Knowle D, Gavini N (2005) Roles of the intracellular regions of angiotensin II receptor AT2 in mediating reduction of intracellular cGMP levels. Cell Signal 17:395-404

Ramser J, Abidi FE, Burckle CA, Lenski C, Toriello H, Wen G, Lubs HA, Engert S, Stevenson RE, Meindl A, Schwartz CE, Nguyen G (2005) A unique exonic splice enhancer mutation in a family with X-linked mental retardation and epilepsy points to a novel role of the renin receptor. Hum Mol Genet 14:1019-1027

Reagan-Shaw S, Ahmad N (2005) Silencing of polo-like kinase (Plk) 1 via siRNA causes induction of apoptosis and impairment of mitosis machinery in human prostate cancer cells: implications for the treatment of prostate cancer. FASEB J 19:611-613

Reymond N, Fabre S, Lecocq E, Adelaide J, Dubreuil P, Lopez M (2001) Nectin4/PRR4, a new afadin-associated member of the nectin family that trans-interacts with nectin1/PRR1 through V domain interaction. J Biol Chem 276:43205-43215

Ried K, Rao E, Schiebel K, Rappold GA (1998) Gene duplications as a recurrent theme in the evolution of the human pseudoautosomal region 1: isolation of the gene ASMTL. Hum Mol Genet 7:1771-1778

Rigamonti D, Bauer JH, De-Fraja C, Conti L, Sipione S, Sciorati C, Clementi E, Hackam A, Hayden MR, Li Y, Cooper JK, Ross CA, Govoni S, Vincenz C, Cattaneo E (2000) Wild-type huntingtin protects from apoptosis upstream of caspase-3. J Neurosci 20:3705-3713

Rozen S, Skaletsky H (2000) Primer3 on the WWW for general users and for biologist programmers. Methods Mol Biol 132:365-386

Saavedra J (2005) Brain Angiotensin II: New Developements, Unanswered Questions and Therapeutic Opportunities. Cell and Mol Neurobiol 25:485-512

Sakagawa T, Okuyama S, Kawashima N, Hozumi S, Nakagawasai O, Tadano T, Kisara K, Ichiki T, Inagami T (2000) Pain threshold, learning and formation of brain edema in mice lacking the angiotensin II type 2 receptor. Life Sci 67:2577-2585

Senbonmatsu T, Saito T, Landon EJ, Watanabe O, Price E, Jr., Roberts RL, Imboden H, Fitzgerald TG, Gaffney FA, Inagami T (2003) A novel angiotensin II type 2 receptor signaling pathway: possible role in cardiac hypertrophy. Embo J 22:6471-6482

Servant G, Dudley DT, Escher E, Guillemette G (1996) Analysis of the role of N-glycosylation in cell-surface expression and binding properties of angiotensin II type-2 receptor of rat pheochromocytoma cells. Biochem J 313 (Pt 1):297-304

Servant G, Laporte SA, Leduc R, Escher E, Guillemette G (1997) Identification of angiotensin II-binding domains in the rat AT2 receptor with photolabile angiotensin analogs. J Biol Chem 272:8653-8659

Shea TB, Flanagan LA (2001) Kinesin, dynein and neurofilament transport. Trends Neurosci 24:644-648

Sklan EH, Podoly E, Soreq H (2006) RACK1 has the nerve to act: structure meets function in the nervous system. Prog Neurobiol 78:117-134

Smyth G (2005) Limma: linear models for microarray data. Springer, New York

Stevenson RE (2005) Advances in X-linked mental retardation. Curr Opin Pediatr 17:720-724

Stroth U, Meffert S, Gallinat S, Unger T (1998) Angiotensin II and NGF differentially influence microtubule proteins in PC12W cells: role of the AT2 receptor. Mol Brain Res 53:187-195

Sun Y, Kaksonen M, Madden DT, Schekman R, Drubin DG (2005) Interaction of Sla2p's ANTH domain with PtdIns(4,5)P2 is important for actin-dependent endocytic internalization. Mol Biol Cell 16:717-730

Suzuki T, Kwofie MA, Lennarz WJ (2003) Ngly1, a mouse gene encoding a deglycosylating enzyme implicated in proteasomal degradation: expression, genomic organization, and chromosomal mapping. Biochem Biophys Res Commun 304:326-332

Sytnyk V, Leshchyns'ka I, Nikonenko AG, Schachner M (2006) NCAM promotes assembly and activity-dependent remodeling of the postsynaptic signaling complex. J Cell Biol 174:1071-1085

Szabo A, Perou CM, Karaca M, Perreard L, Quackenbush JF, Bernard PS (2004) Statistical modeling for selecting housekeeper genes. Genome Biol 5:R59

Tanaka M, Kadokawa Y, Hamada Y, Marunouchi T (1999) Notch2 expression negatively correlates with glial differentiation in the postnatal mouse brain. J Neurobiol 41:524-539

Tararuk T, Ostman N, Li W, Bjorkblom B, Padzik A, Zdrojewska J, Hongisto V, Herdegen T, Konopka W, Courtney MJ, Coffey ET (2006) JNK1 phosphorylation of SCG10 determines microtubule dynamics and axodendritic length. J Cell Biol 173:265-277

Team RDC (2005) R: A language and environment for statistical computing, Vienna, Austria

Vervoort VS, Beachem MA, Edwards PS, Ladd S, Miller KE, de Mollerat X, Clarkson K, DuPont B, Schwartz CE, Stevenson RE, Boyd E, Srivastava AK (2002) AGTR2 mutations in X-linked mental retardation. Science 296:2401-2403

von Bohlen und Halbach O, Albrecht D (2006) The CNS renin-angiotensin system. Cell Tissue Res 326:599-616

von Bohlen und Halbach O, Walther T, Bader M, Albrecht D (2001) Genetic deletion of angiotensin AT2 receptor leads to increased cell numbers in different brain structures of mice. Regul Pept 99:209-216

Wang S, Chen JZ, Zhang Z, Gu S, Ji C, Tang R, Ying K, Xie Y, Mao Y (2003) Cloning, expression and genomic structure of a novel human GNB2L1 gene, which encodes a receptor of activated protein kinase C (RACK). Mol Biol Rep 30:53-60

Wang W, Huang Y, Zhou Z, Tang R, Zhao W, Zeng L, Xu M, Cheng C, Gu S, Ying K, Xie Y, Mao Y (2002) Identification and characterization of AGTRAP, a human homolog of murine Angiotensin II Receptor-Associated Protein (Agtrap). Int J Biochem Cell Biol 34:93-102

Wruck CJ, Funke-Kaiser H, Pufe T, Kusserow H, Menk M, Schefe JH, Kruse ML, Stoll M, Unger T (2005) Regulation of transport of the angiotensin AT2 receptor by a novel membrane-associated Golgi protein. Arterioscler Thromb Vasc Biol 25:57-64

Wu L, Iwai M, Li Z, Li JM, Mogi M, Horiuchi M (2006) Nifedipine inhibited angiotensin II-induced monocyte chemoattractant protein 1 expression: involvement of inhibitor of nuclear factor kappa B kinase and nuclear factor kappa B-inducing kinase. J Hypertens 24:123-130

Xinh PT, Tri NK, Nagao H, Nakazato H, Taketazu F, Fujisawa S, Yagasaki F, Chen YZ, Hayashi Y, Toyoda A, Hattori M, Sakaki Y, Tokunaga K, Sato Y (2003) Breakpoints at 1p36.3 in three MDS/AML(M4) patients with t(1;3)(p36;q21) occur in the first intron and in the 5' region of MEL1. Genes Chromosomes Cancer 36:313-316

Yaka R, Thornton C, Vagts AJ, Phamluong K, Bonci A, Ron D (2002) NMDA receptor function is regulated by the inhibitory scaffolding protein, RACK1. Proc Natl Acad Sci U S A 99:5710-5715

Yamada T, Horiuchi M, Dzau VJ (1996) Angiotensin II type 2 receptor mediates programmed cell death. Proc Natl Acad Sci U S A 93:156-160

Yee DK, Heerding JN, Krichavsky MZ, Fluharty SJ (1998) Role of the amino terminus in ligand binding for the angiotensin II type 2 receptor. Brain Res Mol Brain Res 57:325-329

Yee H (2005) marray: Exploratory analysis for two-color spotted microarray data. R package version 1.8.0

Ylisaukko-ojo T, Rehnstrom K, Vanhala R, Tengstrom C, Lahdetie J, Jarvela I (2004) Identification of two AGTR2 mutations in male patients with non-syndromic mental retardation. Human Genetics 114:211-213

Zuccato C, Tartari M, Crotti A, Goffredo D, Valenza M, Conti L, Cataudella T, Leavitt BR, Hayden MR, Timmusk T, Rigamonti D, Cattaneo E (2003) Huntingtin interacts with REST/NRSF to modulate the transcription of NRSE-controlled neuronal genes. Nat Genet 35:76-83